TWO-DIMENSIONAL FLOW AROUND AN ELLIPTIC AEROFOIL

WITH LAMINAR BOUNDARY LAYER

A Thesis

Submitted to the Faculty

of

Graduate Studies

The University of Manitoba

by

KANWALJIT SINGH BHATIA

In Partial Fulfillment of the

Requirements for the Degree

of

Master of Science

Department of Mechanical Engineering

May 1983

THE UNIVERSITY OF MANITOBA

FACULTY OF GRADUATE STUDIES

The undersigned certify that they have read, and recommend to the Faculty of Graduate Studies for acceptance, a Master's thesis entitled: Two-Dimensional Flow Around an Elliptic Aerofoil with Laminar Boundary Layer

submitted by Kanwaljit Singh BHATIA

in partial fulfilment of the requirements for the degree of

Master of Science (Mechanical Engineering)

S. Tinkler
(Dr. S. Tinkler) Advisor - Mech. Eng'g

A C Trupp
(Dr. A.C. Trupp) - Mech. Eng'g

D W Trim
(Dr. D. W. Trim) - Applied Math.

....

....
External Examiner

Date March 8, 1983.

....

Oral Examination is:

Satisfactory /x/ Not Required / /

[Unless otherwise specified by the major Department, thesis students must pass an oral examination on the subject of the thesis and matters relating thereto.]

TWO-DIMENSIONAL FLOW AROUND AN ELLIPTIC AEROFOIL WITH LAMINAR BOUNDARY LAYER

BY

KANWALJIT SINGH BHATIA

A thesis submitted to the Faculty of Graduate Studies of the University of Manitoba in partial fulfillment of the requirements of the degree of

MASTER OF SCIENCE

ABSTRACT

The aim of this study was to develop a computational technique to predict the incompressible, two-dimensional flow around an elliptic aerofoil at low Reynolds number at angles of attack up to and beyond the stall. The potential flow was to be calculated by a uniform flow and a distribution of vortices on the elliptic aerofoil. The displacement effects of the boundary layer and the separated wake were to be represented by a distribution of sources on the surface of aerofoil.

An elliptic cylinder with a fineness ratio of 6:1 at a Reynolds number of 800 was used as a representative aerofoil. Its shape was approximated by an inscribed polygon of flat elements. The vortices with linearly increasing strength were distributed on these elements. The potential flow around the aerofoil was computed by satisfying the zero-normal velocity condition at the mid-point of each element and the downstream end of the elliptic aerofoil as a stagnation point. The boundary layer calculations and the separation points were predicted using Thwaites' method. Another potential flow solution with a different stagnation point was developed. These two potential flows were combined to adjust the circulation to the value needed to equalize the upper and lower surface separation velocities. This modified the surface pressure gradient; the boundary layer was recalculated and the process iterated until the separation points stabilized. The sources were distributed on the same flat elements as were used in developing the potential solutions. The strengths of the sources were adjusted iteratively so that the surface streamline was

displaced by an amount equal to the displacement thickness of the attached boundary layer and the separated wake was a constant pressure region.

For angles of attack between 0 and 7 degrees, the flow was represented successfully. The coefficients of lift, drag and pitching moment were caculated. The coefficients of lift were compared with those calculated by Howarth. A slight difference in these results was due to different methods of boundary layer calculations. For angles of attack from 8 to 11 degrees, the iterative process for circulation adjustment failed to converge. The solution predicted oscillatory leading edge and trailing edge separation points. This may be indicative of an unsteady flow and requires further study. For angles of attack greater than 12 degrees, the separated flow model predicted source strengths which gave velocities incompatible with the constant pressure criterion. Further work is required to model the separated wake at higher angles of attack.

ACKNOWLEDGEMENTS

I would like to thank Professor J. Tinkler for the invaluable guidance he has rendered to me both as a teacher and research supervisor. His encouragement has inspired me to achieve the goals sought for. I also wish to express thanks to Mrs. Ingrid Trestrail for typing this thesis promptly.

My thanks are also due to the fellow graduate students for the fruitful discussions during the research work.

TABLE OF CONTENTS

LIST OF TABLES

LIST OF FIGURES

NOMENCLATURE

a	radius of circular cylinder
An_{ij}	normal velocity at i due to uniform source of strength of 1 at element j.
At_{ij}	tangential velocity at i due to uniform source of strength of 1 at element j.
b	semi-minor axis of the elliptic cylinder
c	semi-major axis of the elliptic cylinder
C	distance defined by $c^2 - b^2$
C_D	coefficient of form drag
C_L	coefficient of lift
C_m	coefficient of pitching moment
C_p	coefficient of pressure $\left(= \frac{p-p_\infty}{1/2\ \rho U_\infty^2}\right)$
d	major axis of the elliptic cylinder (chord)
F_x	force in x-direction
F_y	force in y-direction
f	a fraction
H	shape factor
k	strength of circulation in classical method and a counter in the surface vortex method
ℓ	a parameter used in Thwaites' method, $\ell = \frac{\Theta}{U} \left(\frac{du}{dy}\right)_{\text{surface}}$

$L(m)$	function of m
m	a parameter used in Thwaites' method, $m = \frac{\Theta^2}{U} (\frac{d^2u}{d\bar{y}^2})_{surface}$
n_i	unit vector at point i
N	number of surface elements
p	pressure of the fluid
p_∞	pressure of the uniform stream at infinity
r	distance of a point from the origin
r_1	distance of a point as shown in Figure 14
r_2	distance of a point as shown in Figure 14
R	distance in the Z-plane
Re	Reynolds number based on the major axis and the uniform stream ($Re = U_\infty d/\nu$)
s	distance along the surface as measured from the downstream end of the elliptic cylinder
u	velocity component parallel to x-axis
U	tangential velocity at the surface of the aerofoil due to distributed vortices and onset flow
U_∞	velocity of the uniform stream at infinity
U_{ij}	velocity induced at point i parallel to and due to vorticity distributed at element j
$\bar{u}$	velocity in the real axis direction in conformal transformation method
V_i	Vector velocity induced at a point i
Vn_i	normal velocity at a point i in the attached part
V_{ij}	velocity induced at a point i perpendicular to and due to

vorticity distributed at element j

$\bar{v}$ velocity in the direction perpendicular to real axis direction in conformal transformation method

v velocity component parallel to y

V_{sep} velocity at the point of separation

W complex potential of flow around a cylinder

x axis and distance parallel to major axis of the elliptic cylinder

$\bar{x}$ distance parallel to the surface of the elliptic cylinder

y axis and distance parallel to minor axis of the elliptic cylinder

$\bar{y}$ axis and distance perpendicular to the surface of the elliptic cylinder

Z plane containing the circular cylinder section

α angle of attack

β angular position of a point on circular cylinder in polar coordinates

γ_j uniform vorticity strength on element j

γ_j' gradient of linearly increasing vorticity strength on element j

Γ circulation around the elliptic cylinder

δ inclination of surface element with x-axis

δ^* displacement thickness

Φ angular position of a point on elliptic cylinder in polar coordinates

ϕ_1 angle as shown in Figure 14

ϕ_2 angle as shown in Figure 14

ρ fluid density

σ uniform source strength

σ'	gradient of linearly increasing source strength
θ	momentum thickness
ξ	axes parallel to surface elements
η	axes perpendicular to surface elements
ξ_{ij}	distance of point i in direction of ξ from point j
η_{ij}	distance of point i in direction of η from point j
τ_w	shear stress on the surface
	plane containing the elliptic cylinder
ϕ	angle on circle with diameter as the major axis of the elliptic cylinder as shown in Figure 3
Δ_j	half the length of the j-th surface element
ν	kinematic viscosity of the fluid
$\bar{\theta}$	angle as shown in Fig. 14 and Fig. 15
L	lift force
D	drag force
M	pitching moment

1. INTRODUCTION

It has always been one of the interests of aerodynamists to be able to predict the performance of an aerofoil in flight, or conversely, to design an aerofoil for a given flight performance. Experiments are carried out to measure the characteristics (coefficients of lift, drag, pitching moment, etc.) of an aerofoil, involving wind tunnels of various sizes. These experiments are time consuming and expensive. It is also difficult to achieve exact flight conditions in the wind tunnel tests. Despite these shortcomings, the wind tunnel tests are carried out as the present computational techniques are unable to include the complete boundary layer effects.

It has been observed that for two-dimensional aerofoils at low angles of attack, the boundary layer around the aerofoil is thin and a separated region, if it exists, is small. The inviscid flow theory gives fairly close results to those obtained experimentally. The inviscid fluid flow pressure gradients can be used with the boundary layer theory to predict the skin friction for the attached region. As the angle of attack increases the theoretical results for the inviscid flow show marked differences from the experimental results (for example - the predicted coefficient of lift is too high). This probably can be attributed mainly to the separated flow which modifies the circulation around the aerofoil. The pressure in the separated region is nearly constant. This real pressure distribution around the aerofoil can determine the form drag.

At high Reynolds number encountered in actual flights the boundary layer is usually turbulent leading to turbulent separation at higher angles of attack. It is difficult, theoretically, to model the separated region. In a recent attempt Zumwalt and Elangovan (Ref. 1) have tried to represent the separated region using some empirical relations from jet mixing theory. They have achieved good agreement with the experimental results for their chosen aerofoils. Their results are dependent on the empirical relations used. It has been observed that the laminar boundary layer is more predictable with good methods available to compute the displacement thickness and the separation points. The separated region still remains to be analysed.

The aim of the present study is to develop a technique to compute the characteristics of an aerofoil accounting for the effects of both the boundary layer thickness and the separation. The computational technique to be developed is intended to be a general one and thus applicable to any aerofoil. Here, this technique will be applied to a two-dimensional elliptic aerofoil in an incompressible flow at low Reynolds numbers so that the boundary layer is laminar. If this technique is successful then it can be extended to aerofoils with sharp trailing edges, multi-element aerofoils, and to a boundary layer which is initially laminar and undergoes transition to turbulent flow. The elliptic aerofoil is chosen to work with as an exact analytical solution for the potential flow can be obtained easily. Howarth (Ref. 2) has made a first approximation of the effects of laminar boundary layer separation on the coefficient of lift of an elliptic aerofoil and his results are available for comparison.

In the present study the potential flow will be represented by a uniform flow and distributed vortices on the aerofoil surface. It is intended to represent the boundary layer displacement thickness and the separated wake by a distribution of sources on the surface of the elliptic aerofoil. With suitable boundary conditions, this will shift the dividing streamline away from the elliptic aerofoil by a distance equal to the displacement thickness in the attached part of the flow and cause a constant pressure wake region after separation. The assumption of a constant pressure in the wake region has been observed experimentally and reference to these experimental evidences will be made in the later chapters.

2. INVISCID FLUID FLOW

2.1 Classical Method:

This section deals with the classical method of obtaining the pressure and velocity distribution around the two-dimensional body of any shape. The fundamental assumptions made here are that the fluid, through which the body moves, is incompressible, inviscid and irrotational.

The various early approaches for obtaining the surface pressure distributions around aerofoils have been compiled in Ref. 3. For the sake of completeness, the principle used for such computations can be restated here. The aerofoil is first mapped into a pseudo-circle by an inverse Joukowski transformation and then into an exact circle by a second transformation. The procedure can be generalized and improved by replacing the single Joukowski transformation by one or more inverse Karman-Trefftz transformations. If the Karman-Trefftz transformation is used, an aerofoil with any number of surface slope discontinuities can be mapped into a smooth pseudo-circle. The inverse Joukowski transformation can only be used for an aerofoil that has no surface slope discontinuities except at the trailing edge, where the change in slope is 180°. When the inverse Joukowski transformation is used on any other type of aerofoil, the results are incorrect in the region near the surface-slope discontinuities. Although it appears to be a powerful technique, it is limited to a single element aerofoil since it is a mapping technique. The Riemann mapping theorem guarantees that any single body can be mapped into a single circle but says nothing about multiple bodies. However, the potential flow about two lifting circles can be calculated and the circles are then transformed conformally onto two aerofoils (Ref. 4).

An elliptic aerofoil can easily be transformed conformally onto a circle using Joukowski transformation (Ref. 5). The circulation around the ellipse can be obtained by specifying, arbitrarily, the downstream end of the major axis of the elliptic aerofoil to be a stagnation point. This is equivalent to specifying the Kutta-condition for the aerofoil with sharp trailing edge. The theorem of Kutta-Joukowski can be used to evaluate the coefficient of lift. Appendix A gives the derivation of the formulae used to calculate the surface velocity distribution on the elliptic aerofoil.

Appendix A also gives the surface velocity derivatives with respect to the surface distance of the elliptic aerofoil starting at the trailing edge. These values will be used to check the velocity gradients obtained by other approximate methods.

2.2 Approximate Solutions:

In the last section, it was mentioned that the classical method of solving fluid dynamic problems could not be used for flow around more than one body except in a few special cases. In the last five decades researchers have tried two techniques to solve these problems - approximate analytical methods and exact numerical methods. The approximate solutions introduce analytical approximations into the formulation itself and thus place a limit on the accuracy that can be obtained in a given case regardless of the numerical procedures used. In contrast, in exact numerical methods the analytical formulation, including all equations, is exact and numerical approximations are introduced for purposes of calculation. Exact numerical methods have the property that the errors in the calculated solution can be made as small as desired, by sufficiently refining the numerical calculations.

Because exact analytic solutions (classical approach) are scarce for practical aerofoils and exact numerical methods were beyond the capability of hand computation, approximate solutions received the attention of the investigators in the field of inviscid flow. Many approaches have been formulated. Some are analytic in that the general solution can be written in simple closed form and others are numerical in that considerable computation is required to obtain the solution for each specific case. The common property of all approximate solutions is that restrictions are placed on the type of body or body surface about which the flow can be computed. Moreover, it is not always clear whether or not a particular approximate method is valid for a given body.

One type of approximate solution can be obtained by considering one or both of the following assumptions:

(a) the body is slender, with small local surface slope;

(b) the perturbation-velocity components due to the body are small with respect to the uniform stream that is the onset flow.

Thin aerofoil theory based on these assumptions has been developed by Glauert. These approximations are valid for thin aerofoils having small camber and small surface curvatures at small angles of attack. The accuracy of the computed solution is unknown.

Another large and well known approximate solution utilizes a distribution of singularities (sources and vortices) interior to the body surface. For example, the singularities are normally placed along the chord or camber line for two-dimensional aerofoils. The singularities may be discrete or distributed. The location and general properties of the singularities are assumed and their strengths are determined so that the body surface coincides with a streamline of the flow. This method is limited to the bodies with small surface curvatures.

Approximate solutions are therefore unsatisfactory for two reasons. First, they are obviously inapplicable in many cases such as bodies with sharp edges, two bodies in close proximity and many non-uniform flows. Second, their validity in many cases is not predictable, and the accuracy of the computed solutions is unknown. These facts lead to consideration of exact numerical methods of solution.

2.3 Exact Numerical Methods:

Exact numerical methods for the solution of the problem of potential flow are characterized by the fact that, at least in principle, any degree of accuracy may be obtained by sufficiently refining the calculational procedure without changing the analytical formulation. There appear to be two classes of exact numerical solutions that have been applied to the general fluid-dynamics problem: network methods based on finite-difference approximations of the derivatives of the potential and integral equation methods such as the surface singularity method.

2.3.1 Network Method:

Network method is based on distributing a network of points (termed control points) many body lengths in each direction around the body throughout the flow field. The finite-difference of the values of the potential at various control points around the aerofoil can be calculated by satisfying the boundary conditions at the surface in some form. Thus the solution must be obtained for the whole field even if it is required only on the boundary. Moreover, the most common application is that of the exterior flow about a closed body, where the flow field is infinite but the body is finite. The situation is illustrated in Figure 1. This results in the distribution of control points around the body in each direction. A large number of equations need to be solved to obtain the results on the surface of the body.

The results can be refined by decreasing the spacing between the points being considered.

2.3.2 Integral Equation Method:

Exact integral-equation representation of the problem of potential flow may be formulated in a variety of ways, all leading to a Fredholm integral equation of either the first or the second kind. Most of the methods that have been formulated are equivalent to determining a distribution of singularities over the body surface. Both sources and vortex distributions have been used. The boundary conditions are satisfied so that the body surface is a streamline of the flow. There are no restrictions on the shape of the body or the type of flow. Thus it is quite a versatile method and has been used widely. A good survey of the surface-singularity methods is presented in Ref. 6.

2.3.3.1 Present Theoretical Model:

The present method uses the vortex distribution on the surface of the elliptic aerofoil. The basic idea of the surface-vortex method is as follows. The flow, which must satisfy Laplace's equation, is produced by superimposing a uniform stream U_∞ at angle α to the x-axis, (Figure 2), and a continuous distribution of vortices round the perimeter of the aerofoil. The boundary condition must be such as to ensure that the aerofoil surface is a streamline of the flow. It is convenient to stipulate the condition of zero velocity normal to the aerofoil surface. The present formulation generates a Fredholm integral equation of the first kind. This integral equation may be changed to a summation equation by dividing the aerofoil surface into a finite number of elemental arcs and satisfying the boundary condition at a similar number of points.

Mathematically, if the elliptic aerofoil surface is divided into N vortex elements then the boundary condition of zero normal velocity applied to the mid-point of each element (termed control point henceforth) leads to a linear equation of the type

$$\sum_{j=1}^{N} \bar{V}_{ij} \cdot \bar{n}_i + \bar{U}_\infty \cdot \bar{n}_i = 0 \quad \ldots\ldots\ldots\ldots\ldots\ldots\ldots\ldots\ldots\ldots (2.1)$$

where $\bar{n}_i$ is the unit vector normal at the control point; $\bar{U}_\infty$ is the uniform vector onflow and $\bar{V}_{ij}$ is the vector velocity induced at the control point i by the j-th vortex element around the body surface. The mathematical expression for $\bar{V}_{ij}$ depends on the order of approximation demanded by equation (2.1). The zeroth order model developed by Hess and Smith (Ref. 7) utilizes flat surface elements of constant singularity strength. In the surface vortex model considered here, it is convenient to adopt a modest improvement over the zeroth order approximation; namely use of flat elements with linear variation in singularity strength. This improvement, as noted by Gibson and Wilcox (Ref. 8) ensures continuity in vortex strength between adjacent elements and avoids the increase in computation time associated with parabolic approximations.

2.3.3.2 Numerical Formulation:

In this section it is intended to throw some light on the actual numerical formulation of the potential flow problem. The vortex type of singularity distribution is chosen for the present work. It has the distinct advantage that the vortex density, which is determined directly, is equal to the surface velocity.

The two-dimensional elliptic aerofoil is approximated by a large number of surface elements, whose characteristic dimensions are small as compared to those of the elliptic aerofoil itself. The total number of surface elements and their distribution influence the accuracy of the resulting calculations. As noted by Hess and Smith (Ref. 7) elements should be concentrated in regions where the body geometry-slope changes rapidly. The size of the elements should change gradually between the regions of concentrations and regions where the distribution is sparse. In the elliptic aerofoil here, the distribution of elements is achieved by applying the 'cosine rule',

$$x_{\ell} = 0.5\ (1 + \cos\phi_{\ell}) \quad \ldots\ldots\ldots\ldots\ldots\ldots\ldots\ldots\ldots\ldots\ldots\ldots (2.2)$$

which is illustrated in Figure 3, and where ℓ is an integer between 1 and N. The elliptic aerofoil surface is thus approximated by an inscribed polygon of N sides. Solutions with N = 10, 20, 40 and 60 have been tried. With 60 elements it is possible to obtain the pressure distribution up to 0.13% of the chord. It may be noted that the element end-points are on the aerofoil surface. The control points are then located at the mid-point of each element.

After specifying the control points, it is required to determine the velocity at all control points induced by all vortex elements. In Appendix (B) the induced velocity at any point due to a line vortex with linearly increasing vortex strength has been derived. These expressions are used repeatedly for each element and each control point.

If j represents an element over which the distributed vortex strength increases linearly from γ_j to γ_{j+1} with a gradient of γ'_j = $(\gamma_{j+1} - \gamma_j)/2\Delta_j$, then the induced velocities at i-th control point in the directions parallel to and perpendicular to the j-th element, denoted by U_{ij} and V_{ij} respectively are

$$U_{ij} = \frac{\gamma_j}{2\pi}\left[\tan^{-1}\left(\frac{\xi_{ij} - \Delta_j}{\eta_{ij}}\right) - \tan^{-1}\left(\frac{\xi_{ij} + \Delta_j}{\eta_{ij}}\right)\right] + \frac{\gamma'_j}{2\pi}\left[(\xi_{ij} + \Delta_j)\left\{\tan^{-1}\left(\frac{\xi_{ij} + \Delta_j}{\eta_{ij}}\right) - \tan^{-1}\left(\frac{\xi_{ij} + \Delta_j}{\eta_{ij}}\right)\right\} - \eta_{ij}\,\ell n\left\{\frac{(\xi_{ij} - \Delta_j)^2 + \eta_{ij}^2}{(\xi_{ij} + \Delta_j)^2 + \eta_{ij}^2}\right\}^{1/2}\right] \quad (2.3)$$

and

$$V_{ij} = \frac{\gamma_j}{2\pi}\left[\ell n\left\{\frac{(\xi_{ij} + \Delta_j)^2 + \eta_{ij}^2}{(\xi_{ij} - \Delta_j)^2 + \eta_{ij}^2}\right\}^{1/2}\right] + \frac{\gamma'_j}{2\pi}\left[(\xi_{ij} + \Delta_j)\ell n\left\{\frac{(\xi_{ij} + \Delta_j)^2 + \eta_{ij}^2}{(\xi_{ij} - \Delta_j)^2 + \eta_{ij}^2}\right\}^{1/2} - 2\Delta_j - \eta_{ij}\left\{\tan^{-1}\left(\frac{\xi_{ij} - \Delta_j}{\eta_{ij}}\right) - \tan^{-1}\left(\frac{\xi_{ij} + \Delta_j}{\eta_{ij}}\right)\right\}\right] \quad (2.4)$$

where these notations have been explained in Figure (4).

These components are further resolved into a direction normal to the i-th element at the i-th control point. Keeping i-th element to be the same and varying the position j, the total normal component at i is

$$\bar{V}_i \bullet \bar{n}_i = \sum_{j=1}^{N}\left[\{U_{ij}\sin\delta_j + V_{ij}\cos\delta_j\}.\cos\delta_i - \{U_{ij}\cos\delta_j - V_{ij}\sin\delta_j\}\sin\delta_i\right] \quad (2.5)$$

where δ is the inclination of the element with the positive x-axis as shown in Figure (4). Equation (2.5) simply means that the total normal velocity induced at the i-th control point is the sum of the N velocities due to the distributed vortex at each of the j-th elements.

The onset flow (U_∞ at angle of attack α) has a component of velocity normal to the i-th element given by

$$\bar{U}_\infty \cdot \bar{n}_i = U_\infty \sin (\alpha - \delta_i) \qquad (2.6)$$

The boundary condition of zero normal velocity at the body surface at the i-th control point, as given by Equation (2.1) now leads to N equations

$$\sum_{j=1}^{N} \left[(U_{ij}\sin\delta_j + V_{ij}\cos\delta_j)\cos\delta_i - (U_{ij}\cos\delta_j - V_{ij}\sin\delta_j)\sin\delta_i\right] + U_\infty \sin(\alpha-\delta_i) = 0 \qquad (2.7)$$

where $i = 1, 2, \ldots N$

The number of equations is N while the number of unknown γ's is (N+1). The stagnation point is specified at the downstream end of the major axis of the elliptic aerofoil. This gives

$$\gamma_{N+1} = -\gamma_1 \qquad (2.8)$$

Incorporating Equation (2.8) in the Equation (2.7) reduces the number of unknown γ's to the number of equations. The N linear equations with N unknowns can be solved on a computer using any well-known algorithm to find the unknown γ's. Here, the Gaussian elimination technique is used to evaluate the unknown γ's. The surface tangential velocities are the same as the values of the local vortex strength since the internal velocity is zero.

3. LAMINAR BOUNDARY LAYER CONSIDERATIONS

3.1 Theory:

The general problem of the flow in the laminar boundary layer with the prescribed pressure distributions is one of formidable complexity, involving as it does, partial differential equations with two independent variables. The most effective analytic attack on it has been by the so-called series solution method to which Blasius, Howarth and Frossling have made the most important contributions. The essential features of these methods are given in Ref. 9. However, many external velocity distributions of practical interest can not be handled by these methods. The numerical difficulties involved in obtaining exact solutions of the boundary layer equations for the general case has led to much attention being paid to the development of approximate methods. Usually such methods have been developed with the limited objective of predicting the overall characteristics of the boundary layer, e.g. momentum thickness, displacement thickness and the points of separation, if any, rather than the velocity distribution of the boundary layer flow. The momentum integral equation generally provides the basis for such methods and the approximations are manifest in the assumptions adopted to solve that equation.

The momentum integral equation of the boundary layer is obtained by integrating the equation of motion of the boundary layer. Pohlhausen's, Thwaites' and Young's methods are the important ones in which attempts have been made to solve the integral equations using different approximating assumptions. Thwaites' method (Ref. 10) as modified by Curle and Skan (Ref. 11) has been found to give good predictions of the separation point and therefore it is adopted for use in the present work. The pertinent details of the method are repeated below.

Two non-dimensional parameters ℓ and m are defined by the equations:

$$\ell = \frac{\theta}{U} \left(\frac{du}{d\bar{y}}\right)_{wall} \quad \ldots\ldots (3.1)$$

and

$$m = \frac{\theta^2}{U} \left(\frac{d^2u}{d\bar{y}^2}\right)_{wall} \quad \ldots\ldots (3.2)$$

where u is the boundary layer velocity parallel to the solid boundary, U is the value of u at the outer edge of the boundary layer, $\bar{y}$ is the distance perpendicular to the boundary and θ is the momentum thickness.

The parameter ℓ is directly related to the skin friction while m is related to the pressure (or velocity, U) through the only boundary condition in which the external pressure appears, viz. :-

$$\nu \left(\frac{d^2u}{d\bar{y}^2}\right)_{wall} = \frac{1}{\rho}\frac{dp}{d\bar{x}} = \frac{-UdU}{d\bar{x}} \quad \ldots\ldots (3.3)$$

The first part of this equation is obtained from the equation of motion evaluated at the wall; the second part is obtained from Bernoulli's equation. Here $\bar{x}$ is the distance parallel to the boundary and ν is the coefficient of kinematic viscosity.

Combining (3.2) and (3.3),

$$m = \frac{-\theta^2}{\nu}\frac{dU}{d\bar{x}} \quad \ldots\ldots (3.4)$$

where m is a very important parameter of velocity profile and if we assume that the laminar boundary layer velocity profiles form a uniparametric family, then we can regard m as the form parameter. In that case ℓ must be a unique function of m for all velocity profiles, as must be $H = \delta^*/\theta$ where δ^* is the displacement thickness and H is the shape factor. The momentum integral equation can then be written successively as

$$\frac{d\theta}{d\bar{x}} + \theta\ (H+2)(dU/d\bar{x})/U = \frac{\tau_w}{\rho U^2} = \frac{\nu \ell}{U\theta} \qquad \text{..............(3.5)}$$

or,

$$U\frac{d(\theta^2)}{d\bar{x}} = 2\nu\ [m\ (H+2)+\ell]$$

$$= \nu\ L\ (m) \qquad \text{...(3.6)}$$

where $L(m) = 2\ [m(H+2)+\ \ell]$

Thwaites evaluated the expression represented by the right hand side of the Equation (3.6) for velocity profiles given by known exact solutions covering a wide range of pressure gradients and found that the resulting curves lay close to a straight line for which the equation was $L\ (m) = 0.45 + 6m$. Equation (3.6) therefore can be written as

$$U\ \frac{d}{d\bar{x}}(\theta^2) - 0.45\ \nu + \frac{6dU}{d\bar{x}}\ \theta^2 = 0$$

or,

$$\theta^2 = \theta_0^2 + \frac{0.45\nu}{(U^6)} \int_0^{\bar{x}} U^5\ d\bar{x} \qquad \text{..................................(3.7)}$$

where θ_0 is the momentum thickness at the stagnation point. Thus the value of θ^2 can be determined at any point by a simple quadrature. Once θ^2 is determined the parameter m can be obtained from Equation (3.4). Thwaites selected certain of the exact solutions most relevant to the flow past aerofoils as a guide, particularly the case of a constant adverse velocity gradient, and on the basis of these solutions, he devised a table of ℓ and H as unique functions of m.

Thwaites (Ref. 10) suggests the value of m at the stagnation point as −0.075, which, with Equation (3.4) gives the initial values of momentum thickness. The separation point occurs when m reaches the value of 0.082. Later, Curle and Skan (Ref. 11) applied Thwaites' method to more examples of separation and noted that Thwaites' method systematically underestimates the distances to separation from the stagnation point for different types of velocity distributions. Curle and Skan recommended modified values of ℓ and H for values for m greater than 0.06. According to this modification the parameter m is equal to 0.09 at the point of separation. Values of ℓ and H, including Curle and Skan's modifications, are presented in Table 1.

3.2 Numerical Method:

It is intended here to outline, briefly, the numerical technique used to evaluate the laminar boundary layer characteristics, along the surface of the aerofoil, up to the separation points. The momentum thickness, the parameter m and the displacement thickness are given by Equations (3.7), (3.4), Table 1 and the relation $\delta^* = H\theta$ respectively.

Equation (3.7) can be written in non-dimensional form as

$$\left(\frac{\theta}{d}\right)^2 = \left(\frac{\theta}{d}\right)_0^2 + \frac{0.45}{(U/U_\infty)^6 (Re)} \int_0^{\bar{x}/d} \left(\frac{U}{U_\infty}\right)^5 d\left(\frac{\bar{x}}{d}\right) \quad \ldots\ldots\ldots\ldots\ldots(3.8)$$

where d is a characteristic length, here chosen as the major axis of the elliptic aerofoil, U_∞ is the free stream velocity and $Re(=\frac{Ud}{\nu})$ is the Reynolds number based on the main stream velocity and the major axis of the aerofoil. The main task then is to evaluate the integral in Equation (3.8) while $(\frac{U}{U_\infty})$ can be determined from the potential flow solution, as obtained in the previous chapter. The integral can be evaluated by the 10-point Simpson's 1/3 rule. Thus

$$\int_0^{\bar{x}/d} \left(\frac{U}{U_\infty}\right)^5 d\left(\frac{\bar{x}}{d}\right) = \sum_{j=1}^{i-1} \left(\frac{\Delta\bar{x}/d}{3}\right) \left[f\left(\frac{\bar{x}_j}{d}\right) + 4f\left(\frac{\bar{x}_j}{d}+\frac{\Delta\bar{x}}{d}\right) + 2f\left(\frac{\bar{x}_j}{d}+2\frac{\Delta\bar{x}}{d}\right) + \right.$$

$$+ 4f\left\{\frac{\bar{x}_j}{d} + (M-1)\frac{\Delta\bar{x}}{d}\right\} + f\left(\frac{\bar{x}_{j+1}}{d}\right)\Big] \quad \ldots\ldots (3.9)$$

where $\Delta\bar{x} = \dfrac{\bar{x}_{j+1} - \bar{x}_j}{M}$ where $M = 10$, $f(x) = \left(\dfrac{U}{U_\infty}\right)^5$ and i = number of control points after the stagnation point, on each surface, up to the downstream end of the major axis. It can be observed from the Equation (3.9) that in order to find the momentum thickness at a control point the velocities must be interpolated between that point and the previous control point. This interpolation of velocities at intermediate points is carried out using Lagrangian interpolation. Near the stagnation point, these velocities are interpolated linearly.

Once the distribution of momentum thickness is known, the values of the parameter m can be determined from Equation (3.4) as

$$m = -\frac{\theta^2}{\nu}\left(\frac{dU}{d\bar{x}}\right)$$

$$= -\left(\frac{\theta}{d}\right)^2 \cdot \frac{d\left(U/U_\infty\right)}{d\,(\bar{x}/d)} \cdot Re$$

where the velocity gradient $\left(\text{of } \dfrac{U}{U_\infty}\right)$ is calculated by differentiating a cubic spline relating the known values of velocities at control points to the distances of the control points from the trailing edge. The calculation of the parameter m is stopped as soon as m has a value equal to or greater than 0.09. The separation point is located wherever the parameter m has a value 0.09.

The shape factor H is calculated by linear interpolation of the values of the parameter m in Table 1 and the displacement thickness is given by $\delta^* = H\theta$.

4. INVISCID FLOW AND BOUNDARY LAYER REPRESENTATION

4.1 General:

The surface-vortex method, described earlier, determines the tangential velocity distribution around the elliptic aerofoil for the given flow conditions. Then Thwaites' method is used to calculate the distribution of displacement thickness on the upper and lower surfaces in the regions of attached flow and the points of separation on both the surfaces of the elliptic aerofoil. The existence of the boundary layer and separated wake modifies the circulation around the elliptic aerofoil. These effects can be represented by a distribution of sources on the elliptic aerofoil surface. In terms of the surface-vortex method this is accomplished by treating the flow induced by the sources as an additional onset flow. This concept of the boundary layer source flow is termed as the displacement onset flow.

The same surface elements are used for the source distributions as were used for the surface-vortex method. Sources with uniform strength are distributed on each of these elements. In order to calculate the strength of these sources, boundary conditions are applied at the mid points of each of these elements. The boundary conditions differ in the attached and the separated parts of the flow. These are discussed in the following paragraphs.

4.2 Attached Part:

The main flow in the presence of the boundary layer behaves as if it is flowing without friction past a surface displaced outwards by a distance δ^*. The displacing effect is produced here by discharging sources at the surface with velocity normal to the surface given by $V_n = U. \left(\frac{d\delta^*}{d\bar{x}}\right)$. The derivation of this formula is given in Ref. 12. The displacement thickness slope along the surface of the elliptic aerofoil is determined by numerical differentiation of δ^* with respect to the distance from the stagnation point. The boundary condition in the attached region is set by defining the normal velocities at the control points in that region. This effectively means that at a given control point, i, in the attached region, the normal velocity induced by all the sources is $Vn_i = U_i \left(\frac{d\delta^*}{d\bar{x}}\right)_i$. In terms of the strength of sources the equation can be written as

$$\sum_{j=1}^{N} An_{ij} . \sigma_j = Vn_i \quad \text{...(4.1)}$$

where i refers to the control points in the attached region, An_{ij} is the normal velocity induced at i due to a unit source at j, σ_j refers to the uniform strength of the source at the element j and N is the total number of elements around the elliptic aerofoil.

4.3 Separated Part:

Due to the presence of the boundary layer and the separated wake the determination of circulation around the aerofoil is not possible by simply specifying the stagnation point at the downstream end of the major axis of the elliptic aerofoil. For this it is argued that if the flow conditions are steady then the rate at which vorticity is discharged into the wake from the upper and lower surfaces must be equal and opposite (Ref. 13 & 14). It further follows then that the free stream velocity at the edge of the separated wake must be the same for both upper and lower surfaces in the region of the separated wake. This then is the condition that must be applied to determine the circulation. Since the present model is all potential flow, the constant velocity condition in the separated wake leads to a constant pressure wake region. The technique to determine the circulation with a constant pressure wake region is described in Section 4.4.

It must be noted here that main stream velocity at the upper and lower separation points is the resultant of the total tangential component (due to onset, vortex distribution and source distribution) and the normal component (due to the source distribution). Thus the separation velocity can be written as

$$V^2_{sep} = \left(U_i + \sum_{j=1}^{N} At_{ij}\, \sigma_j\right)^2 + \left(\sum_{j=1}^{N} An_{ij}\, \sigma_j\right)^2 \ldots\ldots\ldots\ldots\ldots\ldots (4.2)$$

where i refers to the control points in the separated region, U_i is the tangential velocity at i-th control point due to the vortex distribution and the onset flow, At_{ij} is the tangential velocity induced at i due to a unit source at j, σ_j refers to the uniform strength of source at the element j and V_{sep} represents the total velocity at the separation point.

Equations (4.1) and (4.2) have N unknowns (σ's) and there are N equations. Since Equation (4.2) is not a linear equation, an iterative procedure is followed to solve the Equations (4.1) and (4.2). The first iteration begins by assuming the tangential component of the velocities induced by the distributed sources is zero. This gives us the first approximation of the strength of the sources from the following equations:

$$\sum_{j=1}^{N} An_{ij} \cdot \sigma_j = \sqrt{V^2_{sep} - U^2_i} \quad \text{for i in the separated region}$$

and

$$\sum_{j=1}^{N} An_{ij} \cdot \sigma_j = V_{ni} \qquad \text{for i in the attached region.}$$

In the subsequent iterations denoted by k, equations (4.1) and (4.2) can be re-written as follows:

$$\sum_{j=1}^{N} An_{ij}\, \sigma_j^k = \sqrt{V^2_{sep} - \left(U_i + \sum_{j=1}^{N} At_{ij} \cdot \sigma_j^{k-1}\right)^2} \quad \ldots\ldots\ldots\ldots\ldots(4.3)$$

for i in the separated region, and

$$\sum_{j=1}^{N} An_{ij}\, \sigma_j^k = Vn_i \quad \ldots\ldots\ldots\ldots\ldots\ldots\ldots\ldots\ldots\ldots\ldots\ldots\ldots\ldots(4.4)$$

for i in the attached region.

Equation (4.3) simply means that for the kth iteration for evaluating the strength of the sources, the tangential velocity induced is due to the sources from the previous iteration. This process of iteration is stopped when the strengths of sources do not vary significantly in the subsequent iterations. The criterion chosen to achieve this is to test the strength of the sources near the upper and lower separation points in the subsequent iterations. If the corresponding strengths of the sources do not vary by more than 1%, the iteration process is stopped.

4.4 Circulation Adjustment With Separated Wake:

As was pointed out earlier, the circulation around the elliptic aerofoil was calculated by specifying the stagnation point at the downstream end of the major axis. This specification is no longer applicable in the presence of the separated wake. The modified condition requires the separation velocities at the upper and lower surfaces to be equal. To satisfy this condition the tangential velocities at the control points nearest to the separation points are equated. If γ_i and γ_j are the vortex strengths at the upper and lower separation points, then

$$\gamma_i = -\gamma_j$$

This reduces the number of unknown γ's from (N+1) to N but by doing so the right hand side of the matrix system is disturbed. Thus the modified Kutta condition can not be applied in the same manner as the conventional Kutta condition in the surface-vortex method.

A different and new approach is followed to satisfy the modified Kutta-condition. Firstly, we have a potential flow solution satisfying the conventional Kutta condition. Using Thwaites' method the separation points on the upper and lower surfaces are determined. Secondly, a new potential flow solution is calculated with an arbitrary stagnation point for the same onset flow conditions. Now, these two potential flow solutions are combined so as to give equal velocities at the upper and lower separation points. However, the new resultant potential flow solution gives a new pressure field for the boundary layer. The boundary layer is recalculated giving new separation points. This leads to an iterative process to follow. These iterations are carried on till the upper and lower separation velocities are not different by more than 1%. The flow is now a potential flow satisfying the conditions that:

(i) far away the flow has a velocity of U_∞ inclined at α to the ellipse major axis,

(ii) in the region where the laminar boundary layer would be attached, the mainstream is displaced from the elliptic aerofoil surface by the same distance as the laminar boundary layer would displace it;

(iii) in the region downstream of separation, the pressure is constant, which is observed to be nearly true in Ref. 13 and 14.

4.5 Estimation of the Lift, Drag and Pitching Moment Coefficients:

Appendix C gives the derivation of the formulae used to estimate the coefficients of lift, drag and pitching moment. Once the potential flow representation of the flow has been made, the coefficients of lift, drag and pitching moment can be estimated.

A flow-chart, Figure 5, lists all the operations carried out to predict these coefficients.

5. RESULTS & DISCUSSION

The problem of the steady, incompressible, low Reynolds number laminar flow around an elliptic aerofoil was formulated in the earlier chapters. A computer program was developed and a copy of the listing is attached in Appendix D. Figure 5 shows a flow-chart of the sequence of computations carried out. The program was tested on an elliptic aerofoil with a fineness ratio of 6:1 at a Reynolds number of 800. The program was used on an Amdahl 470/V8 computer of the University of Manitoba. The program was tested for angles of attack from zero to 20 degrees. This program was intended to be a general one and hence will accept coordinates of any aerofoil and any Reynolds number appropriate for laminar boundary layers.

5.1 Potential Flow:

The adequacy of the surface-vortex method for the potential flow was tested by predicting the flow about the elliptic aerofoil at several angles of attack using from 20 to 60 elements. When the number of elements chosen was 20, the control point nearest to the upstream end of the elliptic aerofoil was 1.2% aft of the front point. This was not good enough to represent the true contour because the shape of the aerofoil changed rapidly in the vicinity of either end. Therefore, to obtain the rapid velocity changes near both ends, it was decided to use 60 elements which made it possible to calculate the tangential velocity at 0.138% chord.

Table 2 represents the velocities obtained at chord positions from 57.8% to 99.8% using 60-element surface-vortex method at an angle of attack of 0 degree. Table 2 also includes the corresponding velocities obtained by the exact Conformal Transformation method and the error in the surface-vortex method which was defined as

$$\text{Percentage error} = \frac{(\text{Approximate velocity} - \text{Exact velocity}) \times 100\%}{\text{Exact velocity}}$$

It was found that the error was much less than 1% over most of the aerofoil surface for all angles of attack, but near the stagnation point it was 8 to 10%. This high percentage of error is due to the small value of the denominator.

Figure 6 represents the pressure distribution calculated from the velocities obtained by the surface-vortex method at an angle of attack of 8 degrees. The differences in pressures obtained by surface-vortex method and the exact method are difficult to distinguish on the graph.

In general, the 60-element surface-vortex method predicted the potential flow around the elliptic aerofoil with high accuracy and was used for the subsequent work. Ref. 7 mentions that numerical difficulties may arise while solving the Fredholm equation of the first kind. But no such difficulties were encountered here and one reason for the present success is that the non-uniform distribution of vorticity on the elements leads to a better conditioned matrix than when uniform vorticity is used: the latter gives a zero diagonal in the coefficient matrix.

The surface velocity gradients, required for the boundary layer calculations, were calculated from the velocity distribution using cubic splines; the details of the method are given in Appendix B. An example of the accuracy of this method is given in Table 3 where the gradients calculated by the Conformal Transformation method are used as the basis of comparison.

5.2 Potential Flow Results for Circulation Determined by Boundary Layer Separation:

The boundary layer calculations began by calculating the momentum thickness using Thwaites' method. Then the parameter m was calculated up to a position where m reached the value 0.09; the displacement thickness was also calculated for each of the control points on both upper and lower surfaces. The exact positions of the points of separation (determined by m= 0.09) were calculated. The normal components of velocity due to the boundary layer growth at the separation points on both the surfaces were calculated. If the upper and lower separation velocities were not equal, a potential flow with an arbitrarily chosen stagnation point was calculated (loop 1, Figure 5). A fraction f of this new potential flow was combined with a fraction (1-f) of the original (rear stagnation point) flow in proportions required to equalize the upper and lower separation velocities, and at the same time keep the onset flow unchanged. This resulted in a modified surface pressure distribution; the boundary layer was recalculated and the process iterated until the separation points were stabilized with equal separation velocities.

The growth of momentum thickness when the angle of attack was 7 degrees is shown in Figure 7a for the final iteration. The momentum thickness on both the surfaces increases rapidly from the stagnation point and then grows more slowly. The predicted values appear to be quite smooth.

The distribution of parameter m was studied for each angle of attack on both the upper and lower surfaces of the aerofoil. Figure 7b shows the distribution of m, in the final iteration at an angle of attack of 7 degrees. It is observed that for both the surfaces, near the stagnation point, the m-values were irregular. But these smooth out away from the stagnation point. The lower surface m - values rise steeply near the separation point. Since separation occurs when m = 0.09, the values of m downstream of separation were not calculated.

This displacement thickness up to the separation point was then estimated. Figure 7c shows the final iteration result for an angle of attack of 7 degrees. The growth is rapid near the stagnation point because of the high shear stress at the surface. The growth is again very rapid as the separation points are approached. These large slopes of the displacement thickness would imply unrealistically high normal velocities. It was observed that, after the initial rapid growth, the displacement thickness rate of growth decreased as $\bar{x}$ increased except near the separation points. In the absence of a better technique, the displacement thickness growth was arbitrarily restricted near the separation points*. The modified values of δ^* are shown dotted on Figure 7c. The normal velocities at the separation points were thus small as compared to the tangential velocities.

Table 4 shows the locations of the nearest control points where the separation occurred on each surface at various angles of attack. The Table also shows the number of iterations required to adjust the circulation so that the upper and lower separation velocities were equal. The magnitudes of these velocities are also given. It is observed that from angles of attack of 0 to 7 degrees, only 2 to 4 iterations were required to adjust the circulation so that the upper and lower separation velocities were equal.

From 8 degrees up to 11 degrees the iteration process failed to converge. It was observed that at 8 degrees, the value of parameter m on the upper surface reached 0.09 very close to the upstream end of the elliptic aerofoil. When the circulation was adjusted, as a next step, the

* The values of $\frac{d\delta^*}{d\bar{x}}$ were checked for a few control points upstream the separation point. Whenever $\frac{d\delta^*}{d\bar{x}}$ began to rise rapidly the displacement thickness was not allowed to grow more than the average growth of the previous interval in proportion to its length.

separation point moved way back on the upper surface. On readjusting the circulation, the separation point moved again close to the upstream end of the aerofoil. This oscillatory behaviour continued between upstream and downstream separations and a unique solution could not be obtained. The same was true for angles of attack from 9 to 11 degrees. Some further discussion of this problem is given later.

For angles of attack of 12 degrees, a unique stable solution was obtained after about 14 iterations. As a matter of investigation, angles of attack well beyond the stall up to 20 degrees, in steps of 2 degrees, were tried. The circulation was able to be adjusted in 4 to 6 iterations. These separation results are also included in Table 4.

There are two possible explanations for the behaviour of the solution between 8 and 11 degrees. First, the iterative computational procedure itself might have been the cause of failure to converge. Second, the real flow may be oscillatory, like Karman vortex shedding, for these angles of attack.

Therefore, whenever a unique solution was not obtained, further investigation was carried out. For example, at an angle of attack of 8 degrees, the parameter m was calculated for the full range of control points even after m had first acquired the value of 0.09. It was observed that m was greater than 0.09 for only four or five control points. Beyond these, the values of m became and stayed less than 0.09 for quite a distance downstream. Eventually, m exceeded 0.09 again where "trailing edge" separation would normally be expected. It was postulated that this trailing edge separation was close to the real separation position and the circulation was adjusted to make the upper and lower separation velocities equal. The process was iterated and after the solution stabilized, the values of m were checked. It was found that m still had upper surface values greater than 0.09 near the upstream end of the aerofoil. This meant that the solution obtained was invalid and a leading edge separation would occur. Similar results were obtained for angles of attack of 9 and 10 degrees.

Since this method failed to produce a unique valid solution, it is possible that the flow may be naturally unstable for angles of attack between 8 and 11 degrees. As mentioned in Chapter IV of Reference 12, it is possible that a vortex street may occur under these conditions. This unsteady flow cannot be predicted by the computer program developed here because steady flow was postulated.

A few values of the parameter m greater than 0.09 near the upstream end of the aerofoil may lead to another conclusion that a separation bubble may have been formed. The treatment required to handle the separation bubble near the leading edge of an aerofoil is dependent on empirical relations (Reference 1) and is beyond the scope of the present study.

Further work is necessary to investigate whether the iteration process can be modified to give a steady solution for angles of attack between 8 and 11 degrees.

5.3 The Iterative Solution for Displacement and Wake Effects:

To represent the boundary layer displacement effects and the separated wake, uniform sources were distributed over the surface elements. The strengths of these sources were calculated to satisfy the normal velocity and constant pressure boundary conditions in the attached and separated regions respectively as discussed in Chapter 4. As illustrated by the flow chart (Figure 5), the strengths of these sources were calculated as a first approximation by neglecting the contribution of the tangential velocities induced by the sources. In the subsequent iteration (loop 2, Figure 5), the tangential velocities induced by the sources of the previous iteration were considered. This iterative process was continued till the strengths of these sources did not vary. An average of two iterations was required.

As shown in Figure 5, during the last pass through loop 2, the normal and tangential velocities due to sources were combined with the tangential velocities obtained by the onset flow and the distributed vortices. This resulted in modified surface velocities. The boundary layer calculations were performed again to predict the separation points. If the velocities at the separation points were not equal, loop 3, Figure 5 was followed in which the modified velocity distribution was combined with a potential flow to adjust the circulation till equal velocities resulted. The source-calculation was performed again and the process iterated till equal velocities resulted at the upper and lower separation points. The number of iterations required were 1 to 3 for various cases.

The cases of angles of attack from 0 to 7 degrees were obtained with the boundary layer displacement thickness and the wake represented by source distributions. Figure 8 shows the pressure distribution at an angle of attack of 1 degree satisfying the above conditions. The full solution could not be applied to the cases with angles of attack between 8 and 11 degrees because the separation points were not stationary. When the full solution was sought for angles of attack between 12 and 20 degrees, it was found that the sources generated such high tangential and normal velocities that a constant pressure separated wake could not be obtained. A possible cause for this is that in the first iteration to obtain the strengths of the sources, the boundary conditions changed too abruptly from the attached region to the separated region. In the attached region the normal velocity was related to the displacement thickness while the normal velocity in the separated region was related to the separation velocity and the tangential velocity due to the onset flow and the distributed vortices. This first approximation produced very high source strengths which were poorly conditioned for input to the subsequent iteration and convergence was not achieved. Proper representation of the separated wake at higher angles of attack will require further study. A recommendation to this effect is to re-specify for the first iteration the normal velocities in the separated region of the upper and lower surfaces. It is suggested that the normal velocities should be specified equal to their values at the separation points. Since these normal velocities are small, the first approximation of the strengths of sources should not induce high tangential and normal velocities.

5.4 Results of Force and Moment Coefficients

5.4.1 The Coefficient of Lift:

The coefficient of lift was calculated at several stages of the calculations. It was first calculated where the inviscid velocity distribution was determined by the rear stagnation point being at the downstream end of the aerofoil. These results show a linear variation with angle of attack right up to 20 degrees. The lower end of the range is plotted on Figure 9.

The coefficient of lift was calculated after the circulation was adjusted to equalize the upper and lower separation velocities. Figure 9 shows these values of the coefficient of lift. These results will be discussed in three parts for three ranges of angle of attack.

For angles of attack up to 7 degrees, the results were well behaved and are very close to those of Howarth who used the same criterion for determining the circulation from the boundary layer separation. The small differences in the lift-coefficients can be attributed to the different methods of calculating the boundary layer. Howarth used a Pohlhausen-type solution which is known to have limited accuracy in predicting separation. The present analysis used Thwaites' method as modified by Curle and Skan specifically for improving the prediction of separation. It is therefore assumed that the slightly higher lift predicted by this method is valid. These results up to an angle of 7 degrees show a marked reduction of lift compared to the potential flow solution. Unfortunately, there are no suitable experimental results for comparison but the computed results are consistent with typical aerofoil data. It is interesting to note that Howarth was able to establish that the lift reached a maximum round about 7 degrees and that the stalling occurred by 8 degrees. The present method seems to indicate that the stalling angle was about 7 degrees but the solutions in the post-stall region require special discussion.

The oscillatory solutions obtained for angles between 8 and 11 degrees are also represented by two possible values of the coefficients of lift at each angle. The higher values of the coefficients of lift are for the cases when the separation occurs near the downstream end of the aerofoil. The lower values correspond to leading edge separation. If the real flow is indeed oscillatory in this range of angles of attack, it is unlikely that the dynamic solution would have such a large amplitude.

The coefficients of lift obtained for angles of attack of 12 degrees and greater are truly in the stalled region and the flow is characterized by the upper surface boundary layer separating near the leading edge.

When the displacing effects of the boundary layer and the wake were taken into consideration, solutions were obtained for angles of attack up to 7 degrees and the coefficients of lift are plotted on Figure 9. These values are a little less than when only the points of separation were allowed for. This can be interpreted as meaning that the displacing effect does not greatly modify the boundary layer growth and its separation. For single element aerofoils, it could be concluded that the lift could be adequately predicted by calculating the boundary layer separation and its effect on circulation. For aerofoils with slotted flops, it is probably more important that the wake of the main aerofoil be represented when calculating the boundary layer behaviour on the flap.

5.4.2 The Coefficient of Drag:

The profile drag force experienced by an aerofoil is due to the frictional stresses called the skin-friction drag and due to a distribution of surface pressures contributing a force component in the direction of the flow, called the form drag.

Figure 10 represents the distribution of the coefficient of skin-friction on the upper surface of aerofoil at an angle of attack of 3 degrees as calculated by Thwaites' method. It is observed that near the stagnation point the skin friction drag is high and reduces downstream of the velocity maximum. The skin friction distribution was calculated up to the separation points. High value of the skin friction near the stagnation point is due to high velocity gradients existing near the stagnation point. Table 5 presents the values of the coefficient of skin friction drag at various angles of attack. It is observed as the angle of attack increases the coefficient of skin-friction drag increases very slowly.

The coefficients of form drag were calculated by integrating the drag forces due to the normal pressure distribution on the surface of the aerofoil. The values of the coefficients of form drag at various angles of attack are presented in Table 5 where it is observed that as the angle of attack increases the coefficient of form drag decreases slightly.

Table 5 and Figure 11 give the values of the coefficients of profile drag at angles of attack up to 7 degrees. The calculations depended on a successful representation of the boundary layer displacement and wake effects by sources.

5.4.3 The Coefficient of Pitching Moment:

The moments of the lift and drag forces about the upstream end of the aerofoil were calculated and normalized to give the pitching moments for angles of attack up to 7 degrees. These coefficients are presented in Figure 12. The sign convention is such that a positive pitching moment tends to increase the angle of attack.

It is observed from Figure 12 that as the angle of attack increases, the pitching moment decreases. This is due to the increasing contribution to the moment by the lift force, which increases as the angle of attack increases.

The compilation and execution times were 0.75 seconds and approximately 40 seconds respectively for the angles of attack between 0 and 7 degrees.

6. CONCLUSIONS

The surface-singularity method to represent two-dimensional, incompressible flow around an elliptic aerofoil of fineness ratio 6:1 with a laminar boundary layer at a Reynolds number of 800 gave the following results:

1. The potential flow is represented accurately by 60 flat elements and a linearly increasing strength of distributed vortices.

2. The boundary layer calculations using Thwaites' method were successful except for the rapid growth of the displacement thickness near the separation point which had to be modified.

3. The displacing effects of the attached boundary layer and a constant pressure wake region were modelled successfully by adding source distribution for angles of attack between 0 and 7 degrees.

4. The oscillatory flow obtained for angles of attack between 8 and 11 degrees may be real or it may be due to the iterative process which failed to converge. Further investigation is needed to establish the genuineness of the oscillatory flow.

5. For angles of attack greater than 12 degrees, the present work predicted excessively high velocity contributions from the source distribution as a result of which the iterative process breaks down. It is recommended that the first approximation of strengths of sources be changed such that the normal components of velocities calculated at the separation points be specified at points aft the separation points on both upper and lower surfaces.

6. The force and moment coefficients were calculated successfully up to 7 degrees of angle of attack.

APPENDIX A

COMPUTATION OF VELOCITY AND VELOCITY GRADIENT - ANALYTICAL METHOD

The potential flow around an elliptic aerofoil can be obtained by conformally transforming it from the flow around a circular cylinder. The velocity distribution and the velocity gradient along the aerofoil surface are calculated as a check for the results obtained by the panel method.

The flow past a circular cylinder of a uniform stream U_∞ inclined at an angle of α to the real axis is shown in Figure (13) and its complex potential, W, in the Z-plane is (Ref. 5)

$$W = U_\infty \left[e^{-i\alpha}Z + a^2 \frac{e^{i\alpha}}{Z}\right] \qquad \text{(A.1)}$$

where a is the radius of the circular cylinder.

The complex potential (in the Z-plane) of a pure circulation of strength k about the origin is given by

$$W = i\,k\,\ell n\,Z \qquad \text{(A.2)}$$

Thus the complex potential of the uniform flow combined with the circulatory flow can be obtained by adding the equations (A.1) and (A.2) as follows:

$$W = U_\infty \left[e^{-i\alpha}Z + \frac{a^2 e^{i\alpha}}{Z}\right] + ik\ell nZ \qquad \text{(A.3)}$$

The position of the rear stagnation point can be used as a condition to calculate the circulation. If $\bar{u}$ and $\bar{v}$ are the velocity components in the x and y directions respectively, then

$$\bar{u} - i\bar{v} = \frac{dW}{dZ} \qquad \text{(A.4)}$$

At a stagnation point, such as B in Figure (13), $\frac{dW}{dZ} = 0$.

For the circular cylinder,

$$\frac{dW}{dZ} = U_\infty \left(e^{-i\alpha} - \frac{a^2}{Z^2} e^{i\alpha}\right) + \frac{ik}{Z}$$

and at the point B ($R = a$, $\beta = 0$),

$$Z = Re^{i\beta} = a$$

so that

$$\frac{dW}{dZ} = 0 = U_\infty \left(e^{-i\alpha} - e^{i\alpha}\right) + \frac{ik}{a}$$

Therefore

$$k = \frac{aU_\infty}{i} \left(e^{i\alpha} - e^{-i\alpha}\right) = 2aU_\infty \sin\alpha \quad \text{.....................(A.5)}$$

Thus the complex potential of a uniform stream at an angle of attack α, with circulation, around the circular cylinder such that the point B is a stagnation point, is given by

$$W = U_\infty \left(e^{-i\alpha} Z + \frac{a^2 e^{i\alpha}}{Z}\right) + i2aU_\infty \sin\alpha . \ln Z \quad \text{.....................(A.6)}$$

The region outside the circular cylinder is mapped on the region outside the elliptic aerofoil in the ζ-plane by using the transformation

$$\zeta = Z + \frac{C^2}{4Z} \quad \text{...(A.7)}$$

where $C^2 = c^2 - b^2$, c is the semi major axis and b is the semi minor axis of the elliptic aerofoil. The velocities in the ζ-plane are given by

$$\frac{dW}{d\zeta} = \frac{dW}{dZ} \cdot \frac{dZ}{d\zeta} \quad \text{...(A.8)}$$

From the equation (A.6),

$$\frac{dW}{dZ} = U_\infty \left[e^{-i\alpha} - \frac{a^2 e^{i\alpha}}{Z^2}\right] + i \frac{2a\, U_\infty \sin\alpha,}{Z}$$

which can be rearranged to give (on the surface of the circular cylinder)

$$\frac{dW}{dZ} = U_\infty \left[\left\{\cos\alpha - \cos(\alpha - 2\beta) + 2\sin\alpha \sin\beta\right\} + i\left\{-\sin\alpha - \sin(\alpha - 2\beta) + 2\sin\alpha\cos\beta\right\}\right]$$

$$\text{.....................(A.9)}$$

Also, from (A.7),

$$\frac{d\zeta}{dZ} = 1 - \frac{C^2}{4Z^2} ,$$

but on the surface of the circular cylinder,

$$Z = ae^{i\beta} ,$$

so that

$$\frac{d\zeta}{dZ} = 1 - \frac{C^2}{4a^2} e^{-2i\beta}$$

or

$$\frac{d\zeta}{dZ} = (1-\frac{C^2}{4a^2}\cos 2\beta) + i\,(\frac{C^2}{4a^2}\sin 2\beta) \quad \text{.......................(A.10)}$$

Therefore the velocities on the surface of the elliptic aerofoil are given by

$$\frac{dW}{d\zeta} = U_\infty\left[\{\cos\alpha-\cos(\alpha-2\beta)+2\sin\alpha\,\sin\beta\}+i\{-\sin\alpha-\sin(\alpha-2\beta)+2\sin\alpha\,\cos\beta\}\right] /$$
$$\left[(1-\frac{C^2}{4a^2}\cos 2\beta) + i\,(\frac{C^2}{4a^2}\sin 2\beta)\right] \quad \text{.....................................(A.11)}$$

It should also be noted that as $Z \to \infty$, $\frac{dZ}{d\zeta} \to 1$, so that $\frac{dW}{dZ} \to \frac{dW}{d\zeta}$. This means that the ellipse is in a stream of strength U_∞ at an angle α to the real axis.

The relationship between the position of a point on the elliptic aerofoil and the corresponding point on the circular cylinder can be found out as follows:

In polar coordinates,

$$\zeta = r\,e^{i\Phi}$$

$$Z = R\,e^{i\beta},$$

therefore the transformation function, Equation (A.7) becomes

$$re^{i\Phi} = Re^{i\beta} + \frac{C^2}{4Re^{i\beta}}$$

or

$$\cos\Phi + i\,\sin\Phi = \frac{R}{r}\cos\beta + \frac{C^2}{4Rr}\cos\beta + i\,(\frac{R}{r}\sin\beta - \frac{C^2}{4Rr}\sin\beta)$$

Equating the real and imaginary parts gives

$$\cos\Phi = (\frac{R}{r} + \frac{C^2}{4Rr})\cos\beta \quad \text{.......(A.12}$$

$$\sin\Phi = (\frac{R}{r} - \frac{C^2}{4Rr})\sin\beta \quad \text{.......(A.13}$$

and elimination of r gives

$$\tan\beta = \frac{R + \frac{C^2}{4R}}{R - \frac{C^2}{4R}}\tan\Phi \quad \text{.......(A.14)}$$

Knowing the position of a point on the ellipse, ie, angle Φ, R (= $\frac{c+b}{2}$) and C (= $(c^2-b^2)^{1/2}$), we get the corresponding position (β) on the circular cylinder. This value of β can be used in the equation (A.11) to compute the velocity at the point Φ on the elliptic aerofoil.

Once the velocity distribution has been obtained on the elliptic aerofoil, the velocity gradients with respect to the distance along the surface of the aerofoil can be computed as follows:

$$\frac{d\bar{u}}{ds} = \frac{d\bar{u}}{d\beta}\cdot\frac{d\beta}{d\Phi}\cdot\frac{d\Phi}{ds} \quad \text{.......(A.15)}$$

$$\frac{d\bar{v}}{ds} = \frac{d\bar{v}}{d\beta}\cdot\frac{d\beta}{d\Phi}\cdot\frac{d\Phi}{ds} \quad \text{.......(A.16)}$$

$$\frac{dV}{ds} = \frac{\bar{u}\,\frac{d\bar{u}}{ds} + \bar{v}\,\frac{dv}{ds}}{(\bar{u}^2 + \bar{v}^2)^{1/2}} \quad \text{.......(A.17)}$$

where $\bar{u}$ and $\bar{v}$ are the x and y components of the velocity on the elliptic aerofoil, s is the distance along the elliptic aerofoil surface, measured as shown in Figure (2) and V represents the resultant of $\bar{u}$ and $\bar{v}$ at a given point on the elliptic aerofoil.

In the Equations (A.15) and (A.16), $\frac{d\bar{u}}{d\beta}$ and $\frac{d\bar{v}}{d\beta}$ are calculated from

(A.11), $\frac{d\beta}{d\Phi}$ is calculated by (A.14) and $\frac{d\Phi}{ds}$ is calculated from the properties of the ellipse as follows. In polar coordinates the equation of the ellipse is

$$\left(\frac{r\cos\Phi}{c}\right)^2 + \left(\frac{r\sin\Phi}{b}\right)^2 = 1 \quad \ldots\ldots (A.18)$$

which gives

$$\frac{dr}{d\Phi} = \frac{-r\sin 2\Phi\left(\frac{c^2}{b^2} - 1\right)}{\left(-1-\frac{c^2}{b^2}\right) - \cos 2\Phi\left(1-\frac{c^2}{b^2}\right)} \quad \ldots\ldots (A.19)$$

and this can be used in the expression for the required derivative

$$\frac{d\Phi}{ds} = \left\{r^2 + \left(\frac{dr}{d\Phi}\right)^2\right\}^{-1/2} \quad \ldots\ldots (A.20)$$

APPENDIX B

COMPUTATION OF VELOCITY & VELOCITY GRADIENT - SURFACE SINGULARITY METHOD

In this section the formulae are developed for the induced velocity at a point due to an element with a distributed vortex of uniform strength, a linearly varying strength and a combination of these two types of distributions.

Similarly, the corresponding formulae are derived for the induced velocities at a point due to distributed sources of uniform strength, linear strength and a combination of these two types.

B.1 Uniformly Distributed Vortex Strength:

Let γ be the strength of uniformly distributed vorticity over a straight element AB with O as the centre such that OA=OB=Δ, as shown in Figure 14. Consider a small portion ds of the element at a distance s from the centre O. Let P (x,y) be the point where the induced velocity is to be found. The velocity induced at P, due to the small length ds, is dV.

Therefore

$$dV = \frac{\gamma ds}{2\pi r}$$

where $r = \{(x-s)^2 + y^2\}^{1/2}$

Assuming positive vorticity gives counter-clockwise flow, the x-component of the induced velocity at P is given by du

$$du = \frac{\gamma \; ds \; \sin\bar{\theta}}{2\pi r} \quad \text{...(B.1)}$$

where $\bar{\theta}$ is the angle between the x-axis and the line joining the point P to a point on the x-axis distant s from the origin.

Similarly, the y-component of the induced velocity at P is given by dv such that

$$dv = \frac{\gamma \, ds \, \cos\bar{\theta}}{2\pi r} \quad \text{...(B.2)}$$

Therefore, u, the total x-component of the induced velocity at P, due to the element AB is given by integrating (B.1) over the length of the element (i.e., from $-\Delta$ to Δ). Then

$$u = \int_{-\Delta}^{\Delta} - \frac{\gamma \sin\bar{\theta} \, ds}{2\pi r}$$

or, $$u = \frac{\gamma}{2\pi} (\phi_1 - \phi_2) \quad \text{...(B.3)}$$

Similarly, v, the total y-component of velocity is given by

$$v = \int_{\Delta}^{\Delta} \frac{\gamma \cos\bar{\theta} \, ds}{2\pi r}$$

or, $$v = \frac{\gamma}{2\pi} \ln \left(\frac{r_1}{r_2}\right) \quad \text{...(B.4)}$$

B.2 Linearly Increasing Strength of Vortex:

Consider a short element AB along the x-axis with its centre at 0 such that AO = OB = Δ, as shown in Figure 14. Let the vortex strength be zero at A and increase linearly towards B at the rate of γ'. A small length ds at a distance s from the centre induces the velocity dV at P(x,y)

$$dV = \frac{\gamma' ds \, (s + \Delta)}{2\pi r}$$

thus, the x and y components are

$$du = \frac{-\gamma'(s + \Delta) \sin\bar{\theta} \, ds}{2\pi r} \quad \text{..................................(B.5)}$$

$$dv = \frac{\gamma'(s + \Delta) \cos\bar{\theta} \, ds}{2\pi r} \quad \text{..................................(B.6)}$$

To find the total x-component of the induced velocity at 0 due to AB, (B.5) is integrated over the length AB (i.e., from $-\Delta$ to Δ)

$$u = \int_{-\Delta}^{\Delta} \frac{-\gamma'(s + \Delta)\sin\bar{\theta}\, ds}{2\pi r}$$

or,
$$u = -\frac{\gamma'}{2\pi}\left[(x + \Delta)(\phi_2 - \phi_1) + y\,\ell n\,\frac{r_2}{r_1}\right] \quad \text{(B.7)}$$

Similarly, for the y-component,

$$v = \int_{-\Delta}^{\Delta} \frac{\gamma'(s + \Delta)\cos\bar{\theta}\, ds}{2\pi r}$$

or,
$$v = \frac{\gamma'}{2\pi}\left[x\,\ell n\,\left(\frac{r_1}{r_2}\right) - 2\Delta + y\,(\phi_2 - \phi_1) + \Delta\,\ell n\,\left(\frac{r_1}{r_2}\right)\right] \quad \text{(B.8)}$$

B.3 Uniformly Distributed and Linearly Increasing Vortex Strength:

Combining Equations (B.3) and (B.7), the x-component of the induced velocity at P due to uniformly distributed vorticity of strength γ_j and linearly varying vortex strength which increases at the rate of γ'_j given by

$$u = \frac{\gamma_j}{2\pi}(\phi_1 - \phi_2) + \left[-\frac{\gamma'_j}{2\pi}\left\{(x + \Delta_j)(\phi_2 - \phi_1) + y\,\ell n\,\frac{r_2}{r_1}\right\}\right] \quad \text{(B.9)}$$

where $\gamma'_j = \frac{\gamma_{j+1} - \gamma_j}{2\Delta_j}$, $r_1 = \{(x + \Delta_j)^2 + y^2\}$, $r_2 = \{(x - \Delta_j)^2 + y^2\}^{1/2}$

$\phi_1 = \tan^{-1}\left(\frac{y}{x + \Delta_j}\right)$, $\phi_2 = \tan^{-1}\left(\frac{y}{x - \Delta_j}\right)$ and ϕ_1 and ϕ_2 vary between 0 and 2π.

Similarly, the y-component of the induced velocity at P is given by combining the equations (B.4) and (B.8)

$$v = \frac{\gamma_j}{2\pi}\,\ell n\,\frac{r_1}{r_2} + \left[\frac{\gamma_j'}{2\pi}\left\{x\,\ell n\,\frac{r_1}{r_2} - 2\Delta_j + y\,(\phi_2 - \phi_1) + \Delta_j\,\ell n\,\frac{r_1}{r_2}\right\}\right] \quad \text{(B.10)}$$

In the above equations (B.9) and (B.10), the distances x and y have been referred to as the parallel and perpendicular distances from the element whose effect is being considered. In the computer program, x and y have been referred to as XI and ETA. In the equations (B.9) and (B.10), special cases arose when trying to find the induced velocities at the centre of the element due to the element itself.

From (B.9), as $x \to 0$ and $y \to +0$

$$u = -\frac{\gamma_j}{2} - \frac{\gamma_j'}{2}(\Delta_j)$$

From (B.10), as $x \to 0$, and $y \to +0$,

$$v = \frac{\gamma_j'}{2\pi}\left(-2\Delta_j\right)$$

B.4 Uniformly Distributed Sources:

Let σ be the strength of a uniformly distributed source over an element AB with O as the centre such that AO = OB = Δ, as shown in Figure 15. Consider a small portion ds of the element at a distance s from the centre O. Let P (x,y) be the point where the induced velocity due to the element AB is to be found. The velocity induced at P, due to the small length ds, is dV

Therefore,

$$dV = \frac{\sigma ds}{2\pi r}$$

where $r = \left\{(x - s)^2 + y^2\right\}^{1/2}$

The x-component, du, of the induced velocity is given as follows:

$$du = dV \cos\bar{\theta} \quad \text{......(B.11)}$$

where $\bar{\theta}$ is the angle between the x-axis and the line joining the point P to a point on the x-axis, distant s from the origin.

Similarly, the y-component, dv, of the induced velocity is given as

$$dv = dV \sin\bar{\theta} \quad \text{......(B.12)}$$

On integrating (B.11) and (B.12) over the element length, the total components of the induced velocities u and v in x and y directions respectively are

$$u = \frac{\sigma}{2\pi} \ln \frac{r_1}{r_2} \quad \text{(B.13)}$$

and
$$v = \frac{\sigma}{2\pi} (\phi_2 - \phi_1) \quad \text{(B.14)}$$

where $r_1 = \{(x + \Delta)^2 + y^2\}^{1/2}$, $r_2 = \{(x - \Delta)^2 + y^2\}^{1/2}$,

$\phi_1 = \tan^{-1} (\frac{y}{x + \Delta})$ and $\phi_2 = \tan^{-1} (\frac{y}{x - \Delta})$

B.5 Linearly Incereasing Strength of Sources:

Consider a short element AB along the x-axis with its centre at 0 such that AO = OB = Δ, as shown in Figure 5. Let the source strength be zero at A and increase linearly towards B at the rate of σ'. A small length ds at a distance s from the centre induces the velocity dV at P(x,y)

$$dV = \frac{\sigma' ds\ (s + \Delta)}{2\pi r} \quad \text{(B.15)}$$

The total x-component of the induced velocity at the point P due to a linearly increasing strength of source is found as

$$u = \frac{\sigma'}{2\pi} \lfloor (x + \Delta) \ln \frac{r_1}{r_2} - 2\Delta - y\ (\phi_1 - \phi_2) \rfloor \quad \text{(B.16)}$$

Similarly, the total y-component of the induced velocity at the point P due to a linearly increasing strength of source is found as

$$v = \frac{\sigma'}{2\pi} \lfloor (x + \Delta)\ (\phi_2 - \phi_1) + y \ln \frac{r_2}{r_1} \rfloor \quad \text{(B.17)}$$

Equation (B.16) is of the same form as Equation (B.8) whereas Equation (B.17) is - of the Equation (B.7).

B.6 Uniformly Distributed & Linearly Increasing Source Strength:

The sources of uniform strength and linearly increasing strength can be combined to evaluate the total x and y components of the induced velocities at a given point in a similar manner to what was done in Section (B.3) for vortices. Thus, combining (B.13) and (B.16) gives the total induced x-component while on adding (B.14) and (B.17), the total y-component of the induced velocities is obtained. These components are:

$$u = \frac{\sigma}{2\pi}\,\ell n\,(\frac{r_1}{r_2}) + \frac{\sigma'}{2\pi}\,\{x + \Delta)\;\ell n\,\frac{r_1}{r_2} - 2\Delta - y\,(\phi_1 - \phi_2)\}\ldots\ldots(B.18)$$

and

$$v = \frac{\sigma}{2\pi}\,(\phi_2 - \phi_1) + \frac{\sigma'}{2\pi}\,\{(x + \Delta)\quad(\phi_2 - \phi_1) + y\ell n(\frac{r_2}{r_1})\}\ldots\ldots(B.19)$$

It is, again, possible to find the induced velocities at the centre of the element itself due to partly uniformly distributed strength and partly linearly increasing strength of the source.

From the equation (B.18), on putting x=o and y=+o,

$$u = \frac{\sigma'}{2\pi}\,(-\,2\Delta)\ldots\ldots\ldots\ldots\ldots\ldots\ldots\ldots\ldots\ldots\ldots\ldots\ldots\ldots(B.20)$$

and

$$v = +\,\frac{\sigma}{2} + \frac{\sigma'\,\Delta}{2}\ldots\ldots\ldots\ldots\ldots\ldots\ldots\ldots\ldots\ldots\ldots\ldots\ldots\ldots(B.21)$$

B.7 Computation of Velocity Gradient on the Surface:

The velocity gradients on the aerofoil surface are determined by differentiating cubic splines fitted to the known velocity distribution along the surface. It was convenient to measure the surface distance counterclockwise from the downstream end of the elliptic aerofoil.

The theory of fitting cubic splines between two variables is given in Reference 15. The principle involved is re-written here. Let the aerofoil surface be divided into N parts. Let S represent the distance and U represent the velocity. Consider the k-th interval which is between

(U_k, S_k) and (U_{k+1}, S_{k+1}). The cubic for the k-th interval is written as

$$f_k(S) = U = A_k(S-S_k)^3 + B_k(S-S_k)^2 + C_k(S-S_k) + D_k \quad \text{..........(B.22)}$$

where A_k, B_k, C_k and D_k are determined so that the slope and curvature of the spline is the same for the splines in (k-1)th interval and (k+1)the interval. If $\Delta S = S_{k+1}-S_k$, then the spline function values from Equation (B.22) at S_k and S_{k+1} are given by

$$U_k = D_k \quad \text{..(B.23)}$$

$$U_{k+1} = A_k\Delta S^3_k + B_k\,\Delta S^2_k + C_k\,\Delta S_k + D_k \quad \text{..............................(B.24)}$$

The first derivatives of the spline function from Equation (B.22) at S_k and S_{K+1} are given by

$$U'_k = C_k \quad \text{..(B.25)}$$

and

$$U'_{k+1} = 3A_k\,\Delta S^2_k + 2B_k\,\Delta S_k + C_k \quad \text{..............................(B.26)}$$

where $U' = \frac{dU}{dS}$.

Then the coefficients A_k, B_k, C_k, D_k for the k-th interval are written as follows:

$$\left.\begin{aligned} A_k &= \frac{1}{\Delta S^2_k}\left(\frac{-2\Delta U_k}{\Delta S_k} + U'_k + U'_{k+1}\right) \\ B_k &= \frac{1}{\Delta S_k}\left(3\frac{\Delta U_k}{\Delta S_k} - 2U'_k - U'_{k+1}\right) \\ C_k &= U'_k \\ D_k &= U_k \end{aligned}\right\} \quad \text{.........(B.27)}$$

where $\Delta U_k = U_{k+1} - U_k$

The continuity condition $\left(f''_{k-1}(S_k) = f''_k(S_k)\right)$ gives

$$6A_{k-1}\,\Delta S_{k-1} + 2B_{k-1} = 2B_k \quad (k=2,.....N-1) \quad \text{.................(B.28)}$$

which leads to N-2 equations in the N unknowns U'_1, -- U'_N viz.:

$$\frac{1}{\Delta S_{k-1}}U'_{k-1} + 2\left(\frac{1}{\Delta S_{k-1}} + \frac{1}{\Delta S_k}\right)U'_{k+1} = \frac{3\,\Delta U_{k-1}}{(\Delta S_{k-1})^2} + \frac{3\Delta U_k}{(\Delta S_k)^2} \quad (k=2,---N-1)\text{..(B.29)}$$

If the quantitites U'_1 and U'_N are given, the Equation (B.29) can be solved for U'_k (k = 2, ---N-1).

The values of U'_1 and U'_n are approximated using the finite difference form and the rest of the velocity derivatives are evaluated.

APPENDIX - C

ESTIMATION OF THE LIFT, DRAG AND PITCHING MOMENT COEFFICIENTS

C.1 The Lift Coefficient by Integration of the Pressure Distribution Around the Elliptic Aerofoil:

Let Figure (16) represent a section of the elliptic aerofoil at an incidence α to the fluid stream, which is assumed to be from left to right at a speed of U_∞. Consider the pressure, p, acting on a small element AB, of length ds, of the surface. Let p_∞ be the static pressure of the undisturbed stream. The normal force on the element is $p\delta s$ inwards. This force per unit span may be resolved into components δD and δL acting parallel and perpendicular to the direction of the undisturbed stream respectively.

Then

$$dL = - \{-pds \sin\delta\} \sin\alpha + \{pds.\cos\delta\} \cos\alpha \quad \text{.................. (C.1)}$$

where δ is the counterclockwise inclination of the element AB from the positive x-axis (Figure 16).

Replacing $ds.\sin\delta$ by dy and $ds.\cos\delta$ by dx, the Equation (C.1) is re-written as

$$dL = (pdy) \sin\alpha + (pdx) \cos\alpha \quad \text{.............................. (C.2)}$$

If this is integrated round the contour of the elliptic aerofoil, the total lift force, acting normal to the direction of the undisturbed stream, can be obtained. The coefficient of lift, C_L, is obtained by dividing the total lift force by $1/2\ \rho U_\infty^2 d$ where d is the chord of the elliptic aerofoil.

Then

$$C_L = \frac{\oint dL}{1/2\rho U_\infty^2 d}$$

or
$$C_L = \oint \left(\frac{p-p_\infty}{1/2\rho U_\infty^2}\right) d\left(\frac{y}{d}\right) \cdot \sin\alpha + \oint \left(\frac{p-p_\infty}{1/2\rho U_\infty^2}\right) d\left(\frac{x}{d}\right) \cdot \cos\alpha \quad \text{(C.3)}$$

since $\oint p_\infty d(\frac{y}{d}) = 0$. Then introducing $C_p = \frac{p-p_\infty}{1/2\rho U_\infty^2}$

$$C_L = \oint C_p \, d\left(\frac{y}{d}\right) \sin\alpha + \oint C_p \, d\left(\frac{x}{d}\right) \cos\alpha \quad \text{(C.4)}$$

C.2 The Lift Coefficient by Calculating the Circulation Around the Elliptic Aerofoil:

The lift force of an aerofoil is given by the Kutta-Joukowski Theorem as

$$L = \rho U_\infty \Gamma \quad \text{(C.5)}$$

where Γ is the total circulation given by

$$\Gamma = \oint U(s) \, ds \quad \text{(C.6)}$$

where s is the arc length of the contour, measured counterclockwise from the down stream end of the elliptic aerofoil. If the fluid is considered inviscid U(s) is the tangential velocity along the surface of the elliptic aerofoil. Combining Equations (C.5) and (C.6) and normalizing by $1/2\rho U_\infty^2 d$, gives the lift coefficient

$$C_L = \frac{L}{1/2\rho U_\infty^2 d} = \frac{\rho U_\infty \oint U(s) ds}{1/2\rho U_\infty^2 d}$$

$$= 2\oint \left(\frac{U(s)}{U_\infty}\right) d\left(\frac{s}{d}\right) \quad \text{(C.7)}$$

C.3 The Form Drag Coefficient by Integration of the Pressure Distribution Around the Elliptic Aerofoil:

The form drag is due to the pressure distribution on the aerofoil in a direction parallel to the stream.

For a small surface element AB, (as in Fig. 16)

$$dD = (-p\ ds.\ \sin\delta)\cos\alpha + (p\ ds\ \cos\delta)\sin\alpha \quad \ldots\ldots\ldots\ldots\ldots\ldots (C.8)$$

$$= -pdy\ .\ \cos\alpha + pdx\ .\ \sin\alpha \quad \ldots\ldots\ldots\ldots\ldots\ldots (C.9)$$

Integration round the aerofoil contour gives the form drag. The coefficient of drag, C_D, is obtained by dividing the drag force by $1/2\rho U_\infty^2 d$.

Then

$$C_D = \frac{\oint dD}{1/2\rho U_\infty^2 d} = \oint \frac{-(p-p_\infty)}{1/2\rho U_\infty^2}\, d(\frac{y}{d})\cos\alpha + \oint \frac{(p-p_\infty)}{1/2\rho U_\infty^2} d(\frac{x}{d})\sin\alpha$$

or

$$C_D = \oint - C_p\ d(\frac{y}{d})\cos\alpha + \oint C_p\ d\ (\frac{x}{d})\sin\alpha \quad \ldots\ldots\ldots\ldots\ldots\ldots (C.10)$$

C.4 The Coefficient of Pitching Moment by Integration of the Pressure Distribution Around the Elliptic Aerofoil:

The pitching moment can be calculated about any point by taking the moments of the lift force and the drag force about that point. Here, the pitching moment about the upstream end of the major axis is calculated by first finding the moments of the lift and the drag forces on the element shown in Fig. 17. Then on integrating this round the contour, the total pitching moment about the leading edge is calculated.

Let dF_x and dF_y be the forces in the element AB as calculated in Section (C.1) and (C.2). x and y are the coordinates of the mid-point of element AB. Then moment of dF_x and dF_y about O' is equal to the moment of the lift and drag force on AB about O'. Thus the pitching moment on the element AB about O' is

$$dM = dF_x.(y-y_o) + dF_y\ .\ x \quad \ldots\ldots\ldots\ldots\ldots\ldots (C.11)$$

The sign convention for the pitching moment is chosen so that a moment which tends to increase the angle of attack is positive. Expressing

dF_x and dF_y in terms of pressure, Equation (C.11) is re-written as

$$dM = (-pds.\sin\delta)(y-y_o) + (pds.\cos\delta).x$$

$$= p\,dy(y-y_0) + pdx.x \quad \text{.......................................(C.12)}$$

The coefficient of moment, C_m is obtained by dividing the total moment by $1/2\ \rho U_\infty^2\ d^2$.

Then

$$C_M = \frac{\oint dM}{1/2\rho U_\infty^2 d^2} = \frac{\oint - (p-p_\infty)\ d\frac{(y-y_0)}{d} \cdot \frac{(y-y_0)}{d}}{1/2\rho U_\infty^2} + \frac{\oint (p-p_\infty)\ \frac{(x)}{d}\ .\ d\frac{(x)}{d}}{1/2\rho U_\infty^2}$$

$$= \oint - C_p d\ (\frac{y-y_0}{d})\ (\frac{y-y_0}{d}) + \oint C_p\ (\frac{x}{d})\ .\ d\ (\frac{x}{d}) \quad \text{.............(C.13)}$$

APPENDIX - D

COMPUTER PROGRAM FOR LAMINAR BOUNDARY LAYER AROUND AN ELLIPTIC AEROFOIL

The computer program for the laminar boundary layer around an elliptic aerofoil is presented here.

```
//AUXLAR JOB '1390,KANBHAT,T=1M','BHATIA'
// EXEC WATFIV,SIZE=1024K
GO.SYSIN DD *
$JOB WATFIV    BHATIA,NOEXT
       DIMENSION X(61),Y(61),PHI(61),XCON(61),YCON(61),DEL(60),
      *ELEN(60),XI(60,60),ETA(60,60),UU(60,60),VU(60,60),UL(60,60),
      *VL(60,60),CONSA(60,60),CONSB(60,60),COEFA(60,60),COEFB(60
      *,60),COEF(60,61),RH(60),GAM(60),GAMMA(61),GAMCON(61),
      *UCIR(60),VCIR(60),RCIR(60),UELL(60),VELL(60),RELL(60),
      *THETA(60),YCIR(60),ERROR(60),Y1US1(61),DAMPF(10)
       DIMENSION THICMU(50),THICML(50),PARAMU(50),PARAML(50)
      *,GAA(4),XR(61),Y1L(61),Y1F(61),GRADC(61),STAGU(50),DSTAGL
      *(50),DUDS(61),DPLAC(50),DPLAL(50),STE(61),GAM4(61),Y1(61)
       COMMON/SPEED/STC,GAMCON,GAM4CO,ROOT
       COMMON/AREA/EH(26),EM(26),EL(26)
       DIMENSION DDDSU(40),DDDSL(40),STC(61),GRADD(61),DSTUP(50),DSTLW
      *(50),CONSLU(50),CONSLL(50),CP(60),CD(60),CMU1(60),CMU2(60),
      *GAM4CO(61),COEFM(60,61),GAM4F(61),RHH(60),CLIFT(60)
       DIMENSION XCONM(60),YCONM(60),ELENM(60),DELM(60)
       DIMENSION SIGCON(60,5),SIG(60),SIGMA(60,5),UT(60),CHK(40),CL(61)
       DIMENSION TUM(50),TLM(50),UN(60),FIRST(61),DP(60)
       INTEGER G,H,R,S,T,U,V,W,IA,IJOB,IZ,IER,CODE
       COMMON/PRESRE/XCON,YCON,CP
C
       REAL COMAT(60,60),WK(3720)
C
       COMPLEX WA(60),ZA(60,60),ZN
C
C      ***********************************************
C       * DISTRIBUTION OF ELEMENTS AROUND AEROFOIL ****
C      **********************************************
C      N=NO. OF ELEMENTS
C      N+1=NO. OF PANEL ENDS
C
C
      PI=4.0*ATAN(1.0)
      N=60
      NN=N+1
      CODE=1
      IF(CODE.EQ.1)GO TO 12
      CALL CORDNT(A,B,C,N)
      GO TO 21
   12 PRINT 5300
 5300 FORMAT('-',45X,'THE COORDINATES ARE GENERATED')
      DO 10 I=1,NN
      PHI(I)=2.0*PI*FLOAT(I-1)/FLOAT(N)
      X(I)=0.5*(1.0+COS(PHI(I)))
      AA=0.5
      BB=AA/6.0
      IF(I.LE.N/2)THEN DO
      Y(I)=BB*SQRT(1.0-((X(I)-0.5)**2/AA**2))+2.0
      ELSE DO
      Y(I)=-BB*SQRT(1.0-((X(I)-0.5)**2/AA**2))+2.0
      END IF
   10 CONTINUE
      PRINT 1,AA/BB
    1 FORMAT('-',20X,'THE FINENESS RATIO OF ELLIPSE',F7.2)
      PRINT 40
   40 FORMAT('-',3X,'N',8X,'X',13X,'Y',13X,'XCON',11X,'YCON',
     *12X,'DELTA',14X,'ELEN',12X,'THETA')
   21 DO 20 J=1,N
      X(NN)=X(1)
      Y(NN)=Y(1)
      XCON(J)=(X(J)+X(J+1))/2.0
```

```
      YCON(J)=(Y(J)+Y(J+1))/2.0
      DEL(J)=ATAN2((Y(J+1)-Y(J)),(X(J+1)-X(J)))
      DEL(J)=DEL(J)*180.0/PI
      IF(DEL(J).LT.0.0) THEN DO
      DEL(J)=360.0+DEL(J)
      END IF
      DEL(J)=PI*DEL(J)/180.0
      ELEN(J)=SQRT((X(J)-X(J+1))**2+(Y(J)-Y(J+1))**2)
      THETA(J)=ATAN2((YCON(J)-2.0),(XCON(J)-0.5))
      THETA(J)=ATAN(TAN(THETA(J))*AA/BB)
      IF(THETA(J).LE.0.0 .AND. J.LE.N/2)THETA(J)=PI+THETA(J)
      IF(THETA(J).GT.0.0 .AND.J.GT.N/2)THETA(J)=PI+THETA(J)
      PRINT 30,J,X(J),Y(J),XCON(J),YCON(J),DEL(J),ELEN(J),
     *THETA(J)
30    FORMAT(' ',1X,I3,1X,6(E14.7,2X),F11.7)
20    CONTINUE
C     CALCULATION OF ANALYTICAL VELOCITIES
      ALPHA=2.00*PI/180.0
      PRINT 1777,ALPHA*180./PI
1777  FORMAT('-',20X,'THE ANGLE OF ATTACK IS=',F5.1)
      DO 160 H=1,N
      UCIR(H)=COS(ALPHA)-COS(ALPHA-2.0*THETA(H))+2.0*SIN(ALPHA)*
     *SIN(THETA(H))
      VCIR(H)=SIN(ALPHA)+SIN(ALPHA-2.0*THETA(H))-2.0*SIN(ALPHA)*
     *COS(THETA(H))
      RCIR(H)=SQRT(UCIR(H)**2+VCIR(H)**2)
      C1=AA**2-BB**2
      RR=(AA+BB)**2
      FACT1=1.0-COS(2.0*THETA(H))*C1/RR
      FACT2=SIN(2.0*THETA(H))*C1/RR
      F1=FACT1/((FACT1)**2+(FACT2)**2)
      F2=-FACT2/((FACT1)**2+(FACT2)**2)
      UELL(H)=UCIR(H)*F1+VCIR(H)*F2
      VELL(H)=-(UCIR(H)*F2-VCIR(H)*F1)
      RELL(H)=SQRT(UELL(H)**2+VELL(H)**2)
      IF(H.LE.N/2)THEN DO
      IF(UELL(H).GE.0.0.AND.VELL(H).LE.0.0)RELL(H)=RELL(H)*(-1)
      IF(UELL(H).GE.0.0.AND.VELL(H).GT.0.0)RELL(H)=RELL(H)*(-1)
      ELSE DO
      IF(UELL(H).LT.0.0.AND.VELL(H).GT.0.0)RELL(H)=-RELL(H)
      END IF
160   CONTINUE
      CALL RHS(ALPHA,DEL,N,RH)
      DO 200 IA=1,N
      COEF(IA,NN)=RH(IA)
200   CONTINUE
      CALL VELOC(XCON,YCON,DEL,ELEN,N,COEF)
      CALL EQN(COEF,GAMMA,N,NN)
      DO 155 IB=1,N
      GAMMA(NN)=-GAMMA(NN-N)
      GAMCON(IB)=(GAMMA(IB)+GAMMA(IB+1))/2.00
      ERROR(IB)=(GAMCON(IB)-RELL(IB))/RELL(IB)*100.0
155   CONTINUE
      PRINT 156
156   FORMAT('-',20X,'THE VELOCITY DISTRIBUTION-PANEL METHI
     *D')
      PRINT 159,(GAMCON(I),I=1,N)
      PRINT 157
157   FORMAT('-',20X,'THE VELOCITY DISTRIBUTION-ANALYTICALLY
     *')
      PRINT 159,(RELL(I),I=1,N)
      PRINT 158
158   FORMAT('-',20X,'THE % ERROR IN VELOCITY DISTRIBUTION')
      PRINT 159,(ERROR(I),I=1,N)
```

```
  159  FORMAT(6(5X,F12.7))
       PRINT 3502
  3502 FORMAT('-',45X,'THE PRESSURE DIST.-INVISCID')
       DO 3503 I=1,N
  3503 CP(I)=1.0-GAMCON(I)**2
       PRINT 159,(CP(I),I=1,N)
C      CALCULATION OF SURFACE SLOPES
C      *****************************
       CALL SLOPE(X,Y,N,NN,XR,Y1L,Y1F,DER1,DER2)
       PRINT 161
  161    FORMAT('-',20X,'THE SURFACE SLOPES AT CONTROL POINTS')
       PRINT 159,(Y1F(I),I=1,N)
C      CALCULATION OF PANEL END DISTANCES FROM TRAILING EDGE')
C      *****************************************************
       CALL SURLEN(X,Y1F,N,XR,Y1L,Y1,STE,DER1,DER2)
       PRINT 162
  162  FORMAT('-',20X,'THE PANEL END DISTANCES FROM TE')
       PRINT 1599,(STE(I),I=1,NN)
  1599 FORMAT(6(5X,F12.7))
       DO 140 J=1,N
       STC(J)=(STE(J+1)+STE(J))/2.0
  140  CONTINUE
       PRINT 141
  141  FORMAT(' ',20X,'THE DISTANCE OF CONTROL POINTS')
       PRINT 1599,(STC(I),I=1,N)
       CALL ANVEGR(ALPHA,NN,DUDS)
       PRINT 163
  163  FORMAT('-',20X,'THE ANALYTICAL VELOCITY GRADIENTS')
       PRINT 159,(DUDS(I),I=1,N)
       Y1US1(1)=(GAMCON(1)-GAMMA(1))/(STC(1)-STE(1))
       Y1US1(60)=(GAMCON(60)-GAMMA(60))/(STC(60)-STE(60))
       CALL CUBICI(60,STC,GAMCON,Y1US1)
       PRINT 1220
  1220 FORMAT('-',20X,'THE VELOCITY GRADIENTS BY CUBIC SPLINE')
       PRINT 1210,(Y1US1(I),I=1,N)
  1210 FORMAT(6(5X,F12.7))
       READ 1440,(EM(I),I=1,26)
       READ 1440,(EH(I),I=1,26)
       READ 1440,(EL(I),I=1,26)
  1440 FORMAT(9(F8.4))
       PRINT 1447
  1447 FORMAT('-',14X,'M',18X,'H',18X,'L')
       DO 1445 LQ=1,26
       PRINT 1446,EM(LQ),EH(LQ),EL(LQ)
  1446 FORMAT(' ',10X,F8.4,10X,F8.4,10X,F8.4)
  1445 CONTINUE
C      ITERATIONS BEGIN HERE FOR BOUNDARY LAYER CALCULATIONS')
C
C
C
C      CALCULATION OF VELOCITY DERIVATIVES BY LAGARANGIAN
       IFLAG=1
       ITER=1
  1510 CALL DERIV(STC,GAMCON,GRADD)
       PRINT 1502
  1502 FORMAT('-',20X,'THE VELOCITY GRADIENTS BY LAGRANGIAN')
       PRINT 1503,(GRADD(I),I=1,60)
  1503 FORMAT(6(5X,F12.7))
       Y1US1(1)=(GAMCON(1)-GAMMA(1))/(STC(1)-STE(1))
       Y1US1(60)=(GAMCON(60)-GAMMA(60))/(STC(60)-STE(60))
       IF(IFLAG.EQ.1)THEN DO
       CALL CUBICI(60,STC,GAMCON,Y1US1)
       PRINT 1220
       PRINT 1210,(Y1US1(I),I=1,N)
```

```
      CALL ZERO(GAMMA,STE,IND,XL1,XLL1,XL,XLL)
      CALL STAGPT(IND,XL,XLL,STE,GAMMA,ROOT)
      PRINT 3509,IND
 3509 FORMAT('-',45X,'THE STAGNATION POINT IS ON PANEL #',I4)
      PRINT 1507,ROOT
 1507 FORMAT(' ',20X,'THE STAGNATION POINT IS AT',F10.7)
      CALL COLIFT(GAMMA,GAMCON,STC,N,CL,STE)
      PRINT 2600
 2600 FORMAT('-',45X,'THE LIFT COEF. FOR INVISCID FLOW')
      PRINT 1980,CL(NN)
 1980 FORMAT('-',20X,'THE COEFFICIENT OF LIFT=',F12.7)
      END IF
      IF(IFLAG.NE.1)THEN DO
      CALL VNOT(GAMCON,STE,IND,ROOT,STC)
      PRINT 3509,IND
      PRINT 1507,ROOT
      END IF
      CALL DISTAG(STE,IND,ROOT,STAGU,DSTAGL,INE)
      PRINT 1381
 1381 FORMAT('-',20X,'THE DISTANCES FROM STAGNATION POINT
     *ON UPPER SURFACE')
      PRINT 1382,(STAGU(I),I=1,IND)
 1382 FORMAT(6(5X,F12.7))
      PRINT 1383
 1383 FORMAT('-',20X,'THE DISTANCES FROM STAGNATION POINT
     *OF NODES')
      PRINT 1382,(DSTAGL(I),I=1,INE)
      CALL DSTNCE(STC,IND,ROOT,DSTUP,DSTLW,LASTUP,LASTDN)
      PRINT 3501,LASTUP,LASTDN
 3501 FORMAT('-',20X,'THE LAST CONTROL PT.UPPER #',I3,2X,'THE LAST
     *CONTROL PT. LOWER #',I3)
      PRINT 1751
 1751 FORMAT('-',20X,'THE CONTROL POINT DISTANCES-UPPER')
      PRINT 1750,(DSTUP(I),I=1,LASTUP)
      PRINT 1752
 1752 FORMAT('-',20X,'THE CONTROL POINT DISTANCES-LOWER')
      PRINT 1750,(DSTLW(I),I=1,LASTDN)
 1750 FORMAT(6(5X,F12.7))
      RE=800.0
      CALL THCKNS(ROOT,GAMCON,RE,DSTUP,DSTLW,LASTUP,LASTDN,LUP,LDN
     *,IND,THICMU,THICML,STC,NSTATU,NSTATL)
      PRINT 1384
 1384 FORMAT('-',20X,'THE MOMENTUM THICKNESS DISTRI.
     *---UPPER SURFACE')
      PRINT 1385,(THICMU(I),I=1,LASTUP)
      PRINT 1386
 1386 FORMAT('-',20X,'THE MOMENTUM THICKNESS DISRRI.
     *---LOWER SURFACE')
      PRINT 1385,(THICML(I),I=1,LASTDN)
 1385 FORMAT(6(5X,F12.7))
      CALL GAUS(ROOT,GAMCON,RE,DSTUP,DSTLW,LASTUP,LASTDN,LUP,LDN
     *,IND,TUM,TLM,STC,NSTATU,NSTATL)
      PRINT 1981
 1981 FORMAT('-',20X,'GAUSSIAN THICKNESS-UPPER')
      PRINT 1385,(TUM(I),I=1,LASTUP)
      PRINT 1982
 1982 FORMAT('-',20X,'GAUSSIAN THICKNESS-LOWER')
      PRINT 1385,(TLM(I),I=1,LASTDN)
      DO 1989 I=1,LUP
      THICMU(I)=TUM(I)
 1989 CONTINUE
      DO 1988 I=1,LDN
      THICML(I)=TLM(I)
 1988 CONTINUE
```

```
      CALL SEPRET(RE,GRADD,THICMU,THICML,LASTUP,LASTDN,PARAMU,
     *PARAML,SEPUP,SEPLOW,VSEPU,VSEPL,DSTUP,DSTLW,ROOT,IND,LSEPU
     *,LSEPL,NSTATU,NSTATL)
      PRINT 1400
 1400 FORMAT('-',20X,'THE PARAMETER M ON UPPER SUR.')
      PRINT 1401,(PARAMU(I),I=1,LSEPU)
      PRINT 1402
 1402 FORMAT('-',20X,'THE PARAMETER M ON LOWER SUR.')
      PRINT 1401,(PARAML(I),I=1,LSEPL)
 1401 FORMAT(6(5X,F12.7))
      PRINT 1403,SEPUP,SEPLOW,VSEPU,VSEPL
 1403 FORMAT('-',20X,F10.7,10X,F10.7//' ',20X,F10.7,10X,
     *F10.7)
      CALL DISPLT(SEPUP,SEPLOW,DSTUP,DSTLW,THICMU,THICML,
     *PARAMU,PARAML,IND,DPLAC,DPLAL,LSEPU,LSEPL,DISPU,DISPL,
     *NUP,NLOW)
      PRINT 1404
 1404 FORMAT('-',20X,'THE DISPLACEMENT THICKNES DIST.
     * ON UPPER SURFACE')
      PRINT 1405,(DPLAC(I),I=1,NUP)
 1405 FORMAT(6(5X,F12.7))
      PRINT 1406
 1406 FORMAT('-',20X,'THE DISPLACEMENT THICKNESS DIST.
     * ON LOWER SURFACE')
      PRINT 1405,(DPLAL(I),I=1,NLOW)
      CALL DISLOP(DSTUP,DSTLW,LSEPU,LSEPL,DPLAC,DPLAL,DISPU,
     *DISPL,DDDSU,DDDSL,DDUP,DDLOW,SEPUP,SEPLOW,NUP,NLOW,CHK)
      PRINT 1979
 1979 FORMAT(' ',20X,'THE DISPLACEMENT SLOPE BY LAGRANGIAN')
      PRINT 1570,(CHK(I),I=2,NUP)
      PRINT 1570,(DDDSU(I),I=1,NUP)
      PRINT 1570,(DDDSL(I),I=1,NLOW)
 1570 FORMAT(6(5X,F12.7))
      PRINT 1575,DDUP,DDLOW
      PRINT 1576,DISPU,DISPL
 1576 FORMAT('-',20X,'THE DIS. TH. AT UPP.',F10.5,2X,'THE DIS.
     * TH. AT LOWER ',F10.5)
 1575 FORMAT('-',20X,'THE DIS. SLOPE AT UPPER SEP.',F10.5,
     *20X,'THE DIS. SLOPE AT LOWER SEP.',F10.5)
      UNRUP=VINT(ROOT-SEPUP)*DDUP
      UNRLOW=VINT(ROOT+SEPLOW)*DDLOW
      PRINT 1560,UNRUP,UNRLOW
 1560 FORMAT('-',20X,'NORMAL VEL. AT UPPER SEP. PT.',F10.5,20X,
     *'NORMAL VEL. AT LOWER SEP PT.',F10.5)
      VELUP=SQRT((VINT(ROOT-SEPUP))**2+UNRUP**2)
      VELLOW=SQRT((VINT(ROOT+SEPLOW))**2+UNRLOW**2)
      PRINT 1550,VELUP,VELLOW
 1550 FORMAT('-',20X,'UPPER SEPARATION VELOCITY',20X,'LOWER
     *SEPARATION VELOCITY'//' ',22X,F12.5,25X,F12.5)
      CALL CDRAG(CP,ALPHA,CLIFT,N,XCON)
      CALL CDRAG2(CP,ALPHA,CD,YCON,N)
      PLIFT=CLIFT(N)*COS(ALPHA)+CD(N)*SIN(ALPHA)
      CODRAG=CLIFT(N)*SIN(ALPHA)-CD(N)*COS(ALPHA)
      PRINT 2365,PLIFT,CODRAG
      CALL SKIN(GAMCON,RE,THICMU,THICML,CONSLU,CONSLL,NUP,NLOW,
     *PARAMU,PARAML,NSTATU,NSTATL)
      PRINT 2360
      PRINT 2361,(CONSLU(I),I=1,NUP)
      PRINT 2362
      PRINT 2361,(CONSLL(I),I=1,NLOW)
      IF((ABS(VELUP)-ABS(VELLOW)).LE.0.01.AND. (ABS(VELLOW)-ABS(VELUP
     *)).LE.0.01)GO TO 1601
      NS=4
      CALL SHIFT(N,NS,XCON,YCON,DEL,ELEN,RH,XCONM,
```

```
     *YCONM,DELM,ELENM,RHH)
      ITER=ITER+1
      CALL VELOC(XCONM,YCONM,DELM,ELENM,N,COEFM)
      DO 1905 IA=1,N
      COEFM(IA,NN)=RHH(IA)
 1905 CONTINUE
      CALL EQN(COEFM,GAM4F,N,NN)
      GAM4F(NN)=-GAM4F(NN-N)
      DO 1910 I=1,NN
      IF(I.GT.(NN-(NS-1)))THEN DO
      GAM4(I+NS-1-N)=GAM4F(I)
      ELSE DO
      GAM4(I+NS-1)=GAM4F(I)
      END IF
 1910 CONTINUE
      PRINT 1605
 1605 FORMAT('-',20X,'THE VEL. DIST. WITH SHIFTED STAGNATION
     * POINT')
      GAM4(NN-N)=GAM4(NN)
      PRINT 1606,(GAM4(I),I=1,NN)
 1606 FORMAT(6(5X,F12.7))
      DO 1660 I=1,N
      GAM4CO(I)=(GAM4(I)+GAM4(I+1))/2.0
 1660 CONTINUE
      PRINT 1661
 1661 FORMAT('-',20X,'THE VELOCITY AT SHIFTED CONTROL POINTS')
      PRINT 1606,(GAM4CO(I),I=1,N)
      VELBUP=VEL(ROOT-SEPUP)
      VELBLW=VEL(ROOT+SEPLOW)
      PRINT 1610,SEPUP,SEPLOW,VELBUP,VELBLW
 1610 FORMAT('-',20X,F10.7,10X,F10.7//' ',20X,F10.7,10X,F10.7)
      AAA=1.0+((VELUP-VELLOW)/(VELBLW-ABS(VELBUP)))
      AAA=1.0/AAA
      PRINT 1915,AAA
 1915 FORMAT('-',20X,'THE ORIGINAL SOLN. *',F12.7)
      DO 1500 KY=1,N
      GAMCON(KY)=GAMCON(KY)*AAA+GAM4CO(KY)*(1.0-AAA)
 1500 CONTINUE
      IF(IFLAG.EQ.1)THEN DO
      DO 2000 KP=1,NN
      GAMMA(KP)=GAMMA(KP)*AAA+GAM4(KP)*(1.0-AAA)
 2000 CONTINUE
      END IF
      DO 5200 I=1,N
      CP(I)=1.0-GAMCON(I)**2
 5200 CONTINUE
      IF(IFLAG.EQ.1)THEN DO
      PRINT 1990
 1990 FORMAT('-',20X,'THE MODIFIED PANEL SOLUTION')
      PRINT 1606,(GAMMA(I),I=1,NN)
      END IF
      PRINT 1501
 1501 FORMAT('-',20X,'THE MODIFIED POTENTIAL FLOW')
      PRINT 1509,(GAMCON(I),I=1,N)
 1509 FORMAT(10(2X,F10.7))
      IF(IFLAG.EQ.1)THEN DO
      CALL COLIFT(GAMMA,GAMCON,STC,N,CL,STE)
      PRINT 2601
 2601 FORMAT('-',45X,'THE LIFT COEFF. AFTER CIRCULATION CHANGE')
      PRINT 1980,CL(NN)
      END IF
      GO TO 1510
C     SURFACE SOURCE DISTRIBUTION
 1601 PRINT 1602,ITER
```

```
 1602 FORMAT('-',20X,'NO. OF ITERATIONS TO EQUALISE
     * VELOCITIES AT SEPARATION POINT=',I3)
      IF(IFLAG.EQ.1) THEN DO
      CALL COLIFT(GAMMA,GAMCON,STC,N,CL,STE)
      PRINT 4440,CL(NN)
 4440 FORMAT('-',20X,'THE CL AFTER EQUAL VELOCITIES',F12.7)
      END IF
      IF(VELLOW.GT.VELUP) THEN DO
      QSEP=VELLOW
      ELSE DO
      QSEP=VELUP
      END IF
      KOD=1
      CALL SOURCE(XCON,YCON,DEL,ELEN,QSEP,LSEPU,LSEPL,NSTATU,NSTATL,
     *SIG,SIGMA,N,NN,GAMCON,DDDSU,DDDSL,UT,UN,IT,KOD)
      PRINT 1950
 1950 FORMAT(' ',20X,'THE TANGENTIAL VELOCITIES BY SOURCES')
      PRINT 1951,(UT(I),I=1,N)
 1951 FORMAT(10(2X,F10.7))
      PRINT 1952
 1952 FORMAT(' ',20X,'THE FIRST APPROX. OF SOURCE STRENGTHS AT PANEL')
      PRINT 1951,(SIG(I),I=1,N)
      PRINT 1953,IT
      IF(KOD.EQ.1)GO TO 1600
      DO 2100 K=1,IT
      PRINT 1951,(SIGMA(I,IT),I=1,N)
 2100 CONTINUE
      PRINT 1983
 1983 FORMAT('-',20X,'THE NORMAL VELOCITIES DUE TO SOURCES')
      PRINT 1951,(UN(I),I=1,N)
      DO 2300 I=1,N
      GAMCON(I)=GAMCON(I)+UT(I)
 2300 CONTINUE
      IF(IFLAG.EQ.1) THEN DO
      PRINT 2603
 2603 FORMAT('-',45X,'THE LIFT COEFF.AFTER SOURCE DISTRIBUTION')
      CALL COLIFT(GAMMA,GAMCON,STC,N,CL,STE)
      PRINT 1980,CL(NN)
      END IF
C
      CALL TEST(ROOT,FI,PRESNT)
      PRINT 1900,FI,PRESNT
 1900 FORMAT('-',20X,'THE INTEGRAL=',F10.7,2X,'AND',F10.7)
C
 1953 FORMAT('-',20X,'THE NO. OF ITERATIONS FOR SOURCES=',I3)
      CALL SKIN(GAMCON,RE,THICMU,THICML,CONSLU,CONSLL,NUP,NLOW,PARAMU,
     *PARAML,NSTATU,NSTATL)
      PRINT 2360
 2360 FORMAT('-',45X,'THE SKIN FRICTION-UPPER SURFACE')
      PRINT 2361,(CONSLU(I),I=1,NUP)
 2361 FORMAT(10(2X,F10.7))
      PRINT 2362
 2362 FORMAT('-',45X,'THE SKIN FRICTION-LOWER SURFACE')
      PRINT 2361,(CONSLL(I),I=1,NLOW)
      DO 2700 I=1,N
      CP(I)=1.0-(GAMCON(I)**2+UN(I)**2)
 2700 CONTINUE
      PRINT 2363
 2363 FORMAT('-',45X,'THE PRESSURE COEFF. DIST.AT CONTROL POINTS')
      PRINT 2361,(CP(I),I=1,N)
      CALL CDRAG(CP,ALPHA,CLIFT,N,XCON)
      CALL CDRAG2(CP,ALPHA,CD,YCON,N)
      PLIFT=CLIFT(N)*COS(ALPHA)+CD(N)*SIN(ALPHA)
      CODRAG=CLIFT(N)*SIN(ALPHA)-CD(N)*COS(ALPHA)
```

```
      PRINT 2365,PLIFT,CODRAG
 2365 FORMAT('-',20X,'THE LIFT COEFF. BY PRESSURE DIST.=',F12.7,2X,
     *'THE DRAG COEFF.=',F12.7)
      CALL CM1(XCON,N,CP,CMU1)
      IA=2
      IB=30
      CALL CM2(IA,IB,CP,YCON,CMU2)
      IA=31
      IB=59
      CALL CM2(IA,IB,CP,YCON,CMU2)
      CMOMNT=-CMU1(N)-CMU2(30)+CMU2(59)
      PRINT 2370,CMOMNT
 2370 FORMAT('-',45X,'THE MOMENT COEFF. ABOUT THE LEADING ED.',F12.7)
      CALL DERIV(STC,GAMCON,GRADD)
      PRINT 1502
      PRINT 1503,(GRADD(I),I=1,60)
      CALL VNOT(GAMCON,STE,IND,ROOT,STC)
      PRINT 3509,IND
      PRINT 1507,ROOT
      CALL DSTNCE(STC,IND,ROOT,DSTUP,DSTLW,LASTUP,LASTDN)
      PRINT 3501,LASTUP,LASTDN
      PRINT 1751
      PRINT 1750,(DSTUP(I),I=1,LASTUP)
      PRINT 1752
      PRINT 1750,(DSTLW(I),I=1,LASTDN)
      CALL THCKNS(ROOT,GAMCON,RE,DSTUP,DSTLW,LASTUP,LASTDN,LUP,LDN,IND
     *,THICMU,THICML,STC,NSTATU,NSTATL)
      PRINT 1384
      PRINT 1385,(THICMU(I),I=1,LASTUP)
      PRINT 1386
      PRINT 1385,(THICML(I),I=1,LASTDN)
      CALL SEPRET(RE,GRADD,THICMU,THICML,LASTUP,LASTDN,PARAMU,PARAML,
     *SEPUP,SEPLOW,VSEPU,VSEPL,DSTUP,DSTLW,ROOT,IND,LSEPU,LSEPL,
     *NSTATU,NSTATL)
      PRINT 1400
      PRINT 1401,(PARAMU(I),I=1,LSEPU)
      PRINT 1402
      PRINT 1401,(PARAML(I),I=1,LSEPL)
      PRINT 1403,SEPUP,SEPLOW,VSEPU,VSEPL
      CALL DISPLT(SEPUP,SEPLOW,DSTUP,DSTLW,THICMU,THICML,PARAMU,
     *PARAML,IND,DPLAC,DPLAL,LSEPU,LSEPL,DISPU,DISPL,NUP,NLOW)
      PRINT 1404
      PRINT 1405,(DPLAC(I),I=1,NUP)
      PRINT 1406
      PRINT 1405,(DPLAL(I),I=1,NLOW)
      CALL DISLOP(DSTUP,DSTLW,LSEPU,LSEPL,DPLAC,DPLAL,DISPU,DISPL,
     *DDDSU,DDDSL,DDUP,DDLOW,SEPUP,SEPLOW,NUP,NLOW,CHK)
      PRINT 1570,(DDDSU(I),I=1,NUP)
      PRINT 1570,(DDDSL(I),I=1,NLOW)
      PRINT 1575,DDUP,DDLOW
      PRINT 1576,DISPU,DISPL
      UNRUP=VINT(ROOT-SEPUP)*DDUP
      UNRLOW=VINT(ROOT+SEPUP)*DDLOW
      PRINT 1560,UNRUP,UNRLOW
      VELUP=SQRT((VINT(ROOT-SEPUP))**2+UNRUP**2)
      VELLOW=SQRT((VINT(ROOT+SEPLOW))**2+UNRLOW**2)
      PRINT 1550,VELUP,VELLOW
      IF((ABS(VELUP)-ABS(VELLOW)).LE.0.01.AND.(ABS(VELLOW)-ABS(VELUP
     *)).LE.0.01)GO TO 1600
      IFLAG=IFLAG+1
      GO TO 1510
C
C
C
```

```
C
C
C
C
C
C
C
C
C
C
C
C
C
C
 1600 STOP
          END
      SUBROUTINE CORDNT(A,B,C,N)
      PRINT 1
 1    FORMAT('-',20X,'THE CORDINATES MISSING')
      RETURN
      END
       SUBROUTINE RHS(ALPHA,DEL,N,RH)
      DIMENSION DEL(N),RH(N)
      DO 1 I=1,N
      RH(I)=-(COS(DEL(I))*SIN(ALPHA)-SIN(DEL(I))*COS(ALPHA))
 1    CONTINUE
      RETURN
      END
      SUBROUTINE TEST(ROOT,FI,PRESNT)
      N=10
      FN=N
      A=0.0050573
      B=0.0162640
      DX=(B-A)/FN
      FI1=FS(ROOT-A)+FS(ROOT-B)
      FI2=0.0
      FI3=0.0
      TDX=2.0*DX
      X=A+DX
      NN=N/2
      DO 3 J=1,NN
      FI2=FI2+FS(ROOT-X)
  3   X=X+TDX
      X=A
      NM=NN-1
      DO 4 J=1,NM
      X=X+TDX
 4    FI3=FI3+FS(ROOT-X)
      FI=DX*(FI1+4.*FI2+2.*FI3)/3.
      A=0.0
      B=.0050573
      DX=(B-A)/FN
      TDX=2.*DX
      FI1=FS(ROOT-A)+FS(ROOT-B)
      FI2=0.0
      FI3=0.0
      NN=N/2
      X=A+DX
      DO 8 J=1,NN
      FI2=FI2+FS(ROOT-X)
  8   X=X+TDX
      X=A
      NM=NN-1
      DO 9 J=1,NM
```

```
      X=X+TDX
    9 FI3=FI3+FS(ROOT-X)
      FI=DX*(FI1+4.*FI2+2.*FI3)/3.0
      PRESNT=FI
      RETURN
      END
C
C
      SUBROUTINE EQN(A,X,N,NN)
      DIMENSION A(N,NN),X(N)
      M=N+1
      L=N-1
      DO 12 K=1,L
      JJ=K
      BIG=ABS(A(K,K))
      KPI=K+1
C     SEARCH FOR LARGEST PIVOT ELEMENT
      DO 7 I=KPI,N
      AB=ABS(A(I,K))
      IF(BIG-AB)6,7,7
    6 BIG=AB
      JJ=I
    7 CONTINUE
C     DECISION OF NECESSITY OF ROW INTERCHANGE
      IF(JJ-K)8,10,8
C     ROW INTERCHANGE
    8 DO 9 J=K,M
      TEMP=A(JJ,J)
      A(JJ,J)=A(K,J)
    9 A(K,J)=TEMP
   10 DO 11 I=KPI,N
      QUOT=A(I,K)/A(K,K)
      DO 11 J=KPI,M
   11 A(I,J)=A(I,J)-QUOT*A(K,J)
      DO 12 I=KPI,N
   12 A(I,K)=0.0
C     FIRST STEP IN BACK SUBSTITUTION PROCESS
      X(N)=A(N,M)/A(N,N)
C     REMAINDER OF BACK SUBSTITUTION PROCESS
      DO 14 MM=1,L
      SUM=0.0
      I=N-MM
      IPI=I+1
      DO 13 J=IPI,N
   13 SUM=SUM+A(I,J)*X(J)
   14 X(I)=(A(I,M)-SUM)/A(I,I)
      RETURN
      END
      SUBROUTINE CUBICI(N,X,Y,Y11)
      DIMENSION X(61),Y(61),F(61),G(61),Y11(61),Y1(61)
      N1=N-1
      G(1)=0.0
      F(1)=0.0
      DO 2 K=1,N1
      J2=K+1
      H2=1.0/(X(J2)-X(K))
      R2=3.*H2*H2*(Y(J2)-Y(K))
      IF(K.EQ.1)GO TO 1
      Z=1.0/(2.0*(H1+H2)-H1*G(J1))
      G(K)=Z*H2
      H=R1+R2
      IF( K.EQ.2)H=H-H1*Y11(1)
      IF(K.EQ.N1)H=H-H2*Y11(N)
      F(K)=Z*(H-H1*F(J1))
```

```
    1      J1=K
           H1=H2
           R1=R2
    2      CONTINUE
           Y11(N1)=F(N1)
           IF(N1.LE.2) RETURN
           N2=N1-1
           DO 3 J1=2,N2
           K=N-J1
           Y11(K)=F(K)-G(K)*Y11(K+1)
    3      CONTINUE
           RETURN
           END
C
C
           FUNCTION VINT(SREQD)
           COMMON /SPEED/STC,GAMCON,GAM4CO,ROOT
           DIMENSION STC(61),GAMCON(61),GAM4CO(61)
           DO 1 I=1,60
           IF(STC(I).LT.SREQD) GO TO 1
           IF(I.EQ.1) GO TO 9
           IF(GAMCON(I-1).LT.0.0.AND.GAMCON(I).GT.0.0) GO TO 11
           VINT=((GAMCON(I)-GAMCON(I-1))/(STC(I)-STC(I-1)))*(SREQD-
     *STC(I-1))+GAMCON(I-1)
           GO TO 7
     1     CONTINUE
     9     VINT=((GAMCON(1)-0.0)/(STC(1)-0.0))*SREQD
           GO TO 7
    11     L=I
           IF(SREQD.GT.ROOT) THEN DO
           VINT=((GAMCON(L)-0.0)/(STC(L)-ROOT))*(SREQD-ROOT)
           ELSE DO
           VINT=((0.0-GAMCON(L-1))/(ROOT-STC(L-1)))*(SREQD-STC(L-1))+
     *GAMCON(L-1)
           END IF
     7     RETURN
           END
C
C
           FUNCTION FS(CLEN)
           COMMON/SPEED/STC,GAMCON,GAM4CO,ROOT
           REAL FS,CLEN
           DIMENSION STC(61),GAMCON(61),VEL5(61),GAM4CO(61)
           DO 2 J=1,60
           VEL5(J)=GAMCON(J)
     2     CONTINUE
           DO 1 I=1,60
           IF(STC(I).LT.CLEN) GO TO 1
           IF(I.EQ.1) GO TO 9
           IF(VEL5(I-1).LT.0.0.AND.VEL5(I).GT.0.0) GO TO 11
           FS=((VEL5(I)-VEL5(I-1))/(STC(I)-STC(I-1)))*(CLEN-STC(I-1))
     *+VEL5(I-1)
           FS=FS**5
           GO TO 7
     1     CONTINUE
     9     FS=((VEL5(1)-0.0)/(STC(1)-0.0))*CLEN
           FS=FS**5
           GO TO 7
    11     L=I
           IF(CLEN .EQ.ROOT) FS=0.0
           IF(CLEN.GT.ROOT) THEN DO
           FS=((GAMCON(L)-0.0)/(STC(L)-ROOT))*(CLEN-ROOT)
           FS=FS**5
           ELSE DO
```

```
      FS=((0.0-GAMCON(L-1))/(ROOT-STC(L-1)))*(CLEN-STC(L-1))+GAMCON(
     *L-1)
      FS=FS**5
      END IF
  7   RETURN
      END
C
C
C
C
      SUBROUTINE FINDRO(A,N,X1,X2,X,ACC)
      DIMENSION A(3)
      J=1
  1   X=X2
  2   Z=A(1)
      DO 3 I=1,N
  3   Z=Z*X+A(I+1)
      GO TO (4,5),J
  4   X=X1
      J=2
      Y=Z
      GO TO 2
  5   IF(ABS(X2-X)-ACC*ABS(X))10,10,6
  6   IF(Y*Z)7,10,8
  7   X1=X
      GO TO 9
  8   X2=X
  9   X=(X1+X2)/2.0
      GO TO 2
 10   RETURN
      END
C
      SUBROUTINE VNOT(GAMCON,STE,IND,ROOT,STC)
      DIMENSION GAMCON(61),STE(61),STC(61)
      DO 1 I=3,59
      IF(GAMCON(I).LT.0.0.AND.GAMCON(I+1).LT.0.0)GO TO 1
      IF(GAMCON(I).GT.0.0.AND.GAMCON(I+1).GT.0.0)GO TO 1
      ROOT=STC(I)+((STC(I+1)-STC(I))/(GAMCON(I+1)-GAMCON(I)))*
     *(-GAMCON(I))
      IF(ROOT.GT.STE(I+1))THEN DO
      IND=I+1
      ELSE DO
      IND=I
      END IF
    1 CONTINUE
      RETURN
      END
C
C
      FUNCTION HPAM(EMREQ)
      COMMON /AREA/EH(26),EM(26),EL(26)
      IF(EMREQ.GT.EM(26).OR.EMREQ.LT.EM(1)) GO TO 6
      DO 1 I=1,25
      IF((EMREQ-EM(I))*(EMREQ-EM(I+1)).LT.0.0)GO TO 2
  1   CONTINUE
  2   HPAM=(EH(I+1)-EH(I))/(EM(I+1)-EM(I))*(EMREQ-EM(I))+EH(I)
      GO TO 7
  6   PRINT 8,EMREQ
  8   FORMAT('-',20X,'M=',F12.7,1X,'IS OUT OF RANGE')
  7   RETURN
      END
C
C
C
```

```
            SUBROUTINE VELOC(XCON,YCON,DEL,ELEN,N,COEF)
      INTEGER R,S,U,V
      DIMENSION XI(60,60),ETA(60,60),COEFA(60,60),COEFB(60,60),
     *COEF(60,61),XCON(60),YCON(60),DEL(60),ELEN(60),
     *UU(60,60),VU(60,60),UL(60,60),VL(60,60),CONSA(60,60),
     *CONSB(60,60)
C
      PI=4.0*ATAN(1.0)
      DO 50 K=1,N
      DO 60 L=1,N
      IF(K.EQ.L)GO TO 70
      XI(K,L)=(XCON(K)-XCON(L))*COS(DEL(L))+(YCON(K)-YCON(
     *L))*SIN(DEL(L))
      ETA(K,L)=(YCON(K)-YCON(L))*COS(DEL(L))-(XCON(K)-XCON(
     *L))*SIN(DEL(L))
      A=XI(K,L)+0.5*ELEN(L)
      B=XI(K,L)-0.5*ELEN(L)
      C=ETA(K,L)
      PHI1=ATAN(ETA(K,L)/(XI(K,L)+0.5*ELEN(L)))
      IF(PHI1.LE.0.00) PHI1=PHI1+PI
      PHI2=ATAN(ETA(K,L)/(XI(K,L)-0.5*ELEN(L)))
      IF(PHI2.LE.0.0)PHI2=PI+PHI2
      UU(K,L)=(PHI1-PHI2)/(2.0*PI)
      VU(K,L)=ALOG(SQRT((A**2+C**2)/(B**2+C**2)))/(2.*PI
     *)
      UL(K,L)=(A*(PHI1-PHI2)-C*ALOG(SQRT((B**2+C**2)/(A**2
     *+C**2))))/(2.0*PI*ELEN(L))
      VL(K,L)=(-A*ALOG(SQRT((B**2+C**2)/(A**2+C**2)))-ELEN
     *(L)-ETA(K,L)*(PHI1-PHI2))/(2.0*PI*ELEN(L))
      CONSA(K,L)=UU(K,L)-UL(K,L)
      CONSB(K,L)=VU(K,L)-VL(K,L)
      COEFA(K,L)=CONSA(K,L)*SIN(DEL(L))*COS(DEL(K))+CONSB(K
     *,L)*COS(DEL(L))*COS(DEL(K))-CONSA(K,L)*COS(DEL(L))*SI
     *N(DEL(K))+CONSB(K,L)*SIN(DEL(L))*SIN(DEL(K))
      COEFB(K,L)=UL(K,L)*SIN(DEL(L))*COS(DEL(K))+VL(K,L)*CO
     *S(DEL(L))*COS(DEL(K))-UL(K,L)*COS(DEL(L))*SIN(DEL(K))+
     *VL(K,L)*SIN(DEL(L))*SIN(DEL(K))
      GO TO 60
   70 COEFA(K,L)=1.0/(2.0*PI)
      COEFB(K,L)=-1.0/(2.0*PI)
   60 CONTINUE
   50 CONTINUE
      DO 80 U=1,N
      DO 90 V=2,N
      COEF(U,V)=COEFA(U,V)+COEFB(U,V-1)
   90 CONTINUE
   80 CONTINUE
      S=1
      DO 100 R=1,N
      COEF(R,S)=COEFA(R,S)-COEFB(R,N)
  100 CONTINUE
      RETURN
      END
C
C
C
C
      SUBROUTINE SUBLEN(X,Y1F,N,XR,Y1L,Y1,STE,DER1,DER2)
      DIMENSION X(61),Y1F(61),STE(61),S1(61),XR(61),Y1L(61)
     *,Y1(61)
      DO 900 IN=1,29
      XINT=(X(IN+1)-X(IN))/9.0
      DINT=(Y1F(IN+1)-Y1F(IN))/8.0
      SUM=0.0
```

```
      DO 910 IP=1,9
      TERM=Y1F(IN)+(IP-1)*DINT
      TERM=SQRT(1.0+TERM**2)
      IF(XINT.LT.0.0) XINT=-XINT
      FACTOR=TERM*XINT
      SUM=SUM+FACTOR
      S1(IN)=SUM
  910 CONTINUE
  900 CONTINUE
      XINT1=(XR(2)-XR(1))/9.0
       DINT1=(DER2-DER1)/8.0
      IF(XINT1.LT.0.0) XINT1=-XINT1
      SUMA=0.0
      DO 920 JK=1,9
      TERM=DER1+(JK-1)*DINT1
      TERM=SQRT(1.0+TERM**2)
      FACTOR=TERM*XINT1
      SUMA=SUMA+FACTOR
  920 CONTINUE
      S1(1)=SUMA
      S1(30)=SUMA
      S1(31)=SUMA
      S1(60)=SUMA
      STE(1)=0.0
      DO 700 M=1,28
      S1(31+M)=S1(30-M)
  700 CONTINUE
      DO 1145 JB=2,61
      STE(JB)=STE(JB-1)+S1(JB-1)
 1145 CONTINUE
      RETURN
      END
C
C
C
      SUBROUTINE SLOPE(X,Y,N,NN,XR,Y1L,Y1F,DER1,DER2)
      DIMENSION X(61),Y(61),Y1F(61),Y1(61),XR(61),YR(61),
     *Y1M(61),
     *XC(61),YC(61),XP(61),YP(61),XF(61),YF(61),Y1L(61),Y1F1(61)
      PI=4.0*ATAN(1.0)
      IA=N/2-1
      DO 640 JJ=1,IA
      XC(JJ)=X(JJ+1)
      YC(JJ)=Y(JJ+1)
  640 CONTINUE
      Y1(1)=-2.38
      Y1(IA)=2.38
      CALL CUBICI(IA,XC,YC,Y1)
      BETA=-30.*PI/180.0
      XO=1.0
      YO=2.0
      DO 710 L=1,16
      XR(L)=(X(L)-XO)*COS(BETA)+(Y(L)-YO)*SIN(BETA)+XO
      YR(L)=(Y(L)-YO)*COS(BETA)-(X(L)-XO)*SIN(BETA)+YO
  710 CONTINUE
      Y1L(1)=-1.7320508
      Y1L(16)=-TAN(ATAN(Y1(15))+BETA)
      CALL CUBICI(16,XR,YR,Y1L)
      DER=ABS(Y1L(1)-Y1L(2))
      DO 740 M=1,16
      Y1L(M)=TAN(ATAN(Y1L(M))+BETA)
  740 CONTINUE
      BETA=30.0*PI/180.0
      XO=0.0
```

```
      YO=2.0
      DO 700 J=16,31
      XR(J)=(X(J)-XO)*COS(BETA)+(Y(J)-YO)*SIN(BETA)+XO
      YR(J)=(Y(J)-YO)*COS(BETA)-(X(J)-XO)*SIN(BETA)+YO
  700 CONTINUE
      DO 750 MM=1,16
      XP(MM)=XR(32-MM)
      YP(MM)=YR(32-MM)
  750 CONTINUE
      Y1M(1)=1.7320508
      Y1M(16)=TAN(ATAN(Y1(15))-BETA)
      CALL CUBICI(16,XP,YP,Y1M)
      DER1=Y1M(1)
      DER2=Y1M(2)
      DO 70 KJ=1,16
      Y1M(KJ)=TAN(ATAN(Y1M(KJ))+BETA)
   70 CONTINUE
      Y1F1(1)=Y1L(2)
      Y1F1(29)=Y1M(2)
      DO 760 MN=1,29
      XF(MN)=X(MN+1)
      YF(MN)=Y(MN+1)
  760 CONTINUE
      CALL CUBICI(29,XF,YF,Y1F1)
      DO 780 MP=1,29
      Y1F(MP+1)=Y1F1(MP)
  780 CONTINUE
      DO 770 MQ=2,30
      Y1F(62-MQ)=-Y1F(MQ)
  770 CONTINUE
      PI=ATAN(1.0)*4.0
      Y1F(1)=TAN(PI/2.)
      Y1F(31)=TAN(PI/2.)
      Y1F(61)=TAN(PI/2.)
      RETURN
      END
C
C
      SUBROUTINE STAGPT(IND,XI,XLL,STE,GAMMA,ROOT)
      DIMENSION STE(61),GAMMA(61),POL(3)
      DUMRUT=((STE(IND+1)-STE(IND))/(GAMMA(IND+1)-GAMMA(IND)
     *)*(-GAMMA(IND)))+STE(IND)
      DIST1=DUMRUT-STE(IND)
      DIST2=STE(IND+1)-DUMRUT
      IF(DIST1.LT.DIST2) GO TO 1368
      NUM=IND+1
      GO TO 1369
 1368 NUM=IND
 1369 CC1=GAMMA(NUM-1)/((STE(NUM-1)-STE(NUM))*(STE(NUM-1)
     *-STE(NUM+1)))
      CC2=GAMMA(NUM)/((STE(NUM)-STE(NUM-1))*(STE(NUM)
     *-STE(NUM+1)))
      CC3=GAMMA(NUM+1)/((STE(NUM+1)-STE(NUM))*(STE(NUM+1)
     *-STE(NUM-1)))
      POL(1)=CC1+CC2+CC3
      POL(2)=-(CC1*(STE(NUM+1)+STE(NUM))+CC2*(STE(NUM-1)+
     *STE(NUM+1))+CC3*(STE(NUM-1)+STE(NUM)))
      POL(3)=(CC1*STE(NUM)*STE(NUM+1))+(CC2*STE(NUM-1)*STE
     *(NUM+1))+(CC3*STE(NUM)*STE(NUM-1))
      ACC=0.000001
      CALL FINDRO(POL,2,XI,XLL,ROOT,ACC)
      ROOT=DUMRUT
      IF(ABS(DUMRUT-ROOT).GT. 0.01)GO TO 1375
      RETURN
```

```
1375 PRINT 1376
1376 FORMAT('-',5X,'THE DIFFERENSE BETWEEN LINEAR & POLY
    *NOMIAL IS LARGE')
     RETURN
     END
C
C
C
     SUBROUTINE ZERO(GAMMA,STE,IND,XL1,XLL1,XL,XLL)
     DIMENSION GAMMA(61),STE(61)
     DO 1365 IQ=1,60
     IF(GAMMA(IQ).LT.0.0.AND.GAMMA(IQ+1) .LT.0.0)GO TO 1365
     IF(GAMMA(IQ).GT.0.0.AND.GAMMA(IQ+1).GT.0.0)GO TO 1365
     IND=IQ
     XL=STE(IQ)
     XLL=STE(IQ+1)
     IF(IQ.LT.15)GO TO 1364
     GO TO 1367
1364 XL1=XL
     XLL1=XLL
     PRINT 1352,XL1,XLL1
1352 FORMAT('-',20X,'THE FIRST STAGNATION POINT IS BETWEEN
    *---',F10.7,' -AND-',F10.7)
1365 CONTINUE
1367 PRINT 1366,XL,XLL
1366 FORMAT('-',20X,'THE FRONT STAGNATION POINT LIES
    *BETWEEN',F10.7,'-AND-',F10.7)
     RETURN
     END
C
     SUBROUTINE DERIV(STE,GAMMA,GRADC)
     DIMENSION STE(60),GAMMA(60),GRADC(60)
     DO 1501 KG=1,58
     CC1=GAMMA(KG)/((STE(KG)-STE(KG+1))*(STE(KG)-STE(KG+2)
    *))
     CC2=GAMMA(KG+1)/((STE(KG+1)-STE(KG))*(STE(KG+1)-STE
    *(KG+2)))
     CC3=GAMMA(KG+2)/((STE(KG+2)-STE(KG))*(STE(KG+2)-STE
    *(KG+1)))
     GRADC(KG+1)=CC1*(2.*STE(KG+1)-STE(KG+2)-STE(KG+1))+CC2
    **(2.*STE(KG+1)-STE(KG)-STE(KG+2))+CC3*(2.*STE(KG+1)-
    *STE(KG+1)-STE(KG))
1501 CONTINUE
     CC1=GAMMA(1)/((STE(1)-STE(2))*(STE(1)-STE(3)))
     CC2=GAMMA(2)/((STE(2)-STE(1))*(STE(2)-STE(3)))
     CC3=GAMMA(3)/((STE(3)-STE(1))*(STE(3)-STE(2)))
     GRADC(1)=CC1*(2.*STE(1)-STE(3)-STE(2))+CC2*(2.*STE(1)-
    *STE(1)-STE(3))+CC3*(2.*STE(1)-STE(1)-STE(2))
     CC1=GAMMA(58)/((STE(58)-STE(59))*(STE(58)-STE(60)))
     CC2=GAMMA(59)/((STE(59)-STE(58))*(STE(59)-STE(60)))
     CC3=GAMMA(60)/((STE(60)-STE(58))*(STE(60)-STE(59)))
     GRADC(60)=CC1*(2.*STE(60)-STE(59)-STE(60))+CC2*(2.*STE(
    *60)-STE(58)-STE(60))+CC3*(2.*STE(60)-STE(58)-STE(59))
     RETURN
     END
C
C
C
     SUBROUTINE DISTAG(STE,IND,ROOT,STAGU,DSTAGL,INE)
     DIMENSION STE(61),STAGU(50),DSTAGL(50)
     DO 1380 IT=1,IND
     STAGU(IT)=ROOT-STE(IND+1-IT)
1380 CONTINUE
     INE=61-IND
```

```
      DO 1460 LR=1,INE
      DSTAGL(LR)=STE(IND+LR)-ROOT
 1460 CONTINUE
      RETURN
      END
C
C
C
      FUNCTION VEL(DIST)
      COMMON/SPEED /STC,GAMCON,GAM4CO,ROOT
      DIMENSION STC(61),GAM4CO(61),GAMCON(61)
      DO 1 I=1,59
      IF(STC(I).LT.DIST)GO TO 1
      DUM=STC(I)-DIST
      IF(DUM.EQ.0.0) GO TO 4
      BUM=DIST-STC(I-1)
      IF(BUM.EQ.0.0)GO TO 5
      IF(DUM.GT.BUM)GO TO 2
      K=I
      GO TO 3
    2 K=I-1
    3 VEL =((DIST-STC(K))*(DIST-STC(K+1))/((STC(K-1)-
     *STC(K))*(STC(K-1)-STC(K+1))))*GAM4CO(K-1)+(((DIS
     *T-STC(K-1))*(DIST-STC(K+1)))/((STC(K)-STC(K-1))*
     *(STC(K)-STC(K+1))))*GAM4CO(K)+(((DIST-STC(K-1))*
     *(DIST-STC(K)))/((STC(K+1)-STC(K-1))*(STC(K+1)-
     *STC(K))))*GAM4CO(K+1)
      GO TO 7
    1 CONTINUE
    4 VEL =GAM4CO(I)
      GO TO 7
    5 VEL =GAM4CO(I-1)
    7 RETURN
      END
      SUBROUTINE THCKNS(ROOT,GAMCON,RE,DSTUP,DSTLW,LASTUP,LASTDN,
     *LUP,LDN,IND,THICMU,THICML,STC,NSTATU,NSTATL)
      DIMENSION GAMCON(61),DSTUP(50),DSTLW(50),THICMU(50),THICML(50)
     *,STC(61)
      D1=STC(IND)-ROOT
      C1=GAMCON(IND-1)/((STC(IND-1)-STC(IND))*(STC(IND-1)-
     *STC(IND+1)))
       C2=GAMCON(IND)/((STC(IND)-STC(IND-1))*(STC(IND)-STC(IND
     *+1)))
      C3=GAMCON(IND+1)/((STC(IND+1)-STC(IND-1))*(STC(IND+1)-
     *STC(IND)))
      DVDS1=C1*(2.*ROOT-STC(IND)-STC(IND+1))+C2*(2.*ROOT-STC(IND-1)
     *-STC(IND+1))+C3*(2.*ROOT-STC(IND-1)-STC(IND))
      IF(D1.GT.0.0)GO TO 1
      THICMU(1)=(0.075/RE)*(1./DVDS1)
      THICML(1)=(0.075/RE)*(1./DVDS1)
      NSTATU=IND
      NSTATL=IND+1
      GO TO 2
    1 THICMU(1)=(0.075/RE)*(1./DVDS1)
      THICML(1)=(0.075/RE)*(1./DVDS1)
      NSTATU=IND-1
      NSTATL=IND
    2 LUP=LASTUP-1
      IF(D1.GT.0.0)THEN DO
      SINT=(ROOT-STC(IND-1))/10.
      UINT=(0.0-GAMCON(IND-1))/10.
      U=UINT
      SUM=0.0
      DO 50 I=1,9
```

```
      F=(U**5)*2.0
      SUM=SUM+F
      U=U+UINT
   50 CONTINUE
      SUM=SUM+(UINT*10.)**5
      THICMU(2)=0.5*SUM*SINT*0.45/(RE*(GAMCON(IND-1)**6))+THICMU(1)
      SINTL=(STC(IND)-ROOT)/10.0
      UINTL=(GAMCON(IND)-0.0)/10.0
      U=UINTL
      SUM=0.0
      DO 30 I=1,9
      F=(U**5)*2.0
      SUM=SUM+F
      U=U+UINTL
   30 CONTINUE
      SUM=SUM+(UINTL*10.0)**5
      THICML(2)=0.5*SUM*SINTL*0.45/(RE*(GAMCON(IND)**6))+THICML(1)
      ELSE DO
      SINT=(ROOT-STC(IND))/10.
      UINT=(0.0-GAMCON(IND))/10.
      U=UINT
      SUM=0.0
      DO 40 I=1,9
      F=(U**5)*2.0
      SUM=SUM+F
      U=U+UINT
   40 CONTINUE
      SUM=SUM+(UINT*10.)**5
      THICMU(2)=0.5*SUM*SINT*0.45/(RE*(GAMCON(IND)**6))+THICMU(1)
      SINTL=(STC(IND+1)-ROOT)/10.0
      UINTL=(GAMCON(IND+1)-0.0)/10.0
      U=UINTL
      SUM=0.0
      DO 60 I=1,9
      F=(U**5)*2.0
      SUM=SUM+F
      U=U+UINTL
   60 CONTINUE
      SUM=SUM+(UINTL*10.)**5
      THICML(2)=0.5*SUM*SINTL*0.45/(RE*(GAMCON(IND+1)**6))+THICML(1)
      END IF
      N=10
      FN=N
      DO 10 I=2,LASTUP
      A=DSTUP(I-1)
      B=DSTUP(I)
      DX=(B-A)/FN
      TDX=2.*DX
      FI1=FS(ROOT-A)+FS(ROOT-B)
      FI2=0.0
      FI3=0.0
      NN=N/2
      X=A+DX
      DO 3 J=1,NN
      FI2=FI2+FS(ROOT-X)
    3 X=X+TDX
      X=A
      NM=NN-1
      DO 4 J=1,NM
      X=X+TDX
    4 FI3=FI3+FS(ROOT-X)
      FI=DX*(FI1+4.0*FI2+2.0*FI3)/3.0
      TMOMUP=0.45*FI/(RE*(GAMCON(NSTATU+2-I)**6))*(-1.)
      THICMU(I)=THICMU(I-1)+TMOMUP
```

```
 10   CONTINUE
      LDN=LASTDN-1
      DO 20 J=2,LASTDN
      A=DSTLW(J-1)
      B=DSTLW(J)
      DX=(B-A)/FN
      TDX=2.0*DX
      FI1=FS(ROOT+A)+FS(ROOT+B)
      FI2=0.0
      FI3=0.0
      NN=N/2
      X=A+DX
      DO 5 K=1,NN
      FI2=FI2+FS(ROOT+X)
  5   X=X+TDX
      X=A
      NM=NN-1
      DO 6 L=1,NM
      X=X+TDX
  6   FI3=FI3+FS(ROOT+X)
      FI=DX*(FI1+4.0*FI2+2.0*FI3)/3.0
      TMOMDN=0.45*FI/(RE*(GAMCON(NSTATL-2+J)**6))
      THICML(J)=THICML(J-1)+TMOMDN
 20   CONTINUE
      RETURN
      END
      SUBROUTINE SEPRET(RE,GRADD,THICMU,THICML,LASTUP,LASTDN,PARAMU,
     *PARAML,SEPUP,SEPLOW,VSEPU,VSEPL,DSTUP,DSTLW,ROOT,IND,LSEPU,LSEPL,
     *NSTATU,NSTATL)
      DIMENSION GRADD(61),THICMU(50),THICML(50),PARAMU(50),PARAML(50),
     *DSTUP(50),DSTLW(50)
C     CALCULATION OF PARAMETER M
      LUP=LASTUP-1
      LDN=LASTDN-1
      PARAMU(1)=-0.075
      PARAML(1)=-0.075
      DO 10 I=2,LASTUP
      PARAMU(I)=-THICMU(I)*RE*GRADD(NSTATU+2-I)
      LSEPU=I
      IF(PARAMU(I).GT.0.09) GO TO 15
 10   CONTINUE
 15   DO 20 J=2,LASTDN
      PARAML(J)=THICML(J)*RE*GRADD(NSTATL+J-2)*(-1.)
      LSEPL=J
      IF(PARAML(J).GT.0.09) GO TO 25
 20   CONTINUE
 25   SEPUP=(DSTUP(LSEPU)-DSTUP(LSEPU-1))/(PARAMU(LSEPU)-PARAMU(
     *LSEPU-1))*(0.09-PARAMU(LSEPU-1))+DSTUP(LSEPU-1)
      SEPLOW=(DSTLW(LSEPL)-DSTLW(LSEPL-1))/(PARAML(LSEPL)-PARAML(
     *LSEPL-1))*(0.09-PARAML(LSEPL-1))+DSTLW(LSEPL-1)
      VSEPU=VINT(ROOT-SEPUP)
      VSEPL=VINT(ROOT+SEPLOW)
      RETURN
      END
      SUBROUTINE DISPLT(SEPUP,SEPLOW,DSTUP,DSTLW,THICMU,
     *THICML,PARAMU,PARAML,IND,DPLAC,DPLAL,LSEPU,LSEPL,
     *DISPU,DISPL,NUP,NLOW)
      DIMENSION DSTUP(50),DSTLW(50),PARAMU(50),PARAML(50),
     *THICMU(50),THICML(50),DPLAC(50),DPLAL(50)
      NUP=LSEPU-1
      DO 10 I=1,NUP
      EMREQ=PARAMU(I)
      DPLAC(I)=HPAM(EMREQ)*SQRT(THICMU(I))
 10   CONTINUE
```

```
      NLOW=LSEPL-1
      DO 20 J=1,NLOW
      EMREQ=PARAML(J)
      DPLAL(J)=HPAM(EMREQ)*SQRT(THICML(J))
   20 CONTINUE
      THIMU=(THICMU(NUP+1)-THICMU(NUP))/(DSTUP(NUP+1)-DSTUP(NUP))*
     *(SEPUP-DSTUP(NUP))+THICMU(NUP)
      DISPU=3.55*SQRT(THIMU)
      THIML=(THICML(NLOW+1)-THICML(NLOW))/(DSTLW(NLOW+1)-DSTLW(NLOW))*
     *(SEPLOW-DSTLW(NLOW))+THICML(NLOW)
      DISPL=3.55*SQRT(THIML)
      RETURN
      END
      SUBROUTINE DISLOP(DSTUP,DSTLW,LSEPU,LSEPL,DPLAC,DPLAL,DISPU,
     *DISPL,DDDSU,DDDSL,DDUP,DDLOW,SEPUP,SEPLOW,NUP,NLOW,CHK)
      DIMENSION DSTUP(50),DSTLW(50),DPLAC(50),DPLAL(50),DDDSU(40),
     *DDDSL(40),CHK(40)
      NUP=LSEPU-1
      DPLAC(NUP+1)=DISPU
      DO 20 I=2,NUP
      C1=DPLAC(I-1)/((DSTUP(I-1)-DSTUP(I))*(DSTUP(I-1)-DSTUP(I+1)))
      C2=DPLAC(I)/((DSTUP(I)-DSTUP(I-1))*(DSTUP(I)-DSTUP(I+1)))
      C3=DPLAC(I+1)/((DSTUP(I+1)-DSTUP(I-1))*(DSTUP(I+1)-DSTUP(I)))
      CHK(I)=C1*(DSTUP(I)*2.-DSTUP(I)-DSTUP(I+1))+C2*(DSTUP(I)*2.-
     *DSTUP(I-1)-DSTUP(I+1))+C3*(DSTUP(I)*2.-DSTUP(I-1)-DSTUP(I))
   20 CONTINUE
      DO 1516 KT=1,NUP
      DDDSU(KT)=(DPLAC(KT+1)-DPLAC(KT))/(DSTUP(KT+1)-DSTUP(KT))
 1516 CONTINUE
      NLOW=LSEPL-1
      DPLAL(NLOW+1)=DISPL
      DO 1517 KV=1,NLOW
      DDDSL(KV)=(DPLAL(KV+1)-DPLAL(KV))/(DSTLW(KV+1)-DSTLW(KV))
 1517 CONTINUE
      NEW=LSEPU-12
      IF(NEW.LE.0)GO TO 2366
      DO 2360 I=NEW,NUP
      IF(DDDSU(I).LT.DDDSU(I-1))GO TO 2360
      DIFF=ABS(DDDSU(I-3)-DDDSU(I-4))
      GO TO 2361
 2360 CONTINUE
 2361 DO 2362 J=I,NUP
      DDDSU(J)=DIFF+DDDSU(J-1)
 2362 CONTINUE
 2366 NEW=LSEPL-12
      IF(NEW.LE.0)GO TO 2367
      DO 2363 I=NEW,NLOW
      IF(DDDSL(I).LT.DDDSL(I-1))GO TO 2363
      DIFF=ABS(DDDSL(I-3)-DDDSL(I-4))
      GO TO 2364
 2363 CONTINUE
 2364 DO 2365 J=I,NLOW
      DDDSL(J)=DIFF+DDDSL(J-1)
 2365 CONTINUE
 2367 I=LSEPU-1
      DDUP=((SEPUP-DSTUP(I-2))*(SEPUP-DSTUP(I-1)))/((DSTUP(I-3)-DSTUP
     *(I-2))*(DSTUP(I-3)-DSTUP(I-1)))*DDDSU(I-3)+((SEPUP-DSTUP(I-3))*
     *(SEPUP-DSTUP(I-1)))/((DSTUP(I-2)-DSTUP(I-3))*(DSTUP(I-2)-DSTUP
     *(I-1)))*DDDSU(I-2)+((SEPUP-DSTUP(I-3))*(SEPUP-DSTUP(I-2)))/((DS
     *TUP(I-1)-DSTUP(I-3))*(DSTUP(I-1)-DSTUP(I-2)))*DDDSU(I-1)
      J=LSEPL-1
      DDLOW=((SEPLOW-DSTLW(J-2))*(SEPLOW-DSTLW(J-1)))/((DSTLW(J-3)-DST
     *LW(J-1))*(DSTLW(J-3)-DSTLW(J-
     *2)))*DDDSL(J-3)+((SEPLOW-DSTLW(J-3))*(SEPLOW-DSTLW(J-1)))/((DS
```

```
     *TLW(J-2)-DSTLW(J-3))*(DSTLW(J-2)-DSTLW(J-1)))*DDDSL(J-2)+((SEPLO
     *W-DSTLW(J-3))*(SEPLOW-DSTLW(J-2)))/((DSTLW(J-1)-DSTLW(J-3))*(DST
     *LW(J-1)-DSTLW(J-2)))*DDDSL(J-1)
      DDDSU(NUP+1)=DDUP
      DDDSL(NLOW+1)=DDLOW
      RETURN
      END
      SUBROUTINE ANVEGR(ALPHA,NN,DUDS)
      DIMENSION XN(61),YN(61),THETA(61),PAI(61),UCIR(61),
     *VCIR(61),DUDT(61),DVDT(61),DUDS(61),RELL(61)
     *,UELL(61),VELL(61),PHIN(61),XCON(61),YCON(61)
      N=NN-1
      AA=0.5
      BB=AA/6.0
      PI=4.0*ATAN(1.0)
      CSQR=AA**2-BB**2
      RSQR=(AA+BB)**2
      DO 1330 I=1,NN
      PHIN(I)=2.0*PI*(I-1)/N
      XN(I)=0.5*(1.0+COS(PHIN(I)))
      IF(I.LE.NN/2)THEN DO
      YN(I)=2.0+BB*SQRT(1.0-((XN(I)-.5)**2/AA**2))
      ELSE DO
      YN(I)=2.0-BB*SQRT(1.0-((XN(I)-.5)**2/AA**2))
      END IF
 1330 CONTINUE
      DO 1310 KE=1,N
      XCON(KE)=(XN(KE)+XN(KE+1))/2.0
      YCON(KE)=(YN(KE)+YN(KE+1))/2.0
      PAI(KE)=ATAN2((YCON(KE)-2.0),(XCON(KE)-0.5))
      THETA(KE)=ATAN(6.*TAN(PAI(KE)))
      IF(PAI(KE).GT.0.0.AND.KE.GT.N/2)PAI(KE)=PI+PAI(KE)
      IF(THETA(KE).GT.0.0.AND.KE.LE.N/2)THETA(KE)=PI+THETA(KE)
      IF(THETA(KE).GT.0.0.AND.KE.GT.N/2)THETA(KE)=PI+THETA(KE)
 1310 CONTINUE
      DO 1300 KD=1,N
      UCIR(KD)=COS(ALPHA)-COS(ALPHA-2.0*THETA(KD))+2.
     **SIN(ALPHA)*SIN(THETA(KD))
      VCIR(KD)=SIN(ALPHA)+SIN(ALPHA-2.0*THETA(KD))-2.
     **SIN(ALPHA)*COS(THETA(KD))
      FACT1=1.0-(CSQR/RSQR)*COS(2.0*THETA(KD))
      FACT2=(CSQR/RSQR)*SIN(2.0*THETA(KD))
      F1=FACT1/((FACT1)**2+(FACT2)**2)
      F2=-FACT2/((FACT1)**2+(FACT2)**2)
      UELL(KD)=UCIR(KD)*F1+VCIR(KD)*F2
      VELL(KD)=-(UCIR(KD)*F2-VCIR(KD)*F1)
      RELL(KD)=SQRT(UELL(KD)**2+VELL(KD)**2)
      IF(KD.LE.N/2)THEN DO
      IF(VELL(KD).GT.0.0.AND.UELL(KD).GT.0.0)RELL(KD)=-RELL(KD)
      IF(VELL(KD).LE.0.0.AND.UELL(KD).GT.0.0)RELL(KD)=-RELL(KD)
      ELSE DO
      IF(UELL(KD).LT.0.0.AND.VELL(KD).GT.0.0)RELL(KD)=-RELL(KD)
      END IF
      IF(KD.LE.N/2)THEN DO
      UELL(KD)=-UELL(KD)
      VELL(KD)=-VELL(KD)
      END IF
      IF(KD.GT.N/2.AND.RELL(KD).LT.0.0)THEN DO
      UELL(KD)=-UELL(KD)
      VELL(KD)=-VELL(KD)
      END IF
      DIS=SQRT((XN(KD)-0.5)**2+(YN(KD)-2.0)**2)
      CON1=1.-(CSQR/RSQR)*COS(2.0*THETA(KD))
      CON2=(CSQR/RSQR)*SIN(2.0*THETA(KD))
```

```
      CON3=(CON1**2)+(CON2**2)
      CON4=(ALPHA-2.0*THETA(KD))
      CON5=COS(ALPHA)-COS(CON4)+2.*SIN(ALPHA)*SIN(
     *THETA(KD))
      CON6=SIN(ALPHA)+SIN(CON4)-2.0*SIN(ALPHA)*COS(
     *THETA(KD))
      CON7=4.0*CON1*CON2+4.0*CON2*(CSQR/RSQR)*COS(2.0*
     *THETA(KD))
      CON8=CON3**2
      DUDT(KD)=(-2.0*SIN(CON4)+2.0*SIN(ALPHA)*COS(THE
     *TA(KD)))*(CON1/CON3)+(CON5)*(((CON3*2.0*CON2)-
     *(CON1*CON7))/CON8)+(-2.0*COS(CON4)+2.0*SIN(ALPHA)*SIN
     *(THETA(KD)))*(-CON2/CON3)+(CON6)*(((CON3*(-2.0*(CSQR
     */RSQR)*COS(2.0*THETA(KD))))-(-CON2*CON7))/CON8)
      DVDT(KD)=(-2.0*SIN(CON4)+2.0*SIN(ALPHA)*COS(THETA(KD
     *)))*(-CON2/CON3)+(CON5)*(((CON3*(-2.0*(CSQR/RSQR)*COS(
     *2.00*THETA(KD))))-(-CON2*CON7))/CON8)-(-2.0*COS(CON
     *4)+2.0*SIN(ALPHA)*SIN(THETA(KD)))*(CON1/CON3)-(CON6)
     **(((CON3*2.0*CON2)-(CON1*CON7))/CON8)
      DRDP=-35.*DIS*SIN(2.*PAI(KD))/(37.-35.*COS(2.*PAI(KD)))
      DTDP=6.*(COS(THETA(KD))**2)/(COS(PAI(KD))**2)
      DPDS=1.0/(SQRT(DIS**2+DRDP**2))
      DUDT(KD)=DUDT(KD)*DTDP*DPDS
      DVDT(KD)=DVDT(KD)*DTDP*DPDS
      DUDS(KD)=(UELL(KD)*DUDT(KD)+VELL(KD)*DVDT(KD))/
     *(SQRT(UELL(KD)**2+VELL(KD)**2))
 1300 CONTINUE
      RETURN
      END
      SUBROUTINE SHIFT(N,NS,XCON,YCON,DEL,ELEN,RH,XCONM,
     *YCONM,DELM,ELENM,RHH)
      DIMENSION XCON(60),YCON(60),DEL(60),ELEN(60),RH(60),
     *XCONM(60),YCONM(60),DELM(60),ELENM(60),RHH(60)
      DO 1 MY=1,60
      IF(MY.LE.(N-(NS-1)))THEN DO
      MY3=MY+(NS-1)
      XCONM(MY)=XCON(MY3)
      YCONM(MY)=YCON(MY3)
      ELENM(MY)=ELEN(MY3)
      DELM(MY)=DEL(MY3)
      RHH(MY)=RH(MY3)
      ELSE DO
      MY3=MY-(N-(NS-1))
      XCONM(MY)=XCON(MY3)
      YCONM(MY)=YCON(MY3)
      DELM(MY)=DEL(MY3)
      ELENM(MY)=ELEN(MY3)
      RHH(MY)=RH(MY3)
      END IF
    1   CONTINUE
      RETURN
      END
      SUBROUTINE SOURCE(XCON,YCON,DEL,ELEN,QSEP,LSEPU,LSEPL,NSTATU,
     *NSTATL,SIG,SIGMA,N,NN,GAMCON,DDDSU,DDDSL,UT,UN,IT,KOD)
      DIMENSION XI(60,60),ETA(60,60),XCON(61),YCON(61),CONS1(
     *60,60),CONS2(60,60),CONSA(60,60),CONSB(60,60),DEL(60),ELEN
     *(60),UN(60),UT(60),COEFA(60,60),COEFB(60,60),COEF(60,61),SIG
     *(60),SIGMA(60,5),TANG(60,60),BETA(60),UU(60,60),VU(60,60),
     *GAMCON(61),DDDSU(40),DDDSL(40),COFT(60,60),WKAREA(4000)
      DIMENSION CONSX(60,60),CONSY(60,60),COEFU(60,60),SIG2(60)
      PI=4.0*ATAN(1.0)
      DO 50 K=1,N
      DO 60 L=1,N
      IF(DEL(L).GT.(PI/2.).AND.DEL(L).LT.PI)BETA(L)=DEL(L)-PI
```

```
      IF(DEL(L).GT.PI.AND.DEL(L).LT.(1.5*PI))BETA(L)=DEL(L)-PI
      IF(DEL(L).GT.(1.5*PI).AND.DEL(L).LT.(2.*PI))BETA(L)=DEL(L)-PI
      IF(DEL(L).LE.(PI/2.).AND.DEL(L).GT.0.0)BETA(L)=DEL(L)+PI
      XI(K,L)=(XCON(K)-XCON(L))*COS(BETA(L))+(YCON(K)-YCON(L))*
     *SIN(BETA(L))
      ETA(K,L)=(YCON(K)-YCON(L))*COS(BETA(L))-(XCON(K)-XCCN(L))*
     *SIN(BETA(L))
   60 CONTINUE
   50 CONTINUE
      DO 90 I=1,N
      DO 100 J=1,N
      IF(J.EQ.I)GO TO 110
      R1=SQRT((XI(I,J)+0.5*ELEN(J))**2+ETA(I,J)**2)
      R2=SQRT((XI(I,J)-0.5*ELEN(J))**2+ETA(I,J)**2)
      IF(XI(I,J).GT.0.0.AND.ETA(I,J).GT.0.0)GO TO 31
      IF(XI(I,J).LT.0.0.AND.ETA(I,J).GT.0.0)GO TO 32
      IF(XI(I,J).LT.0.0.AND.ETA(I,J).LT.0.0)GO TO 33
      IF(XI(I,J).GT.0.0.AND.ETA(I,J).LT.0.0)GO TO 34
   32 IF(ABS(XI(I,J)).GE.(.5*ELEN(J)))THEN DO
      PHI1=ATAN(ETA(I,J)/(XI(I,J)+.5*ELEN(J)))
      PHI1=PHI1+PI
      ELSE DO
      PHI1=ATAN(ETA(I,J)/(XI(I,J)+.5*ELEN(J)))
      END IF
      PHI2=ATAN(ETA(I,J)/(XI(I,J)-.5*ELEN(J)))
      PHI2=PHI2+PI
      GO TO 38
  33  IF(ABS(XI(I,J)).GT.(.5*ELEN(J)))THEN DO
      PHI1=ATAN(ETA(I,J)/(XI(I,J)+.5*ELEN(J)))
      PHI1=PHI1+PI
      ELSE DO
      PHI1=ATAN(ETA(I,J)/(XI(I,J)+.5*ELEN(J)))
      PHI1=PHI1+2.*PI
      END IF
      PHI2=ATAN(ETA(I,J)/(XI(I,J)-.5*ELEN(J)))
      PHI2=PHI2+PI
      GO TO 38
   31 IF(ABS(XI(I,J)).GE.(.5*ELEN(J)))THEN DO
      PHI2=ATAN(ETA(I,J)/(XI(I,J)-.5*ELFN(J)))
      ELSE DO
      PHI2=ATAN(ETA(I,J)/(XI(I,J)-.5*ELEN(J)))
      PHI2=PHI2+PI
      END IF
      PHI1=ATAN(ETA(I,J)/(XI(I,J)+.5*ELEN(J)))
      GO TO 38
   34 IF(ABS(XI(I,J)).GE.(.5*ELEN(J)))THEN DO
      PHI2=ATAN(ETA(I,J)/(XI(I,J)-.5*ELEN(J)))
      PHI2=PHI2+2.*PI
      ELSE DO
      PHI2=ATAN(ETA(I,J)/(XI(I,J)-.5*ELEN(J)))
      PHI2=PI+PHI2
      END IF
      PHI1=ATAN(ETA(I,J)/(XI(I,J)+.5*ELEN(J)))
      PHI1=PHI1+2.*PI
   38 A=XI(I,J)+0.5*ELEN(J)
      UU(I,J)=(1./(2.*PI))*ALOG(R1/R2)
      VU(I,J)=(1./(2.*PI))*(PHI2-PHI1)
      IF(DEL(J).LT.PI.AND.DEL(J).GT.(PI/2.))GO TO 111
      IF(DEL(J).GT.PI.AND.DEL(J).LT.(1.5*PI))GO TO 112
      IF(DEL(J).GT.(1.5*PI).AND.DEL(J).LT.(2.*PI))GO TO 113
      IF(DEL(J).LT.(PI/2.).AND.DEL(J).GE.0.0)THEN DO
      CONSX(I,J)=UU(I,J)*COS(DEL(J)+PI)+VU(I,J)*COS((PI/2.)+PI+DEL(J))
      CONSY(I,J)=UU(I,J)*COS(DEL(J)+PI/2.)+VU(I,J)*COS(DEL(J)+PI)
      END IF
```

```
      GO TO 115
  111 CONSX(I,J)=UU(I,J)*COS(PI-DEL(J))+VU(I,J)*COS((PI/2.)-(PI-DEL(J)))
      CONSY(I,J)=UU(I,J)*COS((PI-DEL(J))+PI/2.)+VU(I,J)*COS(PI-DEL(J))
      GO TO 115
  112 CONSX(I,J)=UU(I,J)*COS(DEL(J)-PI)+VU(I,J)*COS((DEL(J)-PI)+PI/2.)
      CONSY(I,J)=UU(I,J)*COS((PI/2.)-(DEL(J)-PI))+VU(I,J)*COS(DEL(J)
     *-PI)
      GO TO 115
  113 CONSX(I,J)=UU(I,J)*COS(DEL(J)-PI)+VU(I,J)*COS(DEL(J)-PI/2.)
      CONSY(I,J)=UU(I,J)*COS((PI/2.)-(2.*PI-DEL(J)))+VU(I,J)*COS
     *(DEL(J)-PI)
  115 COEFU(I,J)=CONSX(I,J)*COS(DEL(I)-PI/2.)+CONSY(I,J)*COS(DEL(I)-PI)
      GO TO 100
  110 COEFU(I,J)=0.5
  100 CONTINUE
   90 CONTINUE
C     CALCULATION OF NORMAL VELOCITIES IN ATTACHED REGION
      NUP=LSEPU-2
      DO 10 I=1,NUP
      UN(NSTATU-I+1)=GAMCON(NSTATU-I+1)*DDDSU(I+1)*(-1.)
   10 CONTINUE
      NLOW=LSEPL-2
      DO 20 J=1,NLOW
      UN(NSTATL+J-1)=DDDSL(J+1)*GAMCON(NSTATL+J-1)
   20 CONTINUE
      NSTU=NSTATU-(LSEPU-2)
      DO 30 K=1,NSTU
      UN(K)=SQRT(QSEP**2-(GAMCON(K))**2)
   30 CONTINUE
      NSTL=NSTATL+LSEPL-2
      DO 40 L=NSTL,N
      C=QSEP**2-(GAMCON(L)**2)
      IF(C.LE.0.0)THEN DO
      UN(L)=0.0
      GO TO 40
      END IF
      UN(L)=SQRT(QSEP**2-(GAMCON(L))**2)
   40 CONTINUE
      DO 850 I=1,N
      SIG(I)=UN(I)
  850 CONTINUE
      IDGT=0
      CALL LEQT2F(COEFU,1,N,N,SIG,IDGT,WKAREA,IER)
      IT=1
      DO 851 J=1,N
      SIGMA(J,IT)=SIG(J)
  851 CONTINUE
C     CALCULATION OF TANGENTIAL VELOCITIES DUE TO SOURCES
  859 DO 852 I=1,N
      SUM=0.0
      DO 853 J=1,N
      IF(J.EQ.I)THEN DO
      TANG(I,J)=0.0
      ELSE DO
      TANG(I,J)=(CONSX(I,J)*COS(DEL(I))+CONSY(I,J)*SIN(DEL(I)))*SIGMA(
     *J,IT)
      END IF
      SUM=SUM+TANG(I,J)
  853 CONTINUE
      UT(I)=SUM
  852 CONTINUE
      KOD=2
      IF(KOD.EQ.1)GO TO 858
      DO 854 I=1,NSTU
```

```
      C=QSEP**2-(GAMCON(I)+UT(I))**2
      IF(C.LT.0.0)THEN DO
      UN(I)=0.0
      ELSE DO
      UN(I)=SQRT(QSEP**2-(GAMCON(I)+UT(I))**2)
      END IF
  854 CONTINUE
      DO 855 J=NSTL ,N
      C=QSEP**2-(GAMCON(J)+UT(J))**2
      IF(C.LT.0.0)THEN DO
      UN(J)=0.0
      ELSE DO
      UN(J)=SQRT(QSEP**2-(GAMCON(J)+UT(J))**2)
      END IF
  855 CONTINUE
      DO 856 I=1,N
      SIG2(I)=UN(I)
  856 CONTINUE
      IT=IT+1
      CALL LEQT2F(COEFU,1,N,N,SIG2,IDGT,WKAREA,IER)
      DO 857 J=1,N
      SIGMA(J,IT)=SIG2(J)
  857 CONTINUE
      IF( ABS((SIGMA(LSEPU,IT)-SIGMA(LSEPU,IT-1))/SIGMA(LSEPU,IT))
     *.LE.0.01)GO TO 858
      GO TO 859
  858 RETURN
      END
      SUBROUTINE DSTNCE(STC,IND,ROOT,DSTUP,DSTLW,LASTUP,LASTDN)
      DIMENSION STC(61),DSTUP(50),DSTLW(50)
      DSTUP(1)=0.0
      DSTLW(1)=0.0
      D1=STC(IND)-ROOT
      IF(D1.GT.0.0)GO TO 5
      INF=IND+1
      DO 10 I=2,INF
      DSTUP(I)=ROOT-STC(IND-I+2)
   10 CONTINUE
      LASTUP=INF
      GO TO 25
    5 IN=IND-1+1
      DO 15 J=2,IN
      DSTUP(J)=ROOT-STC(IND-J+1)
   15 CONTINUE
      LASTUP=IN
   25 IF(D1.GT.0.0)GO TO 20
      INE=60-IND+1
      DO 30 K=2,INE
      DSTLW(K)=STC(IND+K-1)-ROOT
   30 CONTINUE
      LASTDN=INE
      GO TO 40
   20 INE=60-IND+2
      DO 35 L=2,INE
      DSTLW(L)=STC(IND+L-2)-ROOT
   35 CONTINUE
      LASTDN=INE
   40 RETURN
      END
      SUBROUTINE COLIFT(GAMMA,GAMCON,STC,N,CL,STE)
      DIMENSION GAMMA(61),GAMCON(61),STC(61),STE(61),CL(61)
      CL(1)=((GAMCON(1)+GAMMA(1))/2.0)*(STC(1)-STE(1))
      DO 5 I=2,N
      A=STC(I-1)
```

```
      B=STC(I)
      N1=10
      FN=N1
      DX=(B-A)/FN
      TDX=2.0*DX
      FI1=VINT(A)+VINT(B)
      FI2=0.0
      FI3=0.0
      NN1=N1/2
      X=A+DX
      DO 3 J=1,NN1
      FI2=FI2+VINT(X)
    3 X=X+TDX
      X=A
      NM=NN1-1
      DO 4 K=1,NM
      X=X+TDX
    4 FI3=FI3+VINT(X)
      FI=DX*(FI1+4.*FI2+2.*FI3)/3.
      CL(I)=CL(I-1)+FI
    5 CONTINUE
      CL(N+1)=CL(N)+((GAMCON(N)+GAMMA(N+1))/2.0)*(STE(N+1)-STC(N))
      CL(N+1)=2.0*CL(N+1)*(-1.)
      RETURN
      END
      SUBROUTINE GAUS(ROOT,GAMCON,RE,DSTUP,DSTLW,LASTUP,LASTDN,L
     *UP,LDN,IND,TUM,TLM,STC,NSTATU,NSTATL)
      DIMENSION GAMCON(61),DSTUP(50),DSTLW(50),TUM(50),TLM(50)
     *,STC(61),W(3),Z(3)
      D1=STC(IND)-ROOT
      C1=GAMCON(IND-1)/((STC(IND-1)-STC(IND))*(STC(IND-1)-STC(IND
     *+1)))
      C2=GAMCON(IND)/((STC(IND)-STC(IND-1))*(STC(IND)-STC(IND+1)))
      C3=GAMCON(IND+1)/((STC(IND+1)-STC(IND-1))*(STC(IND+1)-STC(IND
     *)))
      DVDS1=C1*(2.*ROOT-STC(IND)-STC(IND+1))+C2*(2.*ROOT-SIC(IND-1)
     *-STC(IND+1))+C3*(2.*ROOT-STC(IND-1)-STC(IND))
      IF(D1.GT.0.0)GO TO 1
      TUM(1)=(.075/RE)*(1./DVDS1)
      TLM(1)=(.075/RE)*(1./DVDS1)
      NSTATU=IND
      NSTATL=IND+1
      GO TO 2
    1 TUM(1)=(.075/RE)*(1./DVDS1)
      TLM(1)=(.075/RE)*(1./DVDS1)
      NSTATU=IND-1
      NSTATL=IND
    2 LUP=LASTUP-1
      LDN=LASTDN-1
      W(1)=.8888888
      W(2)=.5555555
      W(3)=.5555555
      Z(1)=.0000000
      Z(2)=.7745966
      Z(3)=-.7745966
      DO 20 I=2,LASTUP
      A=DSTUP(I-1)
      B=DSTUP(I)
      SUM=0.0
      DO 10 J=1,3
      SUM=SUM+W(J)*FS(ROOT-(Z(J)*(B-A)+(B+A))/2.)
   10 CONTINUE
      TUM(I)=(-1.)*SUM*.5*(B-A)*.45/(RE*(GAMCON(NSTATU+2-I)**6))
     *+TUM(I-1)
```

```
   20 CONTINUE
      DO 30 I=2,LASTDN
      A=DSTLW(I-1)
      B=DSTLW(I)
      SUM=0.0
      DO 25 J=1,3
      SUM=SUM+W(J)*PS(ROOT+(Z(J)*(B-A)+(B+A))/2.)
   25 CONTINUE
      TLM(I)=SUM*0.5*(B-A)*0.45/(RE*(GAMCON(NSTATL+I-2)**6))+TLM
     *(I-1)
   30 CONTINUE
      RETURN
      END
      FUNCTION TPAM(S)
      COMMON/AREA/EH(26),EM(26),EL(26)
      IF(S.GT.EM(26).OR.S.LT.EM(1)) GO TO 6
      DO 1 I=1,25
      IF((S-EM(I))*(S-EM(I+1)).LT.0.0) GO TO 2
    1 CONTINUE
    2 TPAM=(EL(I+1)-EL(I))/(EM(I+1)-EM(I))*(S-EM(I))+EL(I)
      GO TO 7
    6 IF(S.LT.EM(1))TPAM=0.5
      IF(S.GT.EM(26))TPAM=0.0
    7 RETURN
      END
      SUBROUTINE SKIN(GAMCON,RE,THICMU,THICML,CONSLU,CONSLL,NUP,NLOW,
     *PARAMU,PARAML,NSTATU,NSTATL)
      DIMENSION GAMCON(61),THICMU(50),THICML(50),PARAMU(50),PARAML(50),
     *CONSLU(50),CONSLL(50)
      CONSLU(1)=0.0
      CONSLL(1)=0.0
      DO 10 I=2,NUP
      ELREQ=PARAMU(I)
      CONSLU(I)=2.0*TPAM(ELREQ)*GAMCON(NSTATU-I+2)/(RE*SQRT(THICMU(I)))
     **(-1.0)
   10 CONTINUE
      DO 20 J=2,NLOW
      ELREQ=PARAML(J)
      CONSLL(J)=2.0*TPAM(ELREQ)*GAMCON(NSTATL+J-2)/(RE*SQRT(THICML(J)))
   20 CONTINUE
      RETURN
      END
      FUNCTION CPINT(XREQ,NSUR)
      COMMON/PRESRE/XCON,YCON,CP
      DIMENSION XCON(61),YCON(61),CP(60),UREQ(60)
      IF(NSUR.EQ.2) GO TO 2
      DO 1 I=1,30
      IF(XREQ.LT.XCON(30).AND.XREQ.GT.0.0) GO TO 10
      IF(XREQ.LT.XCON(I)) GO TO 1
      IF(I.EQ.1) GO TO 9
      CPINT=((CP(I)-CP(I-1))/(XCON(I)-XCON(I-1)))*(XREQ-XCON(I-1))+
     *CP(I-1)
      GO TO 7
    1 CONTINUE
    9 CPINT=((CP(1)-0.0)/(XCON(1)-0.0))*(XREQ-1.0)+1.0
      GO TO 7
   10 CPINT=(.5*(CP(31)+CP(30))-CP(30))/(0.0-XCON(30))*(XREQ-XCON(30))
     *+CP(30)
      GO TO 7
    2 DO 3 I=31,60
      IF(XREQ.GT.0.0.AND.XREQ.LT.XCON(31)) GO TO 11
      IF(XCON(I).LT.XREQ) GO TO 3
      CPINT=((CP(I)-CP(I-1))/(XCON(I)-XCON(I-1)))*(XREQ-XCON(I-1))+
     *CP(I-1)
```

```
      GO TO 7
 3    CONTINUE
 11   CPINT=-(CP(31)-.5*(CP(30)+CP(31)))/(XCON(31)-0.0)*(XREQ-0.0)+
     *CP(31)
 7    RETURN
      END
      SUBROUTINE CDRAG(CP,ALPHA,CLIFT,N,XCON)
      DIMENSION XCON(61),CLIFT(60),CP(60)
      CLIFT(1)=CP(1)*(1.-XCON(1))
      DO 5 I=2,59
      A=XCON(I)
      B=XCON(I+1)
      N1=10
      FN=N1
      DX=((B-A)/FN)
      TDX=2.*DX
      IF(I.LE.N/2)THEN DO
      NSUR=1
      ELSE DO
      NSUR=2
      END IF
      FI1=CPINT(A,NSUR)+CPINT(B,NSUR)
      FI2=0.0
      FI3=0.0
      NN1=N1/2
      X=A+DX
      DO 3 J=1,NN1
      FI2=FI2+CPINT(X,NSUR)
 3    X=X+TDX
      X=A
      NM=NN1-1
      DO 4 K=1,NM
      X=X+TDX
 4    FI3=FI3+CPINT(X,NSUR)
      FI=DX*(FI1+4.*FI2+2.*FI3)/3.0
      CLIFT(I)=CLIFT(I-1)+FI
 5    CONTINUE
      CLIFT(N)=CLIFT(N-1)+CP(60)*(1.-XCON(60))
      RETURN
      END
      FUNCTION CINT(YREQ,NQUAD)
      COMMON/PRESRE/XCON,YCCN,CP
      DIMENSION YCON(61),CP(60),UREQ(60),XCON(61)
      IF(NQUAD.EQ.1)GO TO 1
      IF(NQUAD.EQ.2)GO TO 2
      IF(NQUAD.EQ.3)GO TO 3
      IF(NQUAD.EQ.4)GO TO 4
      IF(NQUAD.EQ.5)GO TO 12
      IF(NQUAD.EQ.7)GO TO 14
 1    DO 5 I=1,15
      IF(YCON(I).LT.YREQ)GO TO 5
      CINT=(CP(I)-CP(I-1))/(YCON(I)-YCON(I-1))*(YREQ-YCON(I-1))
     *+CP(I-1)
      GO TO 7
 5    CONTINUE
 2    DO 6 I=16,30
      IF(YREQ.LT.YCON(I))GO TO 6
      IF(YREQ.EQ.YCON(16))THEN DO
      CINT=CP(46)
      ELSE DO
      CINT=(CP(I)-CP(I-1))/(YCON(I)-YCON(I-1))*(YREQ-YCON(I-1))
     *+CP(I-1)
      END IF
      GO TO 7
```

```
 6     CONTINUE
 3     DO 8 I=31,45
       IF(YCON(I).GT.YREQ)GO TO 8
       CINT=(CP(I)-CP(I-1))/(YCON(I)-YCON(I-1))*(YREQ-YCON(I-1))
      *+CP(I-1)
       GO TO 7
 8     CONTINUE
 4     DO 9 I=46,60
       IF(YCON(I).LT.YREQ)GO TO 9
        IF(YREQ.EQ.YCON(46))THEN DO
        CINT=CP(46)
        ELSE DO
       CINT=(CP(I)-CP(I-1))/(YCON(I)-YCON(I-1))*(YREQ-YCON(I-1))
      *+CP(I-1)
        END IF
       GO TO 7
 9     CONTINUE
   12  IF(YREQ.LE.2.083333)THEN DO
       CINT=(.5*(CP(16)+CP(15))-CP(15))/(2.083333-YCON(15))*(YREQ
      *-YCON(15))+CP(15)
       ELSE DO
       CINT=-(CP(16)-.5*(CP(15)+CP(16)))/(YCON(16)-2.083333)*(YCON
      *(16)-YREQ)+CP(16)
       END IF
       GO TO 7
  14   IF(YREQ.LE.1.916666)THEN DO
       CINT=(.5*(CP(46)+CP(45))-CP(45))/(1.96666-YCON(45))*(YREQ-
      *YCON(45))+CP(45)
       ELSE DO
       CINT=-(CP(46)-.5*(CP(45)+CP(46)))/(YCON(46)-1.96666)*(YCON(
      *46)-YREQ)+CP(46)
       END IF
   7   RETURN
       END
       SUBROUTINE CDRAG2(CP,ALPHA,CD,YCON,N)
       DIMENSICN CP(60),CD(60),YCON(61)
       CD(1)=0.0
       DO 5 I=2,59
       A=YCON(I)
       B=YCON(I+1)
       N1=10
       FN=N1
       DX=(B-A)/FN
       TDX=2.0*DX
       IF(I.EQ.15)NQUAD=5
       IF(I.EQ.45)NQUAD=7
       IF(I.LT.15)NQUAD=1
       IF(I.GT.15.AND.I.LE.30)NQUAD=2
       IF(I.GT.30.AND.I.LT.45)NQUAD=3
        IF(I.GT.45)NQUAD=4
       FI1=CINT(A,NQUAD)+CINT(B,NQUAD)
       FI2=0.0
       FI3=0.0
       NN1=N1/2
       X=A+DX
       DO 3 J=1,NN1
       FI2=FI2+CINT(X,NQUAD)
  3    X=X+TDX
       X=A
       NM=NN1-1
       DO 4 K=1,NM
       X=X+TDX
 4     FI3=FI3+CINT(X,NQUAD)
       FI=DX*(FI1+4.*FI2+2.*FI3)/3.0
```

```
      CD(I)=CD(I-1)+FI
    5 CONTINUE
      CD(N)=CD(N-1)
      RETURN
      END
      SUBROUTINE CM1(XCON,N,CP,CMU1)
      DIMENSION XCON(61),CP(60),CMU1(60)
C     INTEGRATION CPXDX
      CMU1(1)=0.0
      DO 5 I=2,59
      A=XCON(I)
      B=XCON(I+1)
      N1=10
      FN=N1
      DX=(B-A)/FN
      TDX=2.0*DX
      IF(I.LE.N/2)THEN DO
      NSUR=1
      ELSE DO
      NSUR=2
      END IF
      FI1=CPINT(A,NSUR)*A+CPINT(B,NSUR)*B
      FI2=0.0
      FI3=0.0
      NN1=N1/2
      X=A+DX
      DO 3 J=1,NN1
      FI2=FI2+CPINT(X,NSUR)*X
    3 X=X+TDX
      X=A
      NM=NN1-1
      DO 4 K=1,NM
      X=X+TDX
    4 FI3=FI3+CPINT(X,NSUR)*X
      FI=DX*(FI1+4.*FI2+2.*FI3)/3.0
      CMU1(I)=CMU1(I-1)+FI
    5 CONTINUE
      CMU1(N)=CMU1(N-1)
      RETURN
      END
      SUBROUTINE CM2(IA,IB,CP,YCON,CMU2)
      DIMENSICN CP(60),YCCN(61),CMU2(60)
C     INTEGRATION CPYDY
      IF(IA.EQ.2)THEN DO
      CMU2(IA-1)=0.0
      ELSE DO
      CMU2(IA-1)=CMU2(30)
      END IF
      DO 5 I=IA,IB
      A=YCON(I)
      B=YCON(I+1)
      N1=10
      FN=N1
      DX=(B-A)/FN
      TDX=2.*DX
      IF(I.EQ.15)NQUAD=5
      IF(I.EQ.45)NQUAD=7
      IF(I.LT.15)NQUAD=1
      IF(I.GT.15.AND.I.LE.30)NQUAD=2
      IF(I.GT.30.AND.I.LT.45)NQUAD=3
      NQUAD=4
      FI1=CINT(A,NQUAD)*ABS(A-2.0)+CINT(B,NQUAD)*ABS(B-2.0)
      FI2=0.0
      FI3=0.0
```

```
          NN1=N1/2
          X=A+DX
          DO 3 J=1,NN1
          FI2=FI2+CINT(X,NQUAD)*ABS(X-2.0)
    3     X=X+TDX
          X=A
          NM=NN1-1
          DO 4 K=1,NM
          X=X+TDX
    4     FI3=FI3+CINT(X,NQUAD)*ABS(X-2.0)
          FI=DX*(FI1+4.0*FI2+2.0*FI3)/3.0
          CMU2(I)=CMU2(I-1)+FI
    5     CONTINUE
          RETURN
          END
$ENTRY
  -0.250  -0.200  -0.140  -0.120  -0.100  -0.080  -0.064  -0.048  -0.032
  -0.016   0.000   0.016   0.032   0.040   0.048   0.056   0.060   0.064
   0.068   0.072   0.076   0.080   0.084   0.086   0.088   0.090
   2.00    2.07    2.18    2.23    2.28    2.34    2.39    2.44     2.49
   2.55    2.61    2.67    2.75    2.81    2.87    2.94    2.99     3.04
   3.09    3.15    3.22    3.30    3.39    3.44    3.49    3.55
   0.500   0.463   0.404   0.382   0.359   0.333   0.313   0.291   0.268
   0.244   0.220   0.195   0.168   0.153   0.138   0.122   0.113   0.104
   0.095   0.085   0.072   0.056   0.038   0.027   0.015   0.0
```

REFERENCES

1) Zumwalt, G.W., and Elangovan, R.: "Computation of Low Speed Flow Past Multi-Element Airfoils with Large Flow Separation", 13th Congress of the International Council of the Aeronautical Sciences, August 1982.

2) Howarth, L.: "The Theoretical Determination of the Lift Coefficient for a Thin Elliptic Cylinder", Proceedings of the Royal Society of London, Series A, Vol. 149, 1935.

3) Geising, J.P.: "Potential Flow About Two-Dimensional Airfoils", Douglas Aircraft Co., Report No. LB 31946 (1965).

4) Williams, B.R.: "An Exact Test Case for the Plane Potential Flow About Two Adjacent Lifting Aerofoils, ARC R & M No. 3717 (1973).

5) Milne-Thomson, L.M.: "Theoretical Hydrodynamics", Macmillan Press Ltd., 1977 Edition.

6) Gibson, I., and Tinkler, J.: "A Summary of Surface Singularity Techniques Applied to 2-Dimensional Aerofoil Flows", Dept. of Mechanical Engineering Publications, University of Manitoba, ER 25.36, July 1982.

7) Hess, J.L. and Smith, A.M.O.: "Calculation of Potential Flow About Arbitrary Bodies", Progress in Aeronautical Sciences, Vol. 8, Pergamon Press, 1967.

8) Gibson, I. and Wilcox, D.J.: "The Prediction of 2-Dimensional Aerofoil Performance Utilizing Distributed Surface Vortices and the Fredholm Integral of the First Kind", Dept. of Industrial Engineering Publications, University College, Galway, October 1982.

9) Schlitching, H.: "Boundary-Layer Theory", Chapter X, Seventh Edition, McGraw-Hill Book Company, 1979.

10) Thwaites, B.: "Approximate Calculation of the Laminar Boundary Layer", The Aeronautical Quarterly, Vol. 1, November 1949.

11) Curle, N. and Skan, S.W.: "Approximate Methods for Predicting Separation Properties of Laminar Boundary Layers", The Aeronautical Quarterly, Volume VIII, February-November, 1957.

12) Duncan, W.J.; Thom, A.S. and Young, A.D.: "Mechanics of Fluids", Chapter VI, Second Edition, Edwards Arnold (Publishers) Ltd., 1970.

13) Preston, J.H.; Sweeting, N.E.: "The Experimental Determination of the Boundary Layer and Wake Characteristics of a Simple Joukowski Aerofoil with Particular Reference to the Trailing Edge Region", ARC R & M No. 1998 (1943).

14) Preston, J.H.: Sweeting, N.E.: "The Experimental Determination of the 2-Dimensional Interference on a Large Chord Piercy 12/40 Aerofoil in a Closed Tunnel Fitted with a Flexible Roof and Floor", ARC R & M No. 2007 (1944).

15) Spath, H.: "Spline Algorithms for Curves and Surfaces", Utilitas Mathematica Publishing Inc., Winnipeg 1974.

TABLE 1

PRESCRIBED FUNCTIONS FOR MODIFIED THWAITES' METHOD

m	ℓ	H
-0.25	0.500	2.00
-0.20	0.463	2.07
-0.14	0.404	2.18
-0.12	0.382	2.23
-0.10	0.359	2.28
-0.08	0.333	2.34
-0.064	0.313	2.39
-0.048	0.291	2.44
-0.032	0.268	2.49
-0.016	0.244	2.55
0	0.220	2.61
0.016	0.195	2.67
0.032	0.168	2.75
0.040	0.152	2.81
0.048	0.138	2.87
0.056	0.122	2.94
0.060	0.113	2.99
0.064	0.104	3.04
0.068	0.095	3.09
0.072	0.085	3.15
0.076	0.072	3.22
0.080	0.056	3.30
0.084	0.038	3.39
0.086	0.027	3.44
0.088	0.015	3.49
0.090	0	3.55

TABLE 2

THE SURFACE VELOCITY DISTRIBUTION ON A 6:1 ELLIPTIC AEROFOIL: INVISCID FLOW, $\alpha = 0°$

POSITION		VELOCITY (U/U_∞)		
Chord-Wise Position (x/d)	Control point No.	Conformal Transformation Theory (Exact)	Distributed Vortices (N = 60)	ERROR %
0.998	1	−0.349	−0.320	−8.3
0.993	2	−0.803	−0.780	−2.8
0.982	3	−0.990	−0.982	−0.8
0.966	4	−1.070	−1.066	−0.4
0.945	5	−1.109	−1.107	−0.2
0.918	6	−1.130	−1.129	−0.09
0.888	7	−1.142	−1.142	0.0
0.853	8	−1.150	−1.150	0.0
0.814	9	−1.156	−1.156	0.0
0.772	10	−1.159	−1.159	0.0
0.726	11	−1.162	−1.162	0.0
0.679	12	−1.164	−1.164	0.0
0.629	13	−1.165	−1.165	0.0
0.578	14	−1.166	−1.165	0.0

Note: 1. The velocity is considered positive if it is counterclockwise about the aerofoil.

TABLE 3

SURFACE VELOCITY GRADIENT AROUND A 6:1 ELLIPTIC AEROFOIL:
INVISCID FLOW, $\alpha = 5°$

POSITION		VELOCITY GRADIENT $\frac{d(U/U_\infty)}{d(s/d)}$		
Chord-Wise Location (x/d)	Control point No.	Conformal Transformation Theory (Exact)	Distributed Vortices (N = 60)	ERROR %
0.998	1	-69.82	-62.11	-11.0
0.993	2	-24.29	-25.37	4.0
0.982	3	- 7.51	- 7.85	4.0
0.966	4	- 2.82	- 2.97	5.0
0.945	5	- 1.31	- 1.38	5.3
0.918	6	- 0.72	- 0.76	5.5
0.888	7	- 0.46	- 0.48	4.3
0.853	8	- 0.33	- 0.34	3.0
0.814	9	- 0.25	- 0.27	8.0
0.772	10	- 0.21	- 0.23	9.5
0.726	11	- 0.19	- 0.20	5.0
0.679	12	- 0.17	- 0.19	11.7
0.629	13	- 0.16	- 0.18	12.5
0.578	14	- 0.16	- 0.18	12.5
0.526	15	- 0.18	- 0.19	5.5

Note: $\text{Error (\%)} = 100 \times \left(\frac{\text{Approx. Gradient} - \text{Exact Gradient}}{\text{Exact Gradient}}\right)$

TABLE 4

COMPUTED SEPARATION CHARACTERISTICS FOR 6:1
ELLIPTIC AEROFOIL AT REYNOLDS NUMBER = 800

ANGLE OF ATTACK (DEGREES)	SEPARATION POSITION (Nearest control point)		SEPARATION VELOCITY (U/U_∞)	NO. OF ITERATIONS
	UPPER SURFACE	LOWER SURFACE		
0	8	54	1.14	1
1	8	54	1.14	1
2	9	54	1.15	2
3	9	55	1.15	2
4	9	55	1.15	2
5	10	56	1.16	2
6	11	56	1.17	4
7	12	57	1.18	4
8	NO UNIQUE SOLUTION			
9	NO UNIQUE SOLUTION			
10	NO UNIQUE SOLUTION			
12	21	58	1.72	14
14	28	59	1.91	5
16	29	59	2.10	6
18	29	59	2.28	4
20	29	60	2.47	5

TABLE 5. COEFFICIENT OF DRAG VALUES

ANGLE OF ATTACK (IN DEGREES)	COEFFICIENT OF SKIN FRICTION DRAG	COEFFICIENT OF FORM DRAG	COEFFICIENT OF PROFILE DRAG
0	0.043	0.102	0.145
1	0.044	0.101	0.145
2	0.045	0.101	0.146
3	0.046	0.099	0.145
4	0.051	0.097	0.148
5	0.054	0.095	0.149
6	0.059	0.090	0.149
7	0.066	0.090	0.156

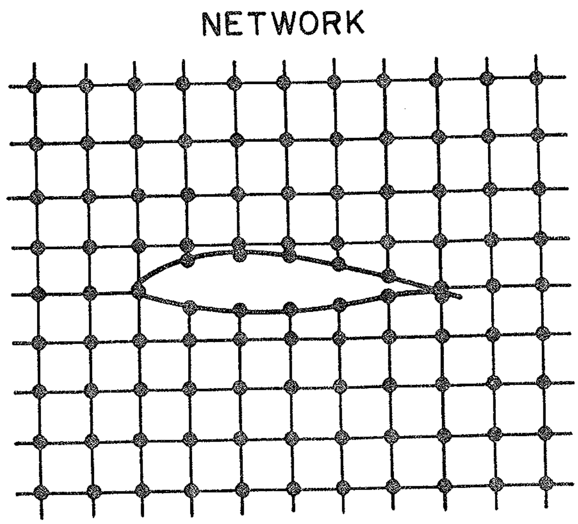

Fig. 1. Control Points for Network Method

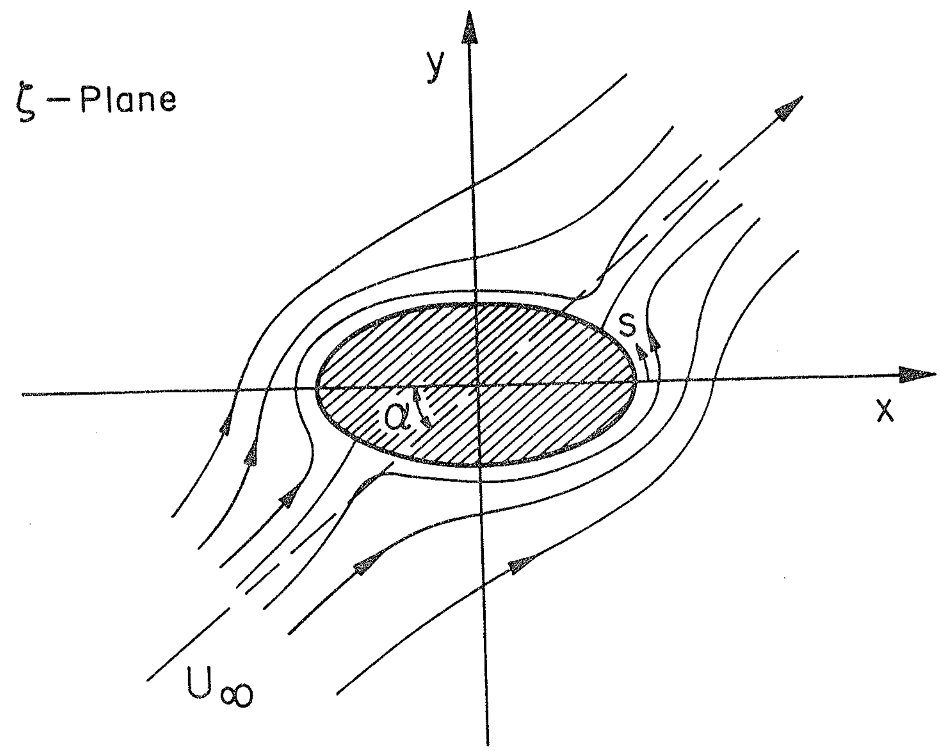

Fig. 2. The Uniform Flow Around an Elliptic Aerofoil

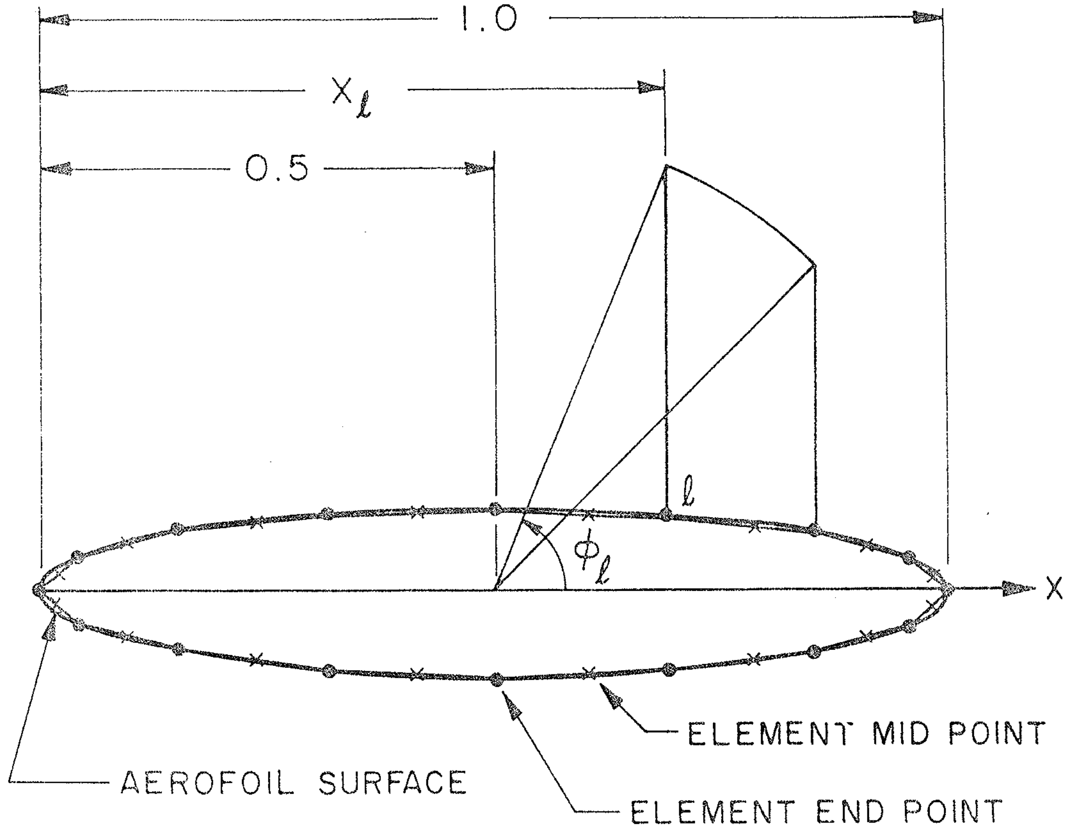

$$X_\ell = 0.5\,(1.0 + \cos\phi_\ell)$$

$$\phi_\ell = 2\pi\,(\ell - 1)/N$$

N = Total number of elements

Fig. 3. Distribution of Elements Around the Aerofoil by Cosine Rule.

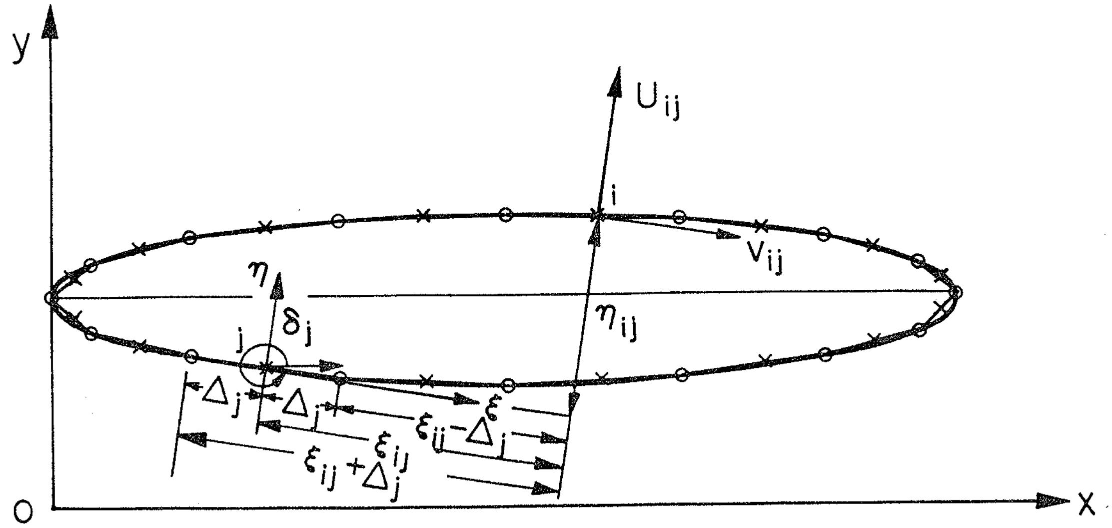

Fig. 4. Induced Velocity Components at a Point due to Distributed Vortices on an Element.

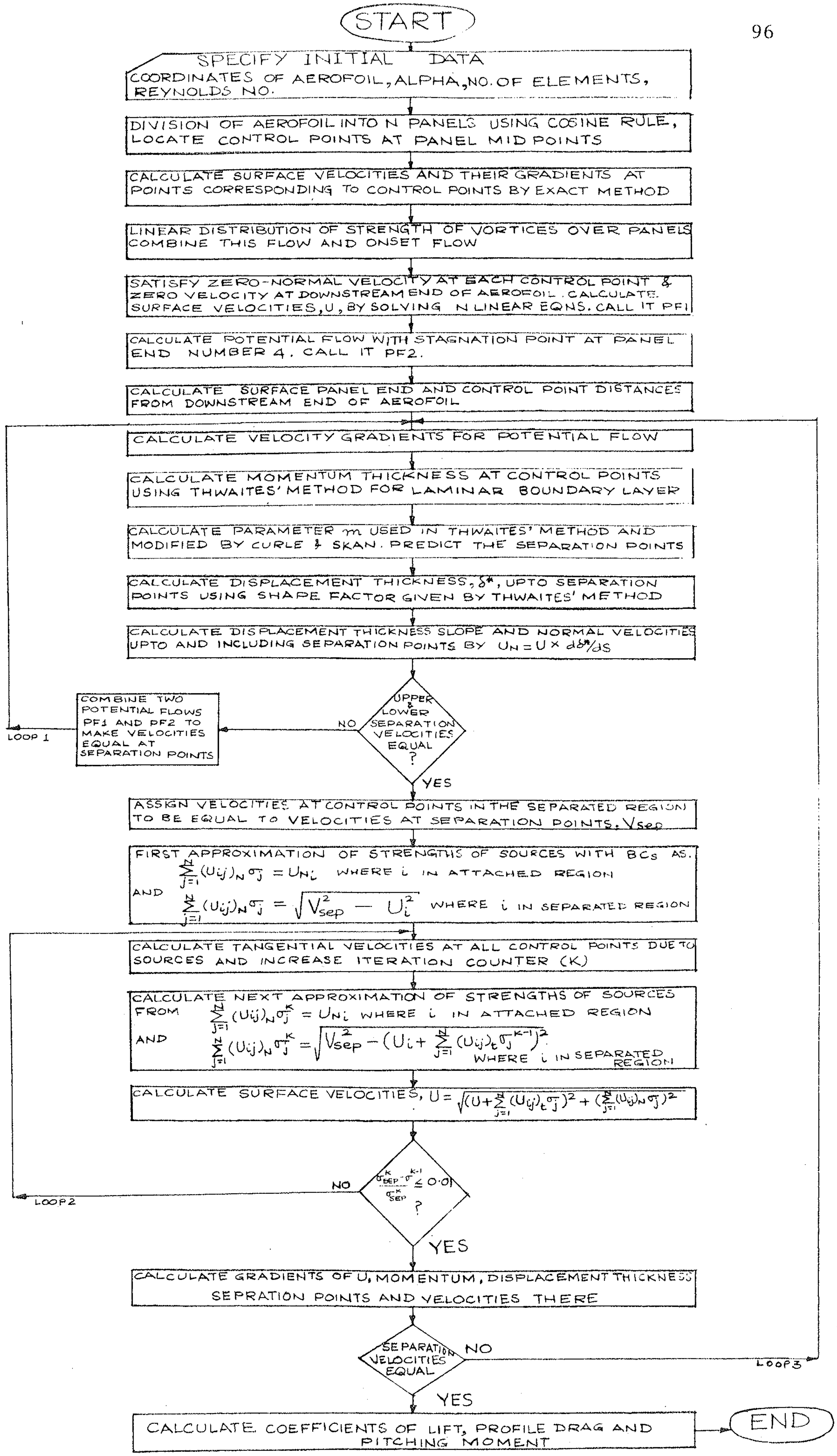

FIG.5 FLOW CHART OF COMPUTER PROGRAM FOR LAMINAR B.L. AROUND AN ELLIPTIC AEROFOIL

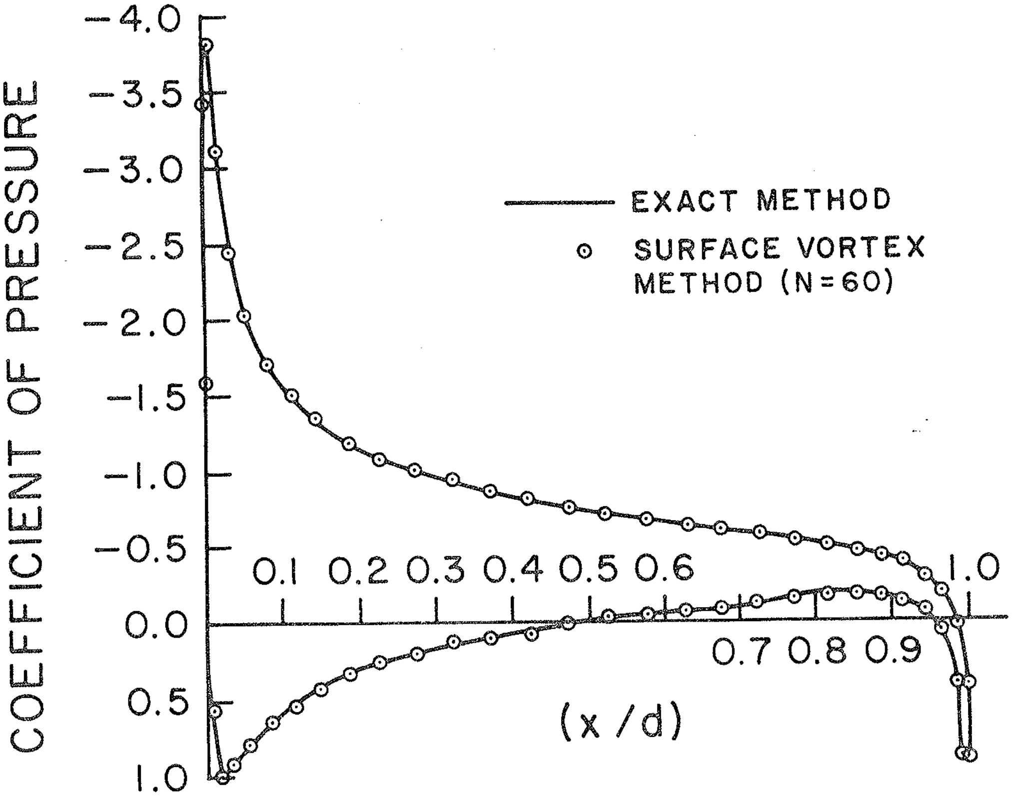

Fig. 6. Inviscid Pressure Distribution at $\alpha = 8°$ by Surface Vortex Method.

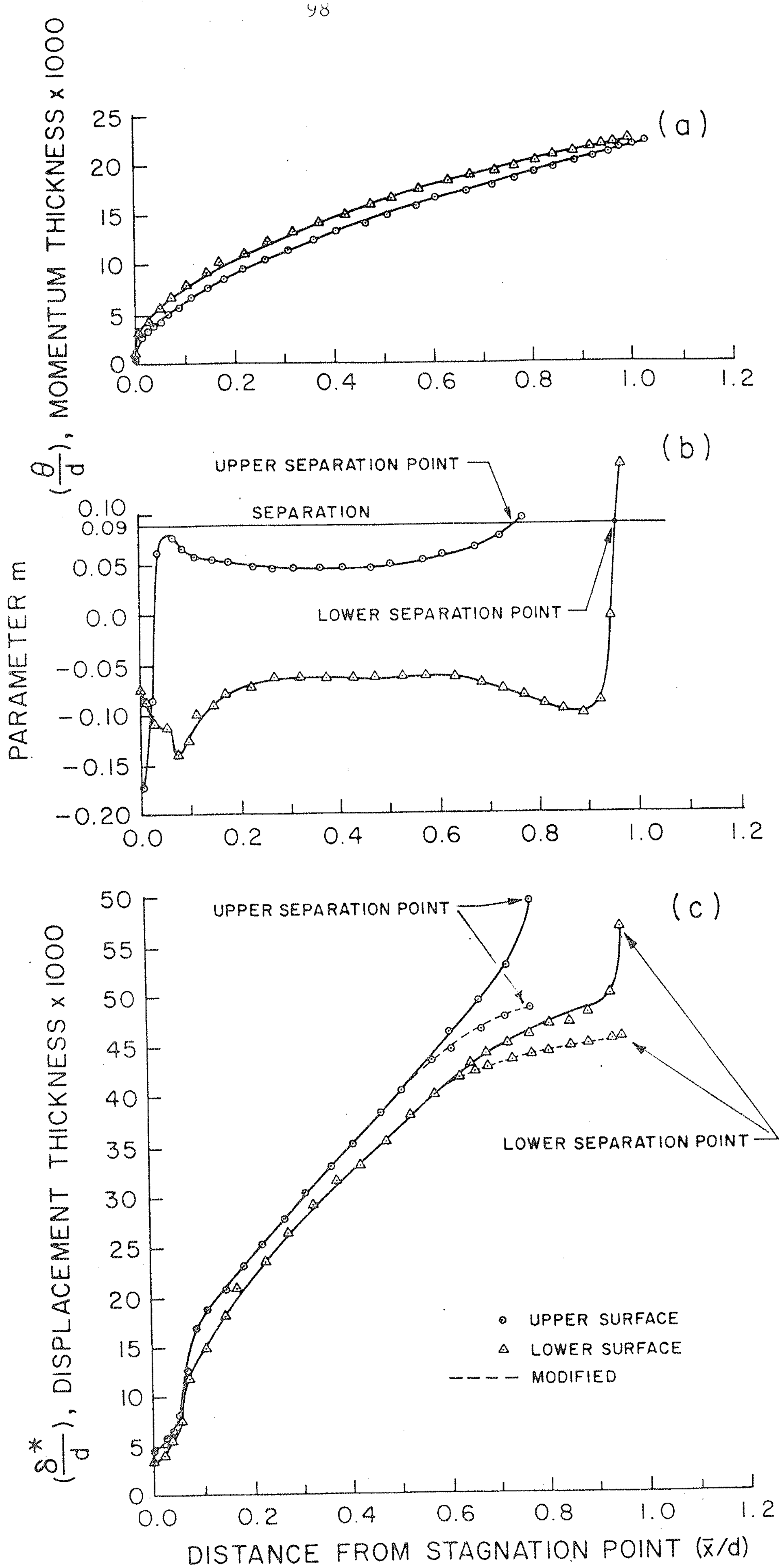

Fig. 7. Boundary Layer Results ($\alpha = 7°$, N = 60, Re = 800)

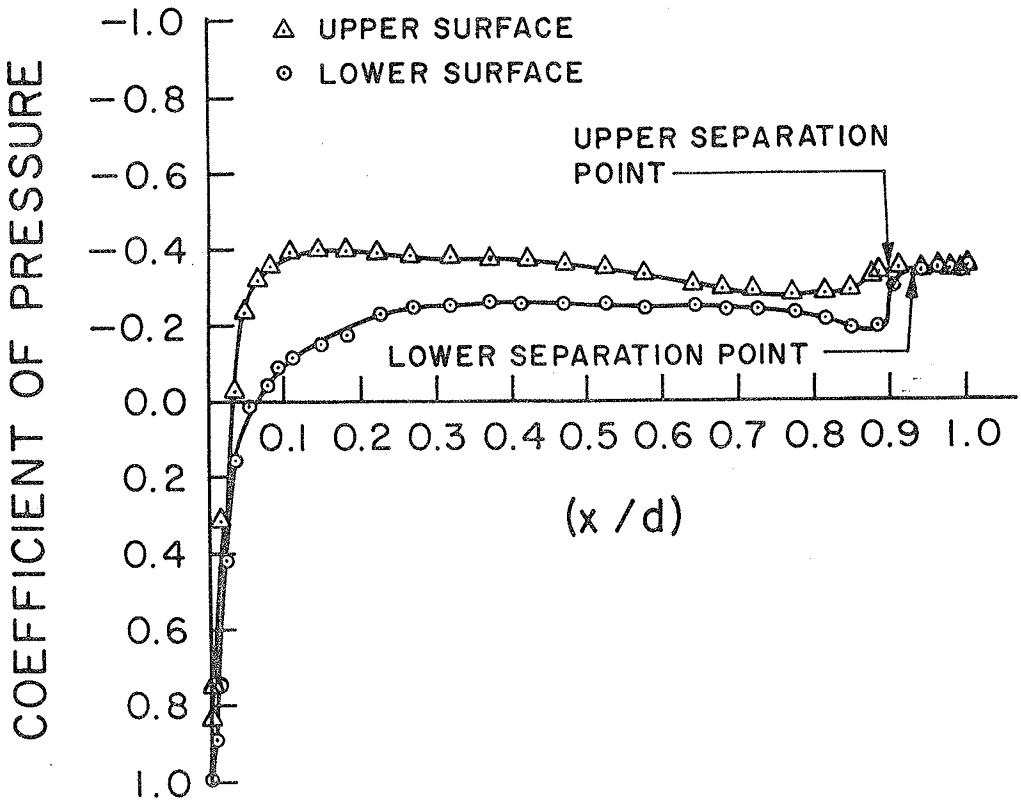

Fig. 8. Pressure Distribution Including Boundary Layer Effects. (N = 60, $\alpha = 1°$)

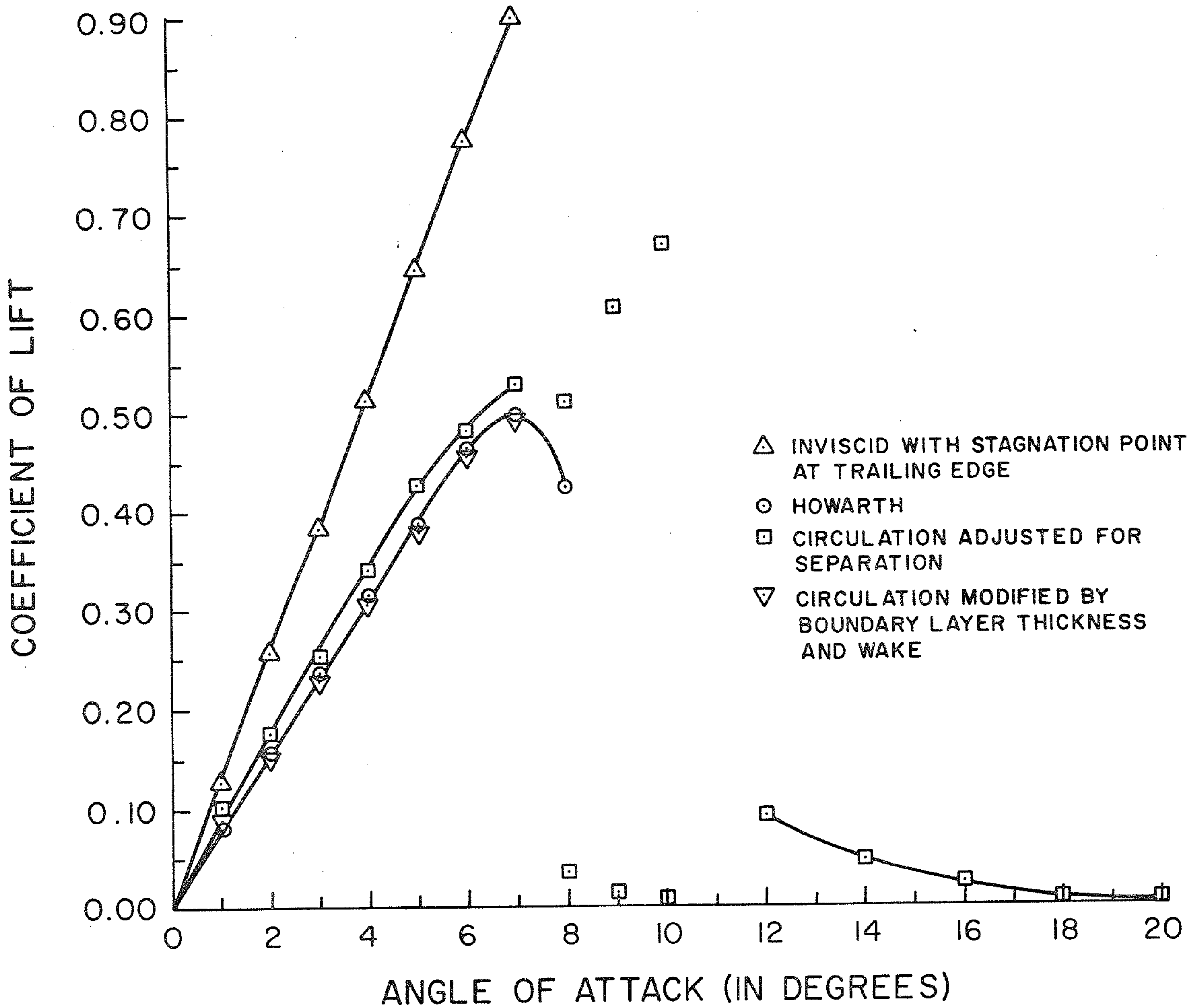

Fig. 9. The Coefficient of Lift Curve.

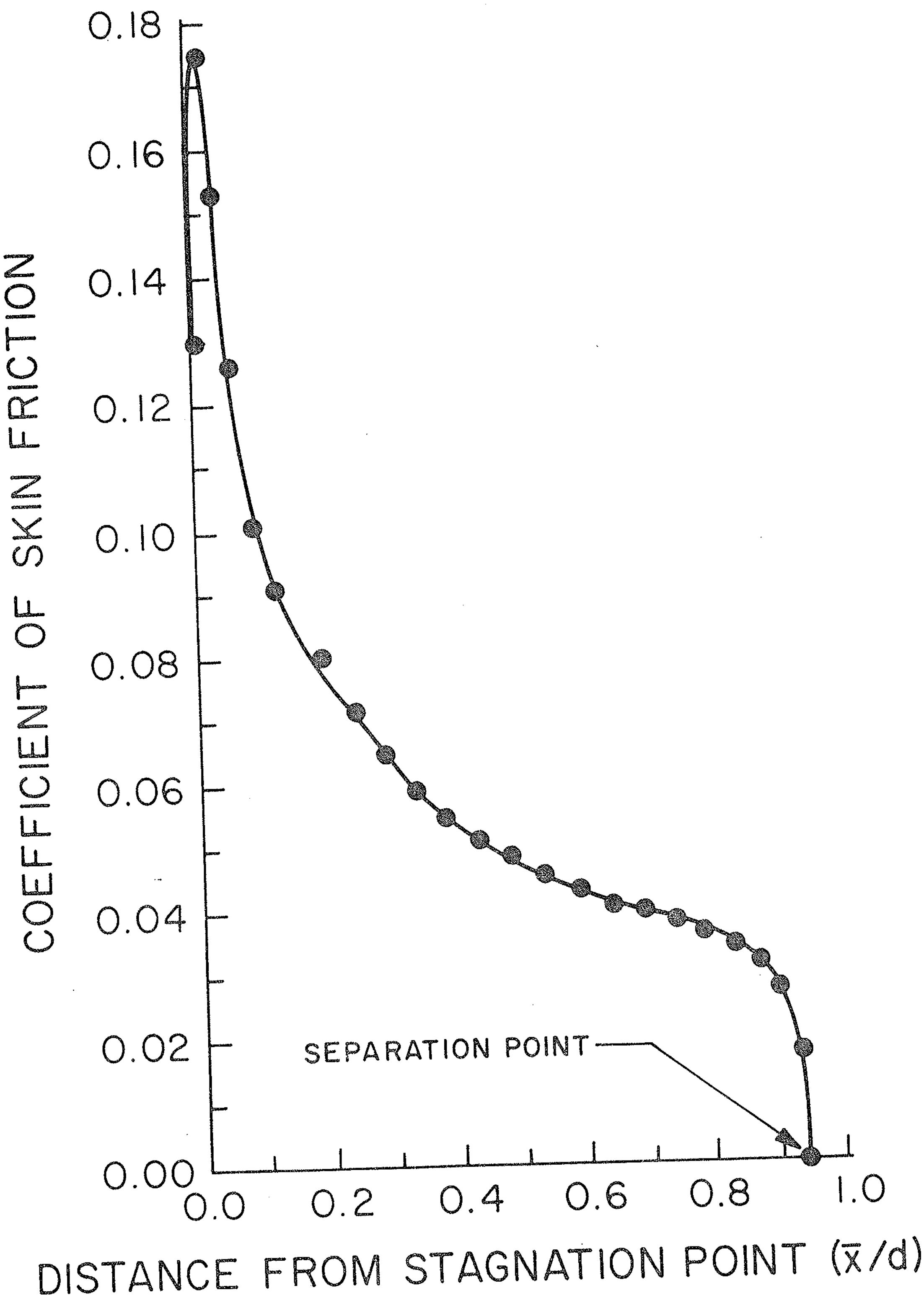

Fig. 10. The Coefficient of Skin Friction Distribution ($\alpha = 3°$)

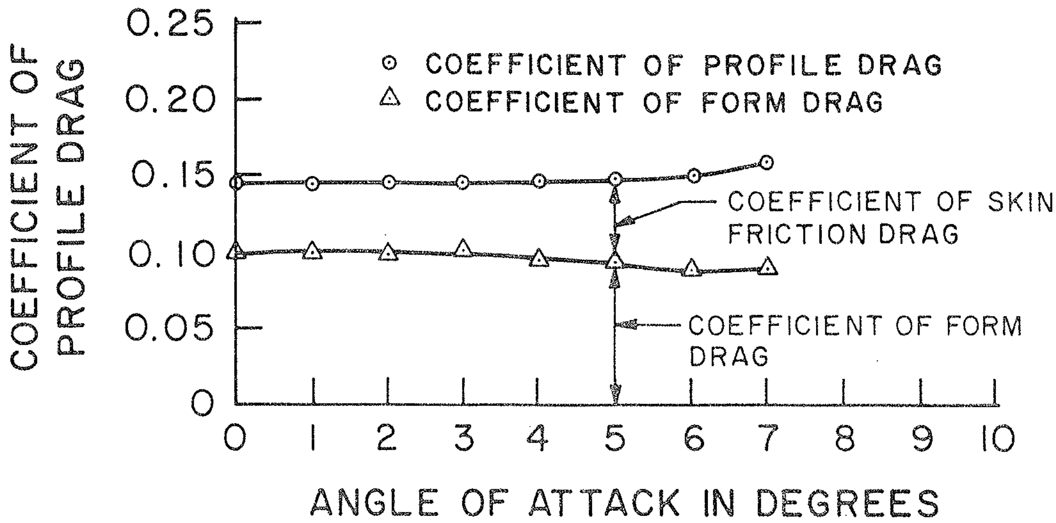

Fig. 11. The Coefficient of Profile Drag Curve.

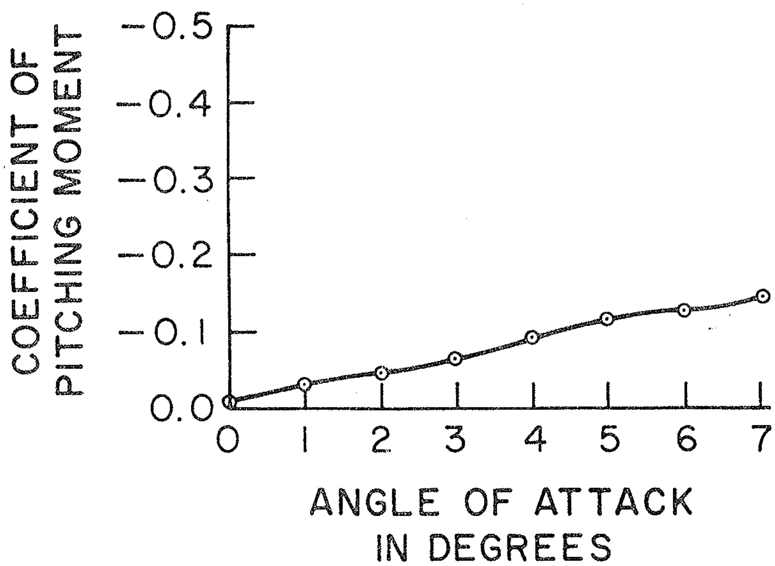

Fig. 12. Coefficient of Pitching Moment Curve.

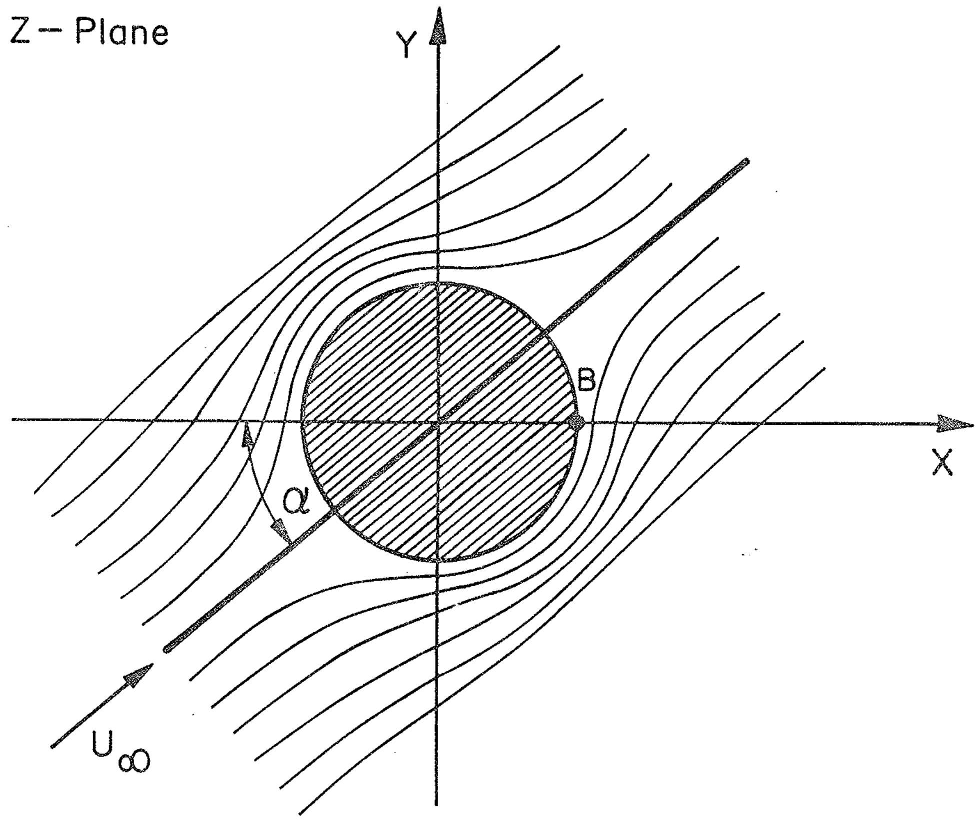

Fig. 13. The Uniform Flow Around a Circular Cylinder

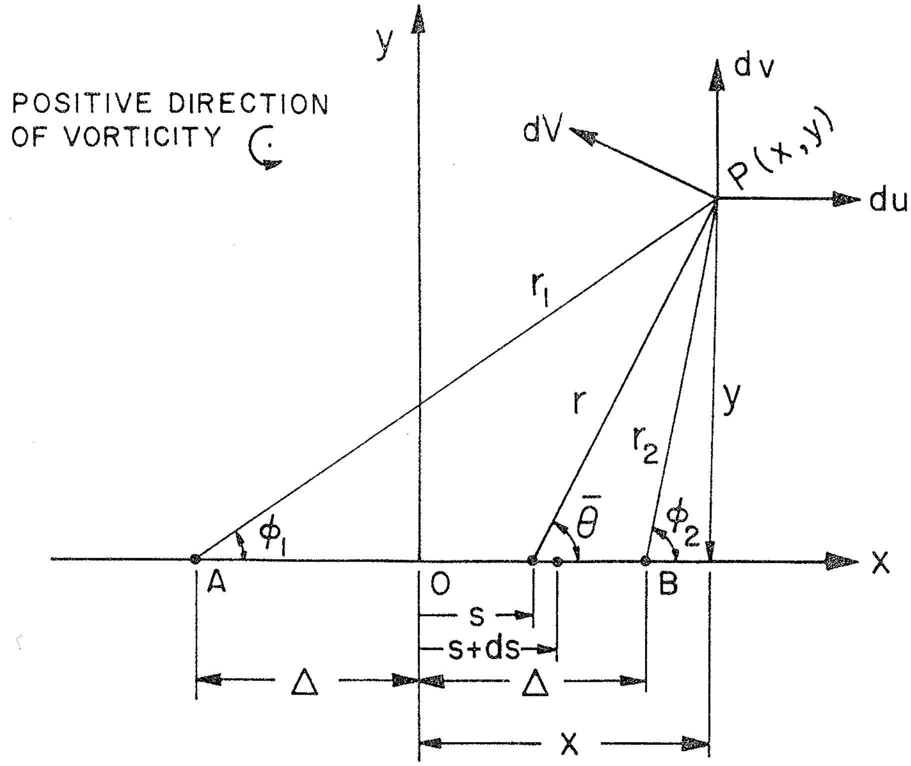

Fig. 14. Induced Velocities at a Point due to Distributed Vortices.

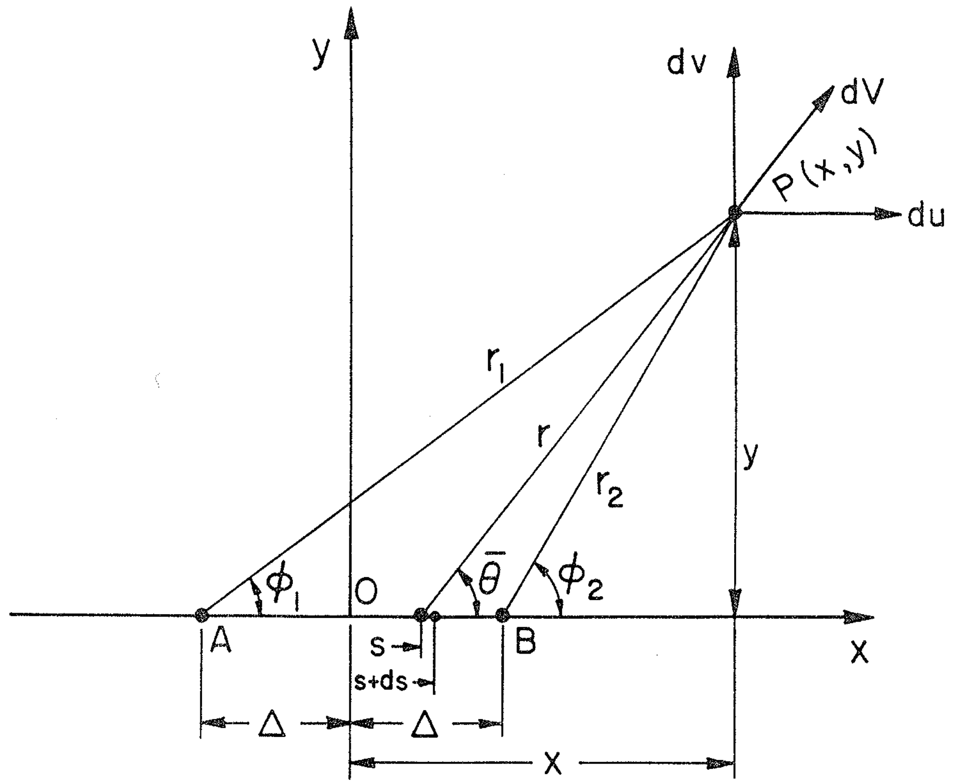

Fig. 15. Induced Velocities at a Point due to Distributed Sources.

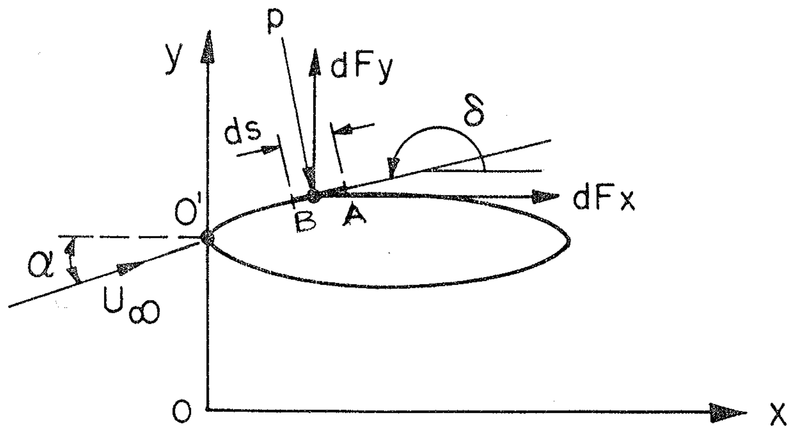

Fig. 16. Normal Pressure on an Element of Aerofoil Surface.

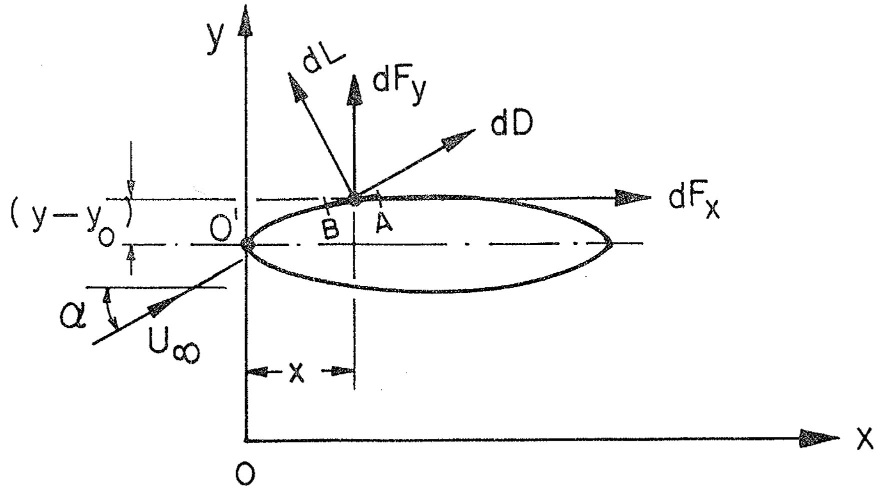

Fig. 17. Pitching Moment About the Leading Edge of the Aerofoil.